Doctoral Dissertations (All Dissertations, All Years)   Electronic Theses and Dissertations

2002-01-08

Computer-Aided Fixture Design Verification

Yuezhuang Kang
Worcester Polytechnic Institute

Follow this and additional works at: https://digitalcommons.wpi.edu/etd-dissertations

COMPUTER-AIDED FIXTURE DESIGN VERIFICATION

by

Yuezhuang Kang

A Ph.D. Dissertation

Submitted to the faculty

of the

WORCESTER POLYTECHNIC INSTITUTE

in partial fulfillment of the requirements for the

Degree of Doctor of Philosophy

in

Manufacturing Engineering

by

_____

December 2001

APPROVED:

_____

Yiming (Kevin) Rong, Advisor, Associate Professor of Manufacturing Engineering

_____

Christopher Brown, Saint-Gobain Professor, Director of Manufacturing
Engineering Program

ABSTRACT

This study presents Computer-Aided Fixture Design Verification (CAFDV) – the methods and implementations to define, measure and optimize the quality of fixture designs. CAFDV verifies a fixture for its locating performance, machining surface accuracy, stability, and surface accessibility. CAFDV also optimizes a fixture for its locator layout design, initial clamping forces, and tolerance specification.

The demand for CAFDV came from both fixture design engineers and today's supply chain managers. They need such a tool to inform them the quality of a fixture design, and to find potential problems before it is actually manufactured. For supply chain managers, they will also be able to quantitatively measure and control the product quality from vendors, with even little fixture design knowledge.

CAFDV uses two models – one geometric and one kinetic – to represent, verify and optimize fixture designs. The geometric model uses the Jacobian Matrix to establish the relationship between workpiece-fixture displacements, and the kinetic model uses the Fixture Stiffness Matrix to link external forces with fixture deformation and workpiece displacement.

Computer software for CAFDV has also been developed and integrated with CAD package I-DEAS™. CAD integration and a friendly graphic user interface allows the user to have easy interactions with 3D models and visual feedback from analysis results.

ACKOWLEDGEMENTS

It is my great pleasure to have this opportunity to thank people who have helped me during my dissertation and my study at Worcester Polytechnic Institute, Massachusetts.

I would like to express my deepest gratitude to Dr. Yiming (Kevin) Rong, my advisor, for helping, guiding and encouraging me to complete this dissertation. Without his numerous suggestions and immense knowledge, this work would have never been completed.

I would like to thank Dr. Juhchin Yang and Mr. Weidong Ma at Ford Motor Co. for their expertise and many discussions that greatly inspired this work.

I also thank Professor Christopher Brown, Professor Richard Sisson, and Professor Joseph Rencis for their enthusiastic service on the dissertation committee.

I appreciate the great help offered by Mr. Weifang Hu, Mr. Yuyun Zhang, Ms. Suqin Yao, and all members in the CAM Lab at WPI..

Finally, I want to devote this work to my mom and my grandparents. It is their endless love that made me what I am today. Thank you, Mom.

TABLE OF CONTENTS

LIST OF FIGURES

LIST OF TABLES

LIST OF SYMBOLS

GCS — global coordinate system

LCS — local coordinate system

LPI — locating performance index

WCS — workpiece coordinate system

$[J]$ — the Jacobian Matrix

$[k]$ — locating point stiffness matrix

$[K]$ — the Fixture Stiffness Matrix

$[T_G^L]$ — 4x4 transformation matrix from LCS to GCS

$[R_G^L]$ — 3x3 rotation matrix from LCS to GCS

$\{q\}$ — workpiece location

$\{\Delta q\}$ — workpiece displacement

$\{\Delta d\}$ — distance between locating point and locating surface

$\{\Delta d\}^T$ — locating point displacement along surface normal

$\{P^G\}$ — a point in global coordinate system

$\{P^W\}$ — a point in workpiece coordinate system

$\{P^L\}$ — a point in local coordinate system

$\{f^G\}$ — reaction force in global coordinate system

$\{f^W\}$ — reaction force in workpiece coordinate system

$\{f^L\}$ — reaction force in local coordinate system

$\{W_i\}$ — internal wrench

$\{W_e\}$ — external wrench

Chapter 1.   Introduction

This chapter gives an introduction of the study – the rationale, the objective, the approaches, the scope and limitations, and the contributions. The organization of the dissertation is listed at the end of this chapter.

1.1.   Rationale

Computer technologies have revolutionized the way products are manufactured today. From standalone CAD/CAM applications to enterprise PDM/ERP (Product Data Management / Enterprise Resource Planning) systems that cross borders, computer technologies have fulfilled the dreams of manufacturers – shortened development time, improved product quality, and lowered cost. As part of this revolution, computer-aided fixture design (CAFD) emerged by integrating fixture design knowledge with CAD platforms. CAFD empowers engineers with its capabilities for fast prototyping with minimal dependence on human interaction.

The primary users of CAFD had been fixture design engineers, who had used it to generate fixture designs. With the advancement of information technology, supply chain managers joined as new users of CAFD. They outsource fixtures to vendors (usually as a part of the production line), and they need tools like CAFD to inspect and control fixture designs from vendors.

An automated fixture design system typically generates more than one solution, sorted by certain criteria. This leaves the questions to CAFD users: which solution is best and how

good is each solution. While design engineers may have enough expertise to answer such questions, supply chain managers usually don't. Seeking solution to this problem raises the demand for Computer-Aided Fixture Design Verification (CAFDV).

1.2. Objective

The objective of CAFDV is to define, measure and optimize the quality of a fixture design. This adds CAFDV as a new stage to CAFD.

Earlier developments generally viewed CAFD as having three stages (Bai, 1995):

- · Setup Planning. To find the number and sequence of all setups, the workpiece orientation, and the machining surfaces for each setup.

- · Fixture Planning. To find locating and clamping positions for each setup.

- · Configuration Design. To design/select detailed fixture components and place them at the right locations.

Now, there is a new and final stage for CAFD:

- · Verification. To define, measure and optimize the quality of fixture designs.

1.3. Approaches and Methodologies

The quality of a fixture design is defined through the requirements from design and manufacturing engineers. Instead of studying all possible requirements, this study focuses on four commonly required areas; other requirements can be similarly integrated. The four studied areas are:

· Locating Performance Analysis. Studies workpiece DOFs (degree of freedom) constrained by locators, workpiece constrained status, locating performance index, and locator layout optimization.

· Tolerance Analysis. Studies machining accuracy provided by the fixture and locator tolerance assignment based on machining surface tolerances.

· Stability Analysis. Studies workpiece stability and minimal clamping forces.

· Accessibility Analysis. Studies point and surface accessibility.

To measure the quality defined above, two models – one geometric and one kinetic – are created to describe the fixture and workpiece relationship.

The geometric model describes the relationship between workpiece displacement and locator displacements, and it is based on the Jacobian Matrix (Asada, 1985). The properties of the Jacobian Matrix can be used in finding locating performance and locating accuracy. The Jacobian Matrix is generally used to formulate the relationship between a 3D object and its locators, and it is also used in robotic hand grasping problems (Xiong, 1999).

The kinetic model describes the relationship between external forces and workpiece displacement. It is based on the Fixture Stiffness Matrix. The creation of the Fixture Stiffness Matrix is discussed in Chapter 4.

In order for the models to handle general as well as specific types of locators, locators are converted into "equivalent locating points". Depending on the type, a locator can be

converted into one or more locating points. The equivalent locating points carry enough information about the actual locator to allow analysis and synthesis. This information includes position, normal direction, tolerance, and stiffness. This study includes the conversion between seven commonly used locators and their equivalent points.

1.4. Scope and Limitations

As mentioned earlier, the quality of a fixture design is defined through its requirements. Four of the most common requirements are considered in this study, but there are more to consider when examining actual fixtures. Machining dynamics, tool path interference, and fixturing ergonomics are also valid requirements for fixture designs.

Instead of studying all possible requirements, this study focuses on building an overall framework of CAFDV and, at the same time, provides solid implementation, with four areas of application. With the framework, other areas of application can be identified, studied, and integrated into CAFDV system in the future.

In the fixture kinetic model, fixtures are assumed to be linear elastic body and the workpiece is assumed as rigid body. In other words, the deformation of workpiece is not considered in the current kinetic model. This is to focus the study on the fixture itself, while workpiece deformation can be calculated with more sophisticated FEA (finite element analysis) methods.

1.5. Contributions

The contributions of this study are categorized into three levels – system, theoretical, and implementation.

System Level

This study as a whole creates a framework for CAFDV, with the geometric and kinetic models as the fundamentals. Based on these two models, analyses are carried out for locating performance, tolerance and stability. The analysis results are further developed to optimize and assist with fixture designs.

Theoretical Level

In the kinetic model, the Fixture Stiffness Matrix is created to link the external forces with fixture deformation.

In locating performance analysis, the Locating Performance Index (LPI) is defined by combining the Jacobian Matrix and the "manipulability" from robotics. With the LPI, locator layout optimization is then accomplished.

For the first time the Jacobian Matrix is used in tolerance analysis, and the surface sensitivity on a locator is defined in tolerance assignment.

In stability analysis, the stability criteria are established with the CSI (contact stability index), and the minimal clamping forces can be optimized with the CSI Matrix.

In accessibility analysis, the Accessible Cylinder is created for point accessibility evaluation.

<u>Implementation Level</u>

To make the CAFDV implementable with computers, conversions between a locator and its locating points are established. These include geometry, tolerance and stiffness conversions. Similarly, machining surfaces are represented by its sample points for tolerance analysis.

Algorithms for all analyses and optimizations have also been developed. These include an implementation for the Jacobian Matrix, and an optimized algorithm for the Fixture Stiffness Matrix.

1.6.   Dissertation Organization

This dissertation is organized into six parts:

Part I (Chapter 1 – 2) Introduction and Review

- · Chapter 1. Introduction (this chapter). Introduces the background, rationale, objective, methodologies, contributions and scope and limitations of this study.

- · Chapter 2. Literature Review. Gives a review of earlier studies related to computer-aided fixture verification. The studies are summarized, categorized, and compared by their research focuses and methods.

Part II (Chapter 3 – 4) Fixture Verification Models

· Chapter 3. Geometric Fixture Model. Introduces the geometric model as the link between workpiece displacement and fixture displacement. It reviews the creation of the Jacobian Matrix and explores the implications of the Jacobian Matrix.

· Chapter 4. Kinetic Fixture Model. Introduces the kinetic model as the link between force and deformation in fixture. It formulates the problem, lists the assumption of the model, and details the derivation of the Fixture Stiffness Matrix.

Part III (Chapter 5 – 8) Fixture Verification Applications

· Chapter 5. Locating Performance Analysis. Studies Locating Performance Index definition, and locator layout optimization.

· Chapter 6. Tolerance Analysis. Includes machining surface accuracy check and locator tolerance assignment.

· Chapter 7. Stability Analysis. Includes stability criteria and minimal clamping force determination.

· Chapter 8. Accessibility Analysis. Defines point and surface accessibility.

Part IV (Chapter 9) Fixture Verification Implementation

· Chapter 9. Algorithms. Lists the detailed implementation algorithms for the Jacobian Matrix and the Fixture Stiffness Matrix.

· Chapter 10. Software Design. Discusses the CAFDV software architecture and user interface screenshots.

Part V (Chapter 10) Summary

    · Chapter 11. Summary. Gives a summary of the study.

Part VI (References and Appendices) Supporting Materials

    · Reference. Gives a list of reference literatures and resources.

    · Appendix A. Conversion Between Locator and Locating Points.

    · Appendix B. Clamping Position Determination.

    · Appendix C. Point Transformation.

Chapter 2.   Literature Review

This chapter gives a review of literature related to this work. First the literature related to general fixture verification is reviewed, and then literature in each of the following areas – locating performance, tolerance, stability, and accessibility – are reviewed.

2.1.   Fixture Verification

Earlier researchers had studied several areas of fixture verification, and each touched one or more areas. Listed below are those important works.

Asada and By (1985) created the Jacobian Matrix to model the fixture-workpiece relationship in 3D space. With this model, they did the following kinetic analysis for a fixture – deterministic positioning, loading/unloading accessibility, bilateral constraint, and total constraint.

Rong et al. have a series of studies (1994/1995b/1996) on tolerance and stability analysis. On tolerance analysis, locating reference planes are modeled as a median layer between locator displacements and workpiece displacement. On stability analysis, 3-D stability problem is converted into 2-D problems, and "acting factor" was introduced to solve friction forces.

Chou et al. (1989) used screw theory for the following fixture analysis and synthesis – deterministic locating, clamping stability, total restraint, clamping point determination, and clamping force determination.

Wu et al. (1995) did both kinetics and force analysis for fixture verification. They modeled the contacts between workpiece and fixture as line and surface contacts. The stability problem is modeled and solved with screw theory and non-linear programming technique. A fixture is stable if solution exists for the non-linear system.

Trappey and Liu (1992) discussed the time-variant stability problem, with considerations of fixturing force limits and directions. In a later work (Trappey, 1995), he used the FEA approach to optimize the fixture layout, which balances between minimal workpiece deformation and maximal machining accuracy.

Besides the works listed above, many other literatures focused on a single aspect of fixture verification. Below is a comparison table based on an in-depth survey of literatures relevant to fixture verification.

Study	Locating Performance	Tolerance Analysis	Stability Analysis	Accessibility
Asada and By, 1985	X	-	-	X
Chou et al. 1989	X	-	X	-
Lee and Cutkosky, 1991	X	-	X	-
Trappey and Liu, 1992	X	-	X	-
Xiong and Xiong, 1998	X	-	X	-
Rong et al. 1994	-	-	X	-
King and Ling, 1995	X	-	X	-
Rong et al. 1995	-	X	-	-
Wu et al. 1995	X	-	X	-
Rong and Bai, 1996	-	X	-	-
DeMeter, 1998	-	-	X	-
Kashyap and DeVries, 1999	X	-	X	-
Li et al. 1999	-	-	-	X
Wang, 1999	X	-	-	-

Table 2.1 Literature Overview for Fixture Verification

2.2.   Locating Performance

Asada and By (1985) established the Jacobian Matrix to formulate the workpiece-fixture relationship in 3-D space. The degrees of freedom (DOFs) constrained by the fixture can be easily derived from the rank of the Jacobian Matrix. Deterministic locating is then equivalent to full rank (rank = 6) of the Jacobian Matrix.

Xiong (1993) applied the kinetic model from multi-fingered robot hand grasping problem to the fixture configuration. Based on contact point positions and normal directions, the fixture configuration matrix (a.k.a. "grasp matrix" in robotics) is established to model the workpiece-fixture relationship in 3-D space. This configuration matrix has similar properties to the Jacobian Matrix, but it's based on assumptions that's true only with robot hand grasping. Since fixtures, unlike the robot hands, the contact point positions will not change with workpiece displacement.

Bicchi (1995) investigated form-closure and force-closure properties of robotic grasping. These two properties indicate the robot hand's capability of inhibiting the workpiece motion. In fixture verification, these two properties are adopted in analysis of total constraint and stability. A robotic grasp or fixture is called form-closure if all possible motions of the workpiece are constrained, and it is called force-closure if the workpiece can maintain its location under all possible wrenches exerted on it. When considering no friction force, form-closure is equivalent to force-closure.

In this work, Asada's Jacobian Matrix is established with detailed mathematical procedures. The model is then used to check if a fixture is well-constrained, i.e., all of its

6 DOFs are constrained. The "stability index" is adopted and developed for automated locating position search.

2.3. Tolerance Analysis

Rong et al (1995b) established three perpendicular locating reference planes, based on locator types and positions. Locator displacements are mapped into the deviations of locating reference planes. The machining surface deviation is then calculated based on the locating reference plane deviations.

Choudhuri and DeMeter (1999) presented a model that relates datum establishment error to locator geometric variability. However, its model is limited to dimensional and profile tolerances applied to spherical tip locators, planar workpiece datum features, and linear, machined features that are bounded by planar workpiece surfaces.

This work developed Asada's Jacobian Matrix to formulate the relationship between machining surface error and locating point displacements. It takes into account the error caused by both locator position error and locator deformation. Given locator tolerance and displacement, this model can predict the deviation for any machining surface. Given machining surface tolerances, it can assign the tolerances for locators. There is no limitation as to which types of locator or tolerance can be included in this model.

2.4. Stability Analysis

Many literatures can be found on stability analysis, in both fixturing and robot grasping areas. There are many different assumptions, approaches, and applications for stability

analysis, such as the consideration of friction force, workpiece and fixture deformation, clamping sequence etc. The comparison table (2.2) shows the focuses of related works.

Study	Friction Force	Workpiece Deformation	Fixture Deformation	Clamping Sequence	Time Varying Cutting Forces	Clamping Force Determination	FEA Method	Optimization
Chou et al. 1989	-	-	-	-	-	X	-	-
Lee and Cutkosky, 1991	X	-	-	-	-	X	-	-
Cogun, 1992	-	-	-	X	-	-	-	-
Trappey and Liu, 1992	X	-	-	-	X	-	-	-
Xiong and Xiong, 1998	-	-	-	-	-	-	-	X
Rong et al. 1994	X	-	-	-	-	-	-	-
Chen, 1995	-	-	-	X	-	-	-	-
King and Ling, 1995	-	-	-	-	-	-	-	X
Wu et al. 1995	X	-	-	-	-	-	-	-
DeMeter, 1998	-	X	-	-	-	-	X	X
Kashyap and DeVries, 1999	-	X	-	-	-	-	X	X

Table 2.2 Literature Overview for Stability Analysis

2.5.   Accessibility Analysis

In fixture design, accessibility is discussed in two senses. Loading / unloading accessibility indicates the easiness to load the workpiece into or detach the workpiece from the fixture, while surface accessibility tells if a fixture unit (locator / clamp) can access the fixturing surface easily. In machining process, accessibility also takes on other meanings. It can be the accessibility for a machine tool to a machining feature, or to a group of machining features. Although these accessibilities are not directly related to the fixturing accessibility, they have similar concepts that are helpful in this research.

Asada and By (1985) discussed the workpiece loading / unloading accessibility based on their Jacobian Matrix model. Their model is well and clearly established, so this approach is adopted and developed in this work.

Chou's "non-obstructive angle" methods (Chou, 1993) is further developed in this work, the "accessible cylinder" is constructed to evaluate the accessibility for a point.

Li et al. (1999) studied the fixturing surface accessibility. He used surface discretization technique, which is commonly used in computer graphics, to assess the surface accessibility. This approach is adopted by this work, and his "surface extrusion and interference detection" algorithm is optimized with ray tracing algorithm in this work.

The table below provides a comparison of all accessibility-related works.

Study	Focus	Technique
Asada and By, 1985	Loading accessibility	Jacobian Matrix
Chou, 1993	Surface accessibility	Non-obstructive angle
Elber, 1994	Machining feature accessibility	Hidden line and surface removal algorithm (computer graphics)
Lim and Menq, 1994	CMM feature inspection accessibility	Heuristic method
Ong and Nee, 1998	Machining feature group accessibility	Fuzzy set
Li et al. 1999	Point accessibility	Surface extrusion Interference detection
	Surface accessibility	Surface discretization

Table 2.3 Literature Overview for Accessibility Analysis

Chapter 3.   Geometric Fixture Model

In fixture tolerance analysis, one major task is to find workpiece displacement that is resulted from locating point displacements. In Figure 3.1, there are three locating points, each with its own tolerance zone. Given the locating point displacements, one question is, how much is the workpiece displacement? On the other hand, if we know the workpiece displacement, can we find the locating point displacements? These questions demand a model for the relationship between workpiece and locating point displacements.
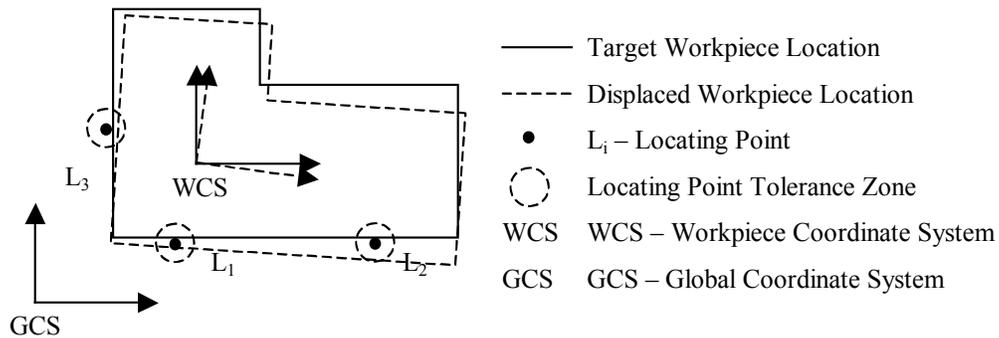
Figure 3.1 Geometric Fixture Model

The geometric model is the link between workpiece displacement and locator displacement. The Jacobian Matrix (Asada, 1985) was adopted to model this relationship. The workpiece displacement can be calculated from locating point displacements, and vice versa. This property forms the foundation for later fixture tolerance analysis, and it is detailed as follows.

In Figure 3.1, assuming the workpiece location is $\{q\} = \{x \quad y \quad z \quad \alpha \quad \beta \quad \gamma\}^T$. When locating points have displacements $\{\Delta d\} = \{\Delta d_1 \quad \Delta d_2 \quad \cdots \quad \Delta d_n\}^T$ along surface normal

direction, they will cause the workpiece to be displaced. The displacements between workpiece $\{\Delta q\}$ and locating points $\{\Delta d\}$ can be linked together by the Jacobian Matrix $[J]$:

$$\{\Delta d\} = [J] \cdot \{\Delta q\} \tag{3.1}$$

or

$$\{\Delta q\} = [J]^{-1} \cdot \{\Delta d\} \tag{3.2}$$

Note: In case $[J]$ is singular, its pseudo-inverse matrix is used in place of $[J]^{-1}$.

where:

- $\{\Delta d\} = \{\Delta d_1 \quad \Delta d_2 \quad \cdots \quad \Delta d_n\}^T$ is the locating point displacements
- $\{\Delta q\} = \{\Delta x \quad \Delta y \quad \Delta z \quad \Delta \alpha \quad \Delta \beta \quad \Delta \gamma\}^T$ is the workpiece displacement

From the equation above we can see that, once the locating point displacements are known, the workpiece displacement can be easily calculated.

3.1.   Derivation of the Jacobian Matrix

Jacobian Matrix is established in Asada's work, based on the distance from locating points to their related locating surfaces. Here the procedure is reorganized and presented in a more systematic view.

In Figure 3.1, let $P_i^G(x_i^G \quad y_i^G \quad z_i^G)$ be the locating point in global coordinate system (GCS), $G_i^W(P_i^W) = A_i x_i^W + B_i y_i^W + C_i z_i^W + D_i = 0$ ($\{A_i \quad B_i \quad C_i\}$ is a normalized vector) be the locating surface represented in the workpiece coordinate system (WCS),

and T_G^W be the 4x4 transformation matrix from WCS to GCS. Then the distance (in WCS) between the ith locating point and its surface is:

$$d_i = G_i^W(P_i^W) = G_i^W(T_W^G \cdot P_i^G) = G_i^W([T_G^W]^{-1} \cdot P_i^G)$$
(3.3)

Since T_G^W is a function of workpiece location $\{q\} = \{x \quad y \quad z \quad \alpha \quad \beta \quad \gamma\}^T$, the distance (in WCS) can then be written as:

$$d_i = d_i^W(\{q\}) = d_i^W(x \quad y \quad z \quad \alpha \quad \beta \quad \gamma)$$
(3.4)

This indicates the locating point to surface distance is a function of workpiece location. Take derivatives on both side of this equation, and we get:

$$\Delta d_i = \frac{\partial d_i}{\partial x} \cdot \Delta x + \frac{\partial d_i}{\partial y} \cdot \Delta y + \frac{\partial d_i}{\partial z} \cdot \Delta z + \frac{\partial d_i}{\partial \alpha} \cdot \Delta \alpha + \frac{\partial d_i}{\partial \beta} \cdot \Delta \beta + \frac{\partial d_i}{\partial \gamma} \cdot \Delta \gamma$$
(3.5)

For distances between all locating points (1, ..., n) and their surfaces, we have:

$$\begin{cases} \Delta d_1 = \dfrac{\partial d_1}{\partial x} \cdot \Delta x + \dfrac{\partial d_1}{\partial y} \cdot \Delta y + \dfrac{\partial d_1}{\partial z} \cdot \Delta z + \dfrac{\partial d_1}{\partial \alpha} \cdot \Delta \alpha + \dfrac{\partial d_1}{\partial \beta} \cdot \Delta \beta + \dfrac{\partial d_1}{\partial \gamma} \cdot \Delta \gamma \\ \Delta d_2 = \dfrac{\partial d_2}{\partial x} \cdot \Delta x + \dfrac{\partial d_2}{\partial y} \cdot \Delta y + \dfrac{\partial d_2}{\partial z} \cdot \Delta z + \dfrac{\partial d_2}{\partial \alpha} \cdot \Delta \alpha + \dfrac{\partial d_2}{\partial \beta} \cdot \Delta \beta + \dfrac{\partial d_2}{\partial \gamma} \cdot \Delta \gamma \\ \vdots \\ \Delta d_n = \dfrac{\partial d_n}{\partial x} \cdot \Delta x + \dfrac{\partial d_n}{\partial y} \cdot \Delta y + \dfrac{\partial d_n}{\partial z} \cdot \Delta z + \dfrac{\partial d_n}{\partial \alpha} \cdot \Delta \alpha + \dfrac{\partial d_n}{\partial \beta} \cdot \Delta \beta + \dfrac{\partial d_n}{\partial \gamma} \cdot \Delta \gamma \end{cases}$$
(3.6)

or:

$$\{\Delta d\} = [J] \cdot \{\Delta q\}$$
(3.7)

17

where the Jacobian Matrix [J] is:

$$J = \begin{bmatrix} \dfrac{\partial d_1}{\partial x} & \dfrac{\partial d_1}{\partial y} & \dfrac{\partial d_1}{\partial z} & \dfrac{\partial d_1}{\partial \alpha} & \dfrac{\partial d_1}{\partial \beta} & \dfrac{\partial d_1}{\partial \gamma} \\ \dfrac{\partial d_2}{\partial x} & \ddots & & & & \dfrac{\partial d_2}{\partial \gamma} \\ \vdots & & & & & \vdots \\ \dfrac{\partial d_m}{\partial x} & \cdots & & & & \dfrac{\partial d_n}{\partial \gamma} \end{bmatrix}$$

(3.8)

Equation (3.7) clearly shows that the Jacobian Matrix [J] links workpiece displacement with locating point displacements.

3.2.   Summary

This chapter introduced the geometric fixture model – the Jacobian Matrix that links workpiece displacement with locating point displacements. The background, creation, and physical meaning of the Jacobian Matrix have also been introduced. More applications for the Jacobian Matrix will be explored in later chapters.

Chapter 4.   Kinetic Fixture Model

If we assume the workpiece to be rigid body and the fixture to be linear elastic, when external forces, i.e., gravity, clamping, machining force, or any combination of them, are applied on the workpiece, the fixture will deform, and the workpiece will be displaced as shown in Figure 4.1. Will the workpiece remain stable? What is the magnitude of the workpiece displacement? How much are the reaction forces on locators and how large are the locator deformations?
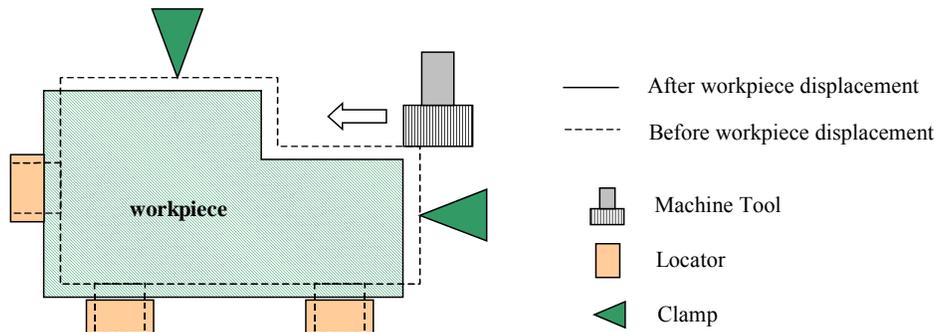
Figure 4.1 Kinetic Fixture Model

The kinetic fixture model serves to answer the above questions. It formulates the relationship between workpiece displacement, fixture deformation, and external forces. Given clamping and machining forces, we are able to calculate the fixture deformation and workpiece displacement.

To establish the model, we assume the workpiece is rigid body, fixtures are linear elastic bodies, and there is friction between fixtures and workpiece. For the workpiece, external forces are balanced by fixture reaction forces.

4.1. Elastic Fixture Assumption

Fixtures are assumed to be linear elastic body, so the reaction forces at locating points are proportional to their displacements. There are three types of coordinate systems used in this study, and they are introduced first.

4.1.1. Three Types of Coordinate Systems

There are three types of coordinate systems (CS) used in this study (Figure 4.2):

· Global Coordinate System (GCS) – the fixed CS in 3D space. It serves as the ultimate reference frame for all other coordinate systems.

· Workpiece Coordinate System (WCS) – the CS attached to each part. In CAD packages, it is determined by user at the part creation.

· Local Coordinate System (LCS) – the CS attached to each contact point. It is generated based on locating position and locator orientation (Appendix B).
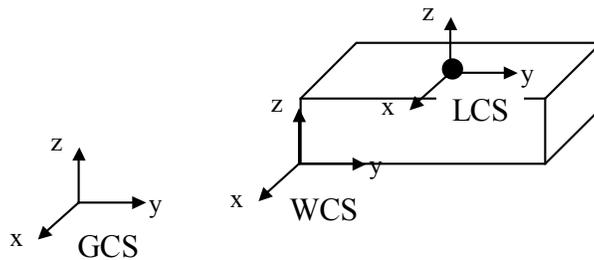
Figure 4.2 Global, Workpiece and Local Coordinate Systems

They are used in different situations as shown in following sections.

4.1.2. Contact Point Stiffness

The contact point (locating/clamping point) is modeled as linear elastic, it has its stiffness on three directions $\{k_x \quad k_y \quad k_z\}$, and it keeps in touch with workpiece surface (Figure 4.3). The estimation of locating point stiffness is list in Appendix B.
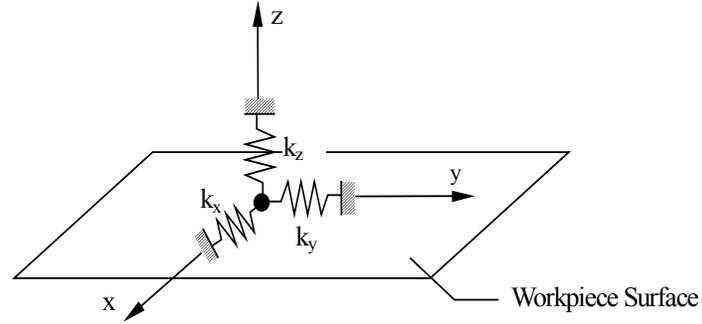
Figure 4.3 Local Stiffness Model

When external forces applied, the workpiece displaces, and the contact point displaces with the surface. The reaction force applied on workpiece in LCS $\{f^L\}$ is:

$$\begin{Bmatrix} f_x^L \\ f_y^L \\ f_z^L \end{Bmatrix} = - \begin{bmatrix} k_x & 0 & 0 \\ 0 & k_y & 0 \\ 0 & 0 & k_z \end{bmatrix} \cdot \begin{Bmatrix} \Delta d_x^L \\ \Delta d_y^L \\ \Delta d_z^L \end{Bmatrix} \tag{4.1}$$

or

$$\{f^L\} = -[k] \cdot \{\Delta d^L\} \tag{4.2}$$

4.2.   Equilibrium Equation Overview

The concept of wrench is borrowed from robotics to describe the combination of force and torque. A wrench in 3-D space $\{W\} = \{F_x, F_y, F_z, M_x, M_y, M_z\}^T$ contains three force elements and three torque elements.

The workpiece is stable when the total external wrench is balanced by the total internal wrench, which is generated by the fixture reaction forces due to workpiece displacement and fixture deformation. This equilibrium equation is:

$$\{W_i\} + \{W_e\} = [K] \cdot \{\Delta q\} + \{W_e\} = 0 \tag{4.3}$$

or,

$$[K] \cdot \{\Delta q\} = -\{W_e\} \tag{4.4}$$

where,

· $\{\Delta q\} = \{\Delta x \quad \Delta y \quad \Delta z \quad \Delta \alpha \quad \Delta \beta \quad \Delta \gamma\}^T$ is the workpiece displacement.

· $\{W_i\} = \{F_{ix}, F_{iy}, F_{iz}, M_{ix}, M_{iy}, M_{iz}\}^T$ is the internal wrench by reaction forces.

· $\{W_e\} = \{F_{ex}, F_{ey}, F_{ez}, M_{ex}, M_{ey}, M_{ez}\}^T$ is the external wrench.

· $[K]$ is the Fixture Stiff Matrix, which is detailed in following sections.

4.3. Formulation of Equilibrium Equation

This section establishes the equilibrium equation for workpiece, and finds the Fixture Stiffness Matrix. First three types of coordinate systems used are introduced, then an outline of the procedures is given, and finally the detailed procedures are introduced.

4.3.1. Formulation Outline

This section outlines the steps of establishing the equilibrium equation, and details of each step are discussed in the sections that follow.

- First, assume we know workpiece displacement in GCS:

$$\{\Delta q\} = \{\Delta x, \Delta y, \Delta z, \Delta \alpha, \Delta \beta, \Delta \gamma\}^T$$

- Then we can find the contact point displacement in GCS $\{\Delta d^G\}$:

$$\{\Delta q\} \rightarrow \{\Delta d^G\}$$

- Then we transform the contact point displacement from GCS into LCS:

$$\{\Delta d^G\} \rightarrow \{\Delta d^L\}$$

- Then we calculate the elastic contact force in LCS:

$$\{\Delta d^L\} \rightarrow \{f^L\}$$

- Then we transform the contact force from LCS into GCS:

$$\{f^L\} \rightarrow \{f^G\}$$

- The we combine all the contact forces into the internal wrench:

$$\{f^G\} \rightarrow \{W_i\}$$

- Finally, by putting them together we have:

$$\{\Delta q\} \rightarrow \{W_i\} = [K] \cdot \{\Delta q\}$$

Those matrices used above are detailed in the following sections.

4.3.2. Contact Point Displacement in GCS

When the workpiece displaces, the contact point on the workpiece surface displaces too. Since the WCS is attached to the workpiece, the contact point coordinates only change in GCS but remain the same in WCS. The displacement of a contact point in GCS is found by the following procedure.

First, the contact point is transformed from WCS $\{p^G\}$ to GCS $\{p^w\}$:

$$\{p^G\} = [T_G^W] \cdot \{p^W\}$$

(4.5)

$\left[T_G^W\right]$ is the transformation matrix from WCS to GCS, and it is a function of workpiece

location $\{q_w\} = \{x_w \quad y_w \quad z_w \quad \alpha_w \quad \beta_w \quad \gamma_w\}^T$.

Then take derivative of $\{q_w\}$ on both sides of equation (4.5), we get:

$$\{d(p^G)\} = \left[\frac{\partial\left(\left[T_G^W\right] \cdot \{p^W\}\right)}{\partial q}\right] \cdot \{dq\} = [G] \cdot \{dq\} \tag{4.6}$$

$$[G] = \left[\left[\frac{\partial T}{\partial x_w}\right]\{p^W\} \quad \left[\frac{\partial T}{\partial y_w}\right]\{p^W\} \quad \left[\frac{\partial T}{\partial z_w}\right]\{p^W\} \quad \left[\frac{\partial T}{\partial \alpha_w}\right]\{p^W\} \quad \left[\frac{\partial T}{\partial \beta_w}\right]\{p^W\} \quad \left[\frac{\partial T}{\partial \gamma_w}\right]\{p^W\}\right]$$

$$\tag{4.7}$$

$[G]$ is a 3x6 matrix, and finding this matrix is similar to finding the Jacobian Matrix

(Chapter 9). For small displacement (as true for fixture deformation), we can have the

approximation:

$$\{\Delta d^G\} = \begin{Bmatrix} \Delta d_x^G \\ \Delta d_y^G \\ \Delta d_z^G \end{Bmatrix} = [G] \cdot \begin{Bmatrix} \Delta x_w \\ \Delta y_w \\ \Delta z_w \\ \Delta \alpha_w \\ \Delta \beta_w \\ \Delta \gamma_w \end{Bmatrix} = [G] \cdot \{\Delta q\} \tag{4.8}$$

From this equation, we get the relation between the contact point displacement in GCS

$\{\Delta d^G\}$ and the workpiece displacement $\{\Delta q\}$.

4.3.3. Contact Point Displacement in LCS

If the contact point displacement in GCS $\{\Delta d^G\}$ is known, this displacement in LCS

$\{\Delta d^L\}$ can be calculated by transforming it from GCS to LCS:

$$\left\{\Delta d^{L}\right\}=\left[T_{G}^{L}\right]^{-1}\cdot\left\{\Delta d^{G}\right\} \tag{4.9}$$

4.3.4. Contacting Force in LCS

At each contact point, the contact force in LCS $\left\{f_{i}^{L}\right\}$ is generated point displacement. As we know the stiffness matrix of the contact point is $\left[k_{i}\right]$ and local displacement is $\left\{\Delta d_{i}^{L}\right\}=\left\{\Delta d_{ix}^{L} \quad \Delta d_{iy}^{L} \quad \Delta d_{iz}^{L}\right\}^{T}$, the contact force in LCS $\left\{f_{i}^{L}\right\}$ can be express as:

$$\left\{f_{i}^{L}\right\}=\left\{\begin{array}{c}f_{ix}^{L}\\f_{iy}^{L}\\f_{iz}^{L}\end{array}\right\}=-\left[\begin{array}{ccc}k_{ix} & 0 & 0\\0 & k_{iy} & 0\\0 & 0 & k_{iz}\end{array}\right]\cdot\left\{\begin{array}{c}\Delta d_{ix}^{L}\\\Delta d_{iy}^{L}\\\Delta d_{iz}^{L}\end{array}\right\}=-\left[k_{i}\right]\cdot\left\{\Delta d_{i}^{L}\right\} \tag{4.10}$$

The contacting forces for all points are:

$$\left\{f^{L}\right\}=\left\{\begin{array}{c}\left\{f_{1}^{L}\right\}\\\left\{f_{2}^{L}\right\}\\\vdots\\\left\{f_{3}^{L}\right\}\end{array}\right\}=-\left\{\begin{array}{cccc}\left[k_{1}\right] & & & \\ & \left[k_{2}\right] & & \\ & & \ddots & \\ & & & \left[k_{m}\right]\end{array}\right\}\cdot\left\{\begin{array}{c}\left\{\Delta d_{1}^{L}\right\}\\\left\{\Delta d_{2}^{L}\right\}\\\vdots\\\left\{\Delta d_{m}^{L}\right\}\end{array}\right\}=-\left[k^{L}\right]\cdot\left\{\Delta d^{L}\right\}$$

$$\tag{4.11}$$

4.3.5. Contacting Force in GCS

The contacting force in GCS can be calculated once the forces in LCS are known. For each contact point, the relationship between global contacting force $\left\{f_{i}^{G}\right\}$ and local contacting force $\left\{f_{i}^{L}\right\}$ is:

$$\left\{f_{i}^{G}\right\}=[T_{Gi}^{L}]\cdot\{f_{i}^{L}\}$$

$[T_{Gi}^{L}]$ is the transformation matrix from LCS to GCS.

The contacting force in GCS for all points can be expressed as:

$$\{f^G\}=\begin{Bmatrix}\{f_1^G\}\\\{f_2^G\}\\\vdots\\\{f_m^G\}\end{Bmatrix}=\begin{Bmatrix}[T_{G1}^L]\\&[T_{G2}^L]\\&&\ddots\\&&&[T_{Gm}^L]\end{Bmatrix}\cdot\begin{Bmatrix}\{f_1^L\}\\\{f_2^L\}\\\vdots\\\{f_m^L\}\end{Bmatrix}=[T_G^L]\cdot\{f^L\} \qquad (4.12)$$

4.3.6. Internal Wrench

A wrench generated by external force is an external wrench, and a wrench generated by reaction force at a contact point is an internal wrench. Let the contact point in GCS be $\{p_i^G\}=\{p_{ix}^G \quad p_{iy}^G \quad p_{iz}^G\}$, the torque generated by contacting force $\{f_i^G\}$ is:

$$\begin{cases}M_{ix}=f_{iz}^G\cdot p_{iy}^G-f_{iy}^G\cdot p_{iz}^G\\M_{iy}=f_{ix}^G\cdot p_{iz}^G-f_{iz}^G\cdot p_{ix}^G\\M_{iz}=f_{iy}^G\cdot p_{ix}^G-f_{ix}^G\cdot p_{iy}^G\end{cases} \qquad (4.13)$$

The internal wrench at this point can be written as:

$$\{W_{ii}\}=\begin{Bmatrix}F_{ix}\\F_{iy}\\F_{iz}\\M_{ix}\\M_{iy}\\M_{iz}\end{Bmatrix}=\begin{bmatrix}1&0&0\\0&1&0\\0&0&1\\0&-p_{iz}^G&p_{iy}^G\\p_{iz}^G&0&-p_{ix}^G\\-p_{iy}^G&p_{ix}^G&0\end{bmatrix}\cdot\begin{Bmatrix}f_{ix}^G\\f_{iy}^G\\f_{iz}^G\end{Bmatrix}=[\Sigma_i]\cdot\{f_i^G\} \qquad (4.14)$$

By combining wrenches at all m contact points, we get the total internal wrench:

$$\{W_i\}=\sum\{W_{ii}\}=[[\Sigma_1]\quad[\Sigma_2]\quad\cdots\quad[\Sigma_m]]\cdot\begin{Bmatrix}\{f_1^G\}\\\{f_w^G\}\\\vdots\\\{f_m^G\}\end{Bmatrix}=[\Sigma]\cdot\{f^G\} \qquad (4.15)$$

4.3.7. Internal Wrench All Together

By combining the previous steps together, we can now get the internal wrench:

$$
\begin{aligned}
\{W\} &\\
&= [\Sigma] \cdot \{f\} \\
&= [\Sigma] \cdot \left[T_G^L\right] \cdot \{f^L\} \\
&= -[\Sigma] \cdot \left[T_G^L\right] \cdot \left[k^L\right] \cdot \{\Delta p^L\} \\
&= -[\Sigma] \cdot \left[T_G^L\right] \cdot \left[k^L\right] \cdot \left[T_G^L\right]^{-1} \cdot \{\Delta p\} \\
&= -[\Sigma] \cdot \left[T_G^L\right] \cdot \left[k^L\right] \cdot \left[T_G^L\right]^{-1} \cdot [J] \cdot \{\Delta q\}
\end{aligned}
\tag{4.16}
$$

4.4.   The Fixture Stiffness Matrix

Now we can re-state the stability equilibrium equation as below, and see the relationship between total external wrench and workpiece displacement:

$$
[K] \cdot \{\Delta q\} = -\{W_e\}
\tag{4.17}
$$

$$
[K] = -[\Sigma] \cdot \left[T_G^L\right] \cdot \left[k^L\right] \cdot \left[T_G^L\right]^{-1} \cdot [G]
\tag{4.18}
$$

[K] is the 6x6 Fixture Stiffness Matrix, which can be obtained as in Equation (4.18).

4.5.   Contact Forces

Once the equation system is solved and the workpiece displacement $\{\Delta q\}$ is known, the contact forces in LCS can be found as:

$$
\{f^L\} = -[k] \cdot \left[T_G^L\right]^{-1} \cdot [G] \cdot \{\Delta q\}
\tag{4.19}
$$

And the forces in WCS can be found through transformation:

$$\{f^G\} = [T_G^L] \cdot \{f^L\} \qquad (4.20)$$

The contact forces in LCS are essential for checking workpiece stability, as will be discussed in Chapter 7 – Stability Analysis.

4.6.   Summary

The kinetic fixture model relates external forces and the workpiece displacement with the Fixture Stiffness Matrix. After obtaining the Fixture Stiffness Matrix, the workpiece displacement can be solved and the contact forces can be calculated. These contact forces are essential for checking workpiece stability.

Chapter 5.   Locating Performance Analysis

Locator layout is the positioning of locators. A sound layout design is vital for the success of the whole fixture design. The figure below shows two similar layouts with different bottom locating positions.
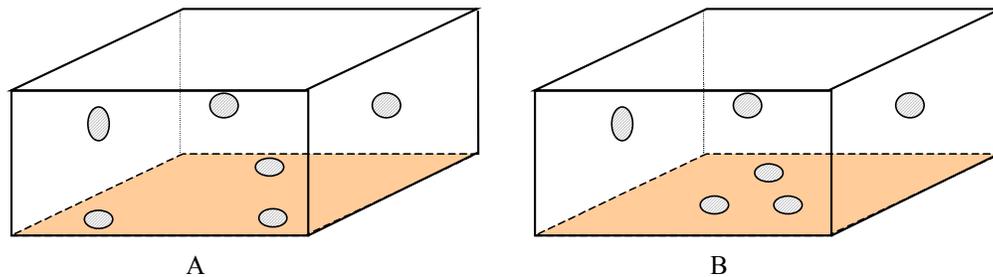
Figure 5.1 Locating Performance Analysis

In layout B, three bottom locators are closer to each other than they are in layout A. Intuitively, we can tell layout A is better, because it looks more "stable". Why it looks more stable, how to define this "stability", and how to improve a layout design are the topics of this chapter. We will define the performance of a locator layout, and then based on the evaluation method, the layout can be optimized.

5.1. Locator Layout Evaluation

A locator layout is evaluated through two measurements: first, the number of workpiece DOFs constrained by locators, and second, is the called Locating Performance Index (LPI). They are discussed as follows.

5.1.1. Constrained DOFs of Workpiece

In Asada's work (1985), it is pointed out that the workpiece DOFs constrained by the fixture equals the rank of the Jacobian Matrix. This result is further extended here so we can know more detail about a locator layout design.

Well-Constrained

A workpiece is well-constrained if the fixture has six locating points and constrains all six DOFs of the workpiece. This is the ideal configuration for fixture designs, among which the "3-2-1" setup and its equivalent are the most popular ones (Figure 5.2-A).

Under-Constrained

A workpiece is under-constrained if there exists a subset of the locating points, that their number is greater than the workpiece DOFs constrained by them. Figure (5.2-B) shows a bottom-locating surface with three locating points. This layout constrains two DOFs with three locating points therefore it is under-constrained.

Over-Constrained

A workpiece is over-constrained if there exists a subset of the locating points, that their number is less than the workpiece DOFs constrained by them. Figure (5.2-C) shows a bottom-locating surface with four locating points. This layout constrains three DOFs with four locating points therefore it is over-constrained. An over-constrained workpiece is likely to have deflection under clamping and machining forces, if locating points are not perfectly aligned.
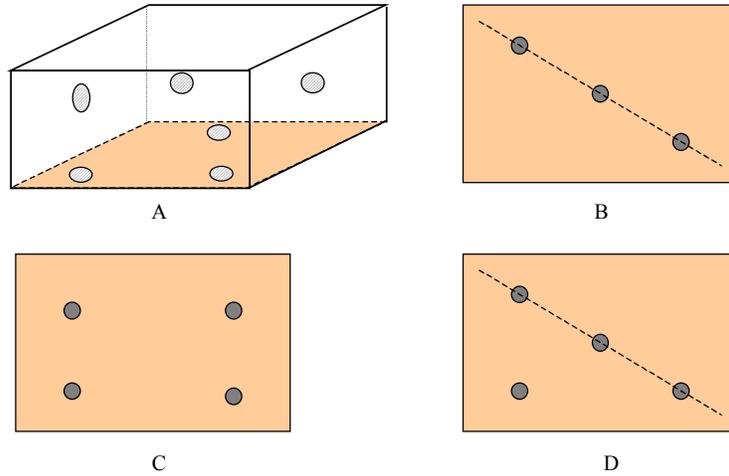
Figure 5.2 Locator Layout and Constrained DOFs

By the definitions above, it is possible for a workpiece to be both under-constrained and over-constrained at the same time. Figure (5.2-D) shows an example.

5.1.2. Locating Performance Index

The Locating Performance Index (LPI) is defined to measure a fixture's ability of tolerating locating errors. This is illustrated in Figure 5.3.
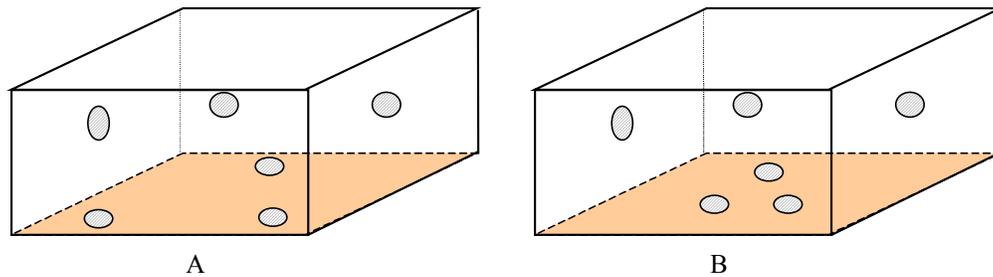
Figure 5.3 Locating Performance Index

Between layout designs A and B, although both constrains 6 DOFs of the workpiece, design A obviously has better performance than design B. The reason is simple – design A will have less workpiece overall displacement, given the same locator displacements. In other words, it can tolerate more locating errors and achieve higher locating accuracy. This "performance index" can now be precisely and confidently calculated.

In multi-fingered robot hand grasping study (Xiong, 1998), the concept "manipulability" is used to measure the control of the grasp over the workpiece. With given finger movements, the grasp with less workpiece displacement has greater manipulability. In other words, this grasp is able to control the workpiece movement more precisely.

This concept of "manipulability" is very similar to the "locating performance" discussed above – they both try to minimize the workpiece displacement. Thus the definition of "manipulability" can be borrowed to define the Locating Performance Index (LPI).

Definition of LPI

$$\mathrm{LPI} = \sqrt{\mathrm{gram}([J])} = \sqrt{\left\| [J]^{\mathrm{T}} \cdot [J] \right\|} \tag{5.1}$$

where,

- $[J]$ is the Jacobian Matrix from the geometric fixture model.
- $\| [J] \|$ is the determinant of matrix $[J]$.
- $\mathrm{gram}([J]) = \left\| [J]^{\mathrm{T}} \cdot [J] \right\|$ is the grammian of a matrix.

LPI is always greater than zero, and its value depends on the size of the workpiece.

Physical Meaning of LPI

The procedure of getting the LPI was not given in Xiong's (1998) work, and it is derived below. This procedure clearly shows the physical meaning LPI implies.

From the geometric fixture model, we have:

$$\{\Delta d\} = [J] \cdot \{\Delta q\}$$

$$\Rightarrow \|\{\Delta d\}\| = \sqrt{\|[J] \cdot \{\Delta q\}\|^2} = \sqrt{\|[J]^T \cdot [J]\| \cdot \|\{\Delta q\}\|^2} = \sqrt{\mathrm{gram}([J])} \cdot \|\{\Delta q\}\|$$

$$\Rightarrow \|\{\Delta d\}\| = \mathrm{LPI} \cdot \|\{\Delta q\}\|$$

$$(5.2)$$

Discussion: From Equation (5.3) we can see that if the locator error $\{\Delta d\}$ is fixed, a larger LPI means less workpiece displacement $\{\Delta q\}$, which also means better machining accuracy. On the other hand, if the workpiece displacement has an upper limit, then larger LPI allows larger tolerances on locators (Figure 5.3).

5.2.   Locator Layout Optimization

From the last section, we know a layout design with maximum LPI provides minimum workpiece displacement and therefore, maximum locating accuracy. Based on LPI, a locator layout can then be optimized. Even if the initial locating positions are unknown, they can be first generated and then optimized.

The procedure for locator layout optimization (and initial locating position generation) is as follows:

- Find the search space, i.e., all possible surface areas for each locating point.

- Determine the constraints between locating points.

- Generate initial positions for the locating points.

- Search the best positions for locating points (which has greatest LPI).

Discussions on several issues are given as follows.

5.2.1. Search Space Representation

The search space for a locating point is the region that the locating point can be positioned in. Because locating points are abstracted from different types of locators, they have different search spaces. (A description of seven included types of locators is given in Appendix A).

For "point" and "plane" type locators, locating points are created on surfaces, and the searchable areas are the locating surfaces, which are represented by UV parameters ($0 \leq U, V \leq 1$).

For "short-v" type locators, locating points are created on the axis of the cylindrical surface, and its searchable area is on the axis, which is represented by parameter U ($0 \leq U \leq 1$).

For other types of locators ("round pin" and "diamond pint" types), their position is fixed once the locating surface is known, so they do not have a searchable area.

5.2.2. Constraints Between Locating Points

Since the locating points are abstracted from the locators, there are some constraints between certain locating points. In other words, they are not totally independent of each other.

For "short-v" type locator, the two locating points always share the same position but with directions perpendicular to each other.

For "pin-hole" type locating (Figure 5.5), two locating points of the round pin share the same position – one points to the diamond pin and the other is perpendicular with the first one. The direction of the locating point from the diamond pin is same with the second locating point of the round pin.

Short Round Pin   Short Diamond Pin

Figure 5.4 Locating Points for Pin-Hole Locating

All these constraints need to be satisfied while optimizing the locating point positions.

5.2.3. Initial Position Generation

The initial locating points for "point" type locator and "plane" type locator are generated around the center of the surface, i.e., $U \cong V \cong 0.5$. For "short-v" type locator, the initial locating points are generated around the center of the axis, i.e., $U \cong 0.5$.

The reason they are generated around center ($\cong 0.5$) instead of at center ($= 0.5$) is that, if two or more points have exactly the same position, the determinant of Jacobian Matrix will be zero (det[J]=0), that will stop those coincide points from optimization. A random number generator is used to generate the initial locating positions around the surface (axis) center. The difference between two initial point coordinates is in the range of [0.001, 0.1]

5.2.4. Position Optimization on Surface

The locating positions are optimized by searching the better position for each locating points. A better position mean the overall fixture will have a larger LPI.

As illustrated in (Figure 5.6), the locating surface is discretized into grids. The locating point was at position "0", and the LPI of the total locator layout is calculated as LPI(0). Then the LPIs are calculated when this locating point is at position "1", "2", "3", and "4", and they are LPI(1), LPI(2), LPI(3), and LPI(4). Compare LPI(0) – LPI(4), the position with the maximum LPI is the best position among these five points. If it's not position "0", then this locating point to the new position with maximum LPI.
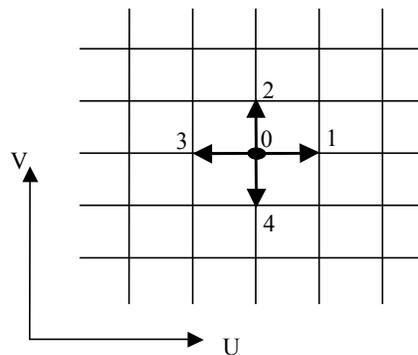
Figure 5.5 Layout Optimization on Surface

For each iteration, each locating point position is optimized as above. The iteration stops when none of the locating point need further optimization (none moved) or reached user specified maximum iteration number.

5.2.5. Position Optimization on Axis

For searchable area which is an axis, the procedure is similar with that of a surface, except it is 1-dimensional (U only) instead of 2-dimensional (U & V).

5.2.6. Post Process

Given the surface, it is very possible that the final locating point position is on the edge of outer loop of the surface. Also, since the U-V parameter of a surface does not have information about the surface details, such as a hole or a boss on the surface, it is possible that the point is located in an inaccessible area. For such types of problems, the post process is needed to adjust the locating point positions to generate a feasible result.

A "margin percentage" (0% – 100%) can be set by user to define the minimal distance allowed for a locating point to be close to the surface outer loop. Any points beyond this limit will be send back to keep the minimal distance. User can set this value based on their fixture component size and workpiece geometry.

If a point fells into an inaccessible area, it relocates itself to the closest accessible position on surface. Then it adjusts its position again to satisfy the "margin percentage".

5.3. Summary

In this chapter, the Locating Performance Index (LPI) is defined to evaluate locator layouts. Base on the LPI, locator layouts can be optimized to achieve best locating accuracy. At the same time, the Jacobian Matrix can be used to find the workpiece DOFs constrained by the fixture. By examining the rank of a Jacobian Matrix, a workpiece can be well-constrained, under-constrained, or over-constrained.

Chapter 6.   Tolerance Analysis

When locators have displacements (caused by manufacturing or positioning error), the workpiece will be displaced, and errors will occur on machining surfaces (Figure 6.1). With the given locator tolerances, can we predict the amount of error it causes for machining surfaces? Can we determine the locator tolerances based on the machining surface tolerance specifications? These questions are to be answered in this chapter.
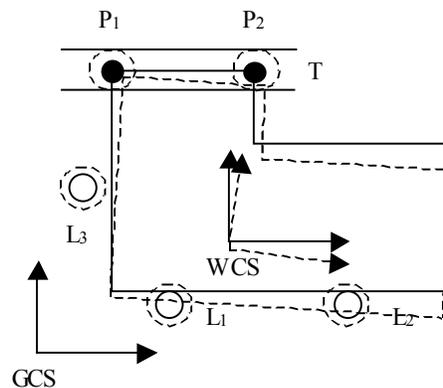
Figure 6.1 Tolerance Analysis

Tolerance analysis in CAFDV studies the relationship between locator tolerances and machining surface tolerances within a single setup. The scope does not include studies on fixture assembly and multi-setup tolerance stack up.

In CAFDV, tolerance analysis has two tasks – machining surface accuracy check and locator tolerance assignment. The former calculates the machining surface accuracy with given locator tolerances, and the latter finds the optimal locator tolerances based on

machining surface tolerance. The figure below best illustrates the relationship between accuracy check and tolerance assignment.
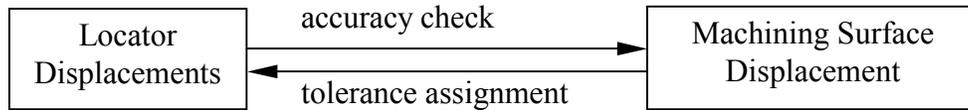
Figure 6.2 Accuracy Check and Tolerance Assignment

In order for computer implementation, machining surfaces are represented by sample points (Section 6.1). Tolerances are then defined based on surface sample points (section 6.2). Then accuracy check and tolerance assignment are discussed (Section 6.1 and 6.2).

6.1.   Machining Surface Sample Points

For computer implementation, machining surfaces must be represented with finite points. These points are sampled from the surface contour, since the largest surface deviation always occurs on the contour. And the surface accuracy is defined by finding the largest deviation among its contour points.
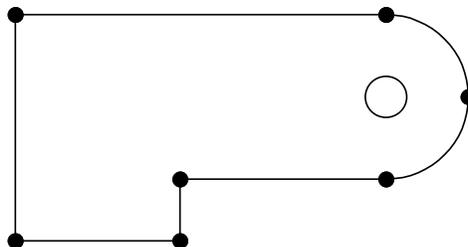
Figure 6.3 Surface Sample Points

For surface deviation calculation, sample points are taken at each vertex on surface, and more points are taken from a curve to increase precision (Figure 6.3).

The deviations of contour points are calculated based on the workpiece location deviation, and the machining surface error is then calculated by its tolerance type.

6.2. Definition of Surface Deviation and Accuracy

For a given tolerance type, the machining surface deviation can be calculated based on its sample point deviations. The calculation follows the standards set in ANSI Y-14.5 (ANSI, 1995). Figure 6.4 shows the target surface and the deviated surface, along with their sample points.
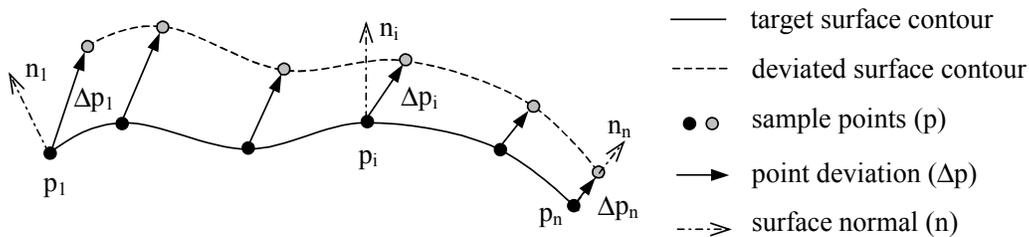
Figure 6.4 Surface Deviation

Machining Surface Accuracy

For a given tolerance type, the surface accuracy is the envelop for all possible deviations, which is equivalent to the maximal deviation (the worst case). For a qualified surface, its accuracy must fall within the specified tolerance.

The calculation for each type of machining accuracy is listed in the following sections.

6.2.1. Surface Profile and Line Profile Deviation

For surface and line profile, they are defined as double the maximum sample point deviation. They can be calculated as (Figure 6.4):

$$\text{dev} = 2 \times \max\{\Delta p_1^n \quad \Delta p_2^n \quad \cdots \quad \Delta p_n^n\} \tag{6.1}$$

where,

- $\Delta p_i^n = \Delta p_i \cdot n_i$ is the sample point deviation along surface normal direction

6.2.2. Parallelism, Perpendicularity and Angularity Deviation

For parallelism, perpendicularity and angularity, their surface deviations are calculated as the difference between maximum and minimum sample point deviations (Figure 6.4):

$$\text{dev} = \max\{\Delta p_1^n \quad \Delta p_2^n \quad \cdots \quad \Delta p_n^n\} - \min\{\Delta p_1^n \quad \Delta p_2^n \quad \cdots \quad \Delta p_n^n\} \tag{6.2}$$

6.2.3. Position Deviation

The deviation calculation for position type is a little different from other types. The sample points are derived from the cylinder axis instead of from the surface contour. It is defined to be double the maximum deviation from the target axis (Figure 6.5):

$$\text{dev} = 2 \times \max\{\Delta d_1^n \quad \Delta d_2^n \quad \cdots \quad \Delta d_n^n\} \tag{6.3}$$
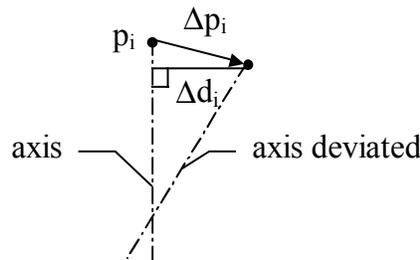
Figure 6.5 Position Deviation

6.2.4. Other Types of Deviations

Other types of deviation, such as plane surface flatness, cylindrical surface run-out, symmetry, are not considered in this work. The reason is that they are not affected by locator displacements.

6.3. Machining Surface Accuracy Check

The machining surface accuracy is the worst case of all possible surface deviations, so the task is to get a set of locating point deviations, and find the largest machining surface deviation.

As shown by the geometric fixture model, once we know locating point deviations $\{\Delta d\}$, we can find the workpiece location deviation $\{\Delta q\}$ as:

$$\{\Delta q\} = [J]^{-1} \cdot \{\Delta d\} \tag{6.4}$$

where:

· $\{\Delta d\} = \{\Delta d_1 \quad \Delta d_2 \quad \cdots \quad \Delta d_n\}$

· $\{\Delta q\} = \{\Delta x \quad \Delta y \quad \Delta z \quad \Delta \alpha \quad \Delta \beta \quad \Delta \gamma\}^T$
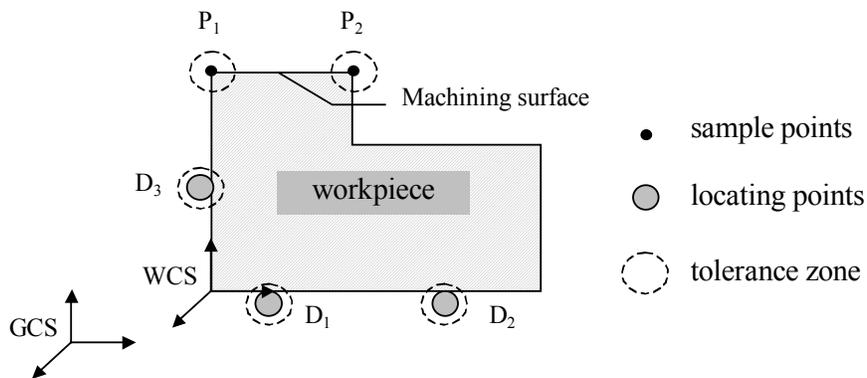
Figure 6.6 Machining Surface Accuracy Check

As shown in Figure 6.6, when the locating points have certain deviations, they will cause deviation for the workpiece. Then the sample points will have deviations, and these deviations can then be used to calculate the surface deviation.

Let $\{q_0\}$ be the ideal workpiece location, $T_G^W(q)$ be the 4x4 workpiece transformation matrix based on location $\{q\}$, and $\{P_i^W\}$ be the surface sample point coordinates in WCS, we can have sample point deviations in GCS $\{\Delta P_i^G\}$ as:

$$
\begin{aligned}
\Delta P_i^G = P_{i2}^G - P_{i1}^G &= \left[T_G^W(q_0 + \Delta q) \right] \cdot P_i^W - \left[T_G^W(q_0) \right] \cdot P_i^W \\
\Rightarrow \Delta P_i^G &= \left[T_G^W(q_0 + \Delta q) - T_G^W(q_0) \right] \cdot P_i^W \\
\Rightarrow \Delta P_i^G &= \left[T_G^W(q_0 + [J]^{-1} \cdot \{\Delta d\}) - T_G^W(q_0) \right] \cdot P_i^W
\end{aligned}
\tag{6.5}
$$

For a given set of locating point deviations $\{\Delta d\}$, the machining surface deviation can then be calculated following the "definition of machining surface deviation":

$$
\begin{aligned}
\Delta p_i^n &= \Delta p_i \cdot n_i \\
dev &= dev\{\Delta p_1^n \quad \Delta p_2^n \quad \cdots \quad \Delta p_n^n\}
\end{aligned}
\tag{6.6}
$$

By varying the locating point displacements in the locating point tolerance zone, we can get a set of machining surface deviations. The machining surface accuracy is the worst case of all surface deviations.

$$
acc = max\{dev_1 \quad dev_2 \quad \cdots \quad dev_m\}
\tag{6.7}
$$

6.4.   Locator Tolerance Assignment

Locator tolerance assignment is to find the tolerance specification for locators, so that all machining surface tolerance requirements can be satisfied. In order to reasonably

distribute tolerances to each locator, first we need to find out how sensitive the machining surface is to each locator. The more sensitive locator should get tighter tolerance specification.

6.4.1.   Surface Sensitivity on Locators

Sensitivity analysis is to evaluate how sensitively the surface deviation depends on a certain locating point deviation. It is used for distributing tolerance to locating points according to their sensitivities.

For certain machining surface tolerance T_j $(j = 1 \cdots m)$, Let P_i $(i = 1 \cdots n)$ be the locating point, $\{\Delta d\} = \{0 \quad \cdots \quad 1 \quad \cdots \quad 0\}$ (only the i'th element is 1) be the locating point normal deviations, then the surface deviation based on this unit locating point deviation is:

$$dev_{ij} = dev(\Delta d) \tag{6.8}$$

And the sensitivity for the tolerance upon the locating point S_{ij} can be found by normalizing the deviations for all locating points:

$$S_{ij} = \frac{dev_{ij}}{dev_{1j} + dev_{2j} + \cdots + dev_{nj}} \qquad \left(\sum_{i=1}^{n} S_{ij} = 1 \right) \tag{6.9}$$

A sensitivity matrix can then be constructed for all surface tolerances and locating points:

Sensitivity S_{ij}	Machining Surface Tolerances T_j $(j = 1 \cdots m)$			
Locating Points P_i $(i = 1 \cdots n)$	S_{11}	S_{12}	$\cdots$	S_{1m}
	S_{21}	S_{22}	$\cdots$	S_{2m}
	$\vdots$	$\vdots$		$\vdots$
	S_{n1}	S_{n2}	$\cdots$	S_{nm}

Table 6.1 Sensitivity Matrix

6.4.2. Tolerance Distribution

For each machining surface tolerance, the locating point tolerances are assigned based on their sensitivities. In the case of multiple machining surface tolerances, the tightest tolerance is selected as the final tolerance for each locating point. This procedure is detailed below.

For machining surface tolerance T_j $(j = 1 \cdots m)$, a reference tolerance t_0 is picked (the selection of t_0 is detailed later) to assign the locating point tolerances t_{ij} $(i = 1 \cdots n)$, based on their sensitivities. This is done through a weight factor w_{ij}:

$$t_{ij} = w_{ij} \cdot t_0 \tag{6.10}$$

Points that has larger sensitivity should have tighter tolerance, so w_i is designed as:

$$w_i = 1 - k \cdot S_{ij} \tag{6.11}$$

The factor 'k' is to prevent zero tolerance when the sensitivity $S_{ij} = 1$. It can be tuned to achieve optimal result. In our implementation of locator tolerance assignment, k = 0.9 is assumed. Combining above equations together, locator tolerances are assigned as:

$$t_{ij} = t_0 \cdot \left(1 - k \cdot S_{ij}\right) \hspace{3cm} (6.12)$$

In the case of multiple tolerances on a machining surface, first the locating point tolerance is assigned for all surface tolerance, and then the tightest tolerance among them is selected as the final locating point tolerance. This is shown in the table below.

Locating Point Tolerance t_{ij}	Machining Surface Tolerances T_j $(j = 1 \cdots m)$				Final Locating Point Tolerance t_i
Locating Points P_i $(i = 1 \cdots n)$	t_{11}	t_{12}	$\cdots$	t_{1m}	$t_1 = \min\{t_{11} \quad \cdots \quad t_{1m}\}$
	t_{21}	t_{22}	$\cdots$	t_{2m}	$t_2 = \min\{t_{21} \quad \cdots \quad t_{2m}\}$
	$\vdots$	$\vdots$		$\vdots$	$\vdots$
	t_{n1}	t_{n2}	$\cdots$	t_{nm}	$t_n = \min\{t_{n1} \quad \cdots \quad t_{nm}\}$

Table 6.2 Tolerance Assignment for Multiple Surface Tolerances

With the assigned tolerances, the locators can ensure that all machining surface tolerances will be satisfied.

6.5.   Summary

Given the locator tolerances, we can predict the machining surface accuracy, based on its tolerance type. On the other hand, given the machining surface tolerance, we are able to determine the locator tolerances.

For computer implementation, machining surfaces are represented by its sample points. Six fixture-related tolerances are then defined with the surface sample points.

In locator tolerance assignment, surface sensitivity on locating point is defined to best distribute tolerances among locating points.

Chapter 7. Stability Analysis

When an external force (gravity, clamping or machining force) is applied on the workpiece, the fixture will deform, and the workpiece will be displaced (Figure 7.1). Will the workpiece remain stable? What are the criteria for it to be stable? If the workpiece depends on friction forces to remain stable, what are the minimal clamping forces required? These questions are answered in this chapter.
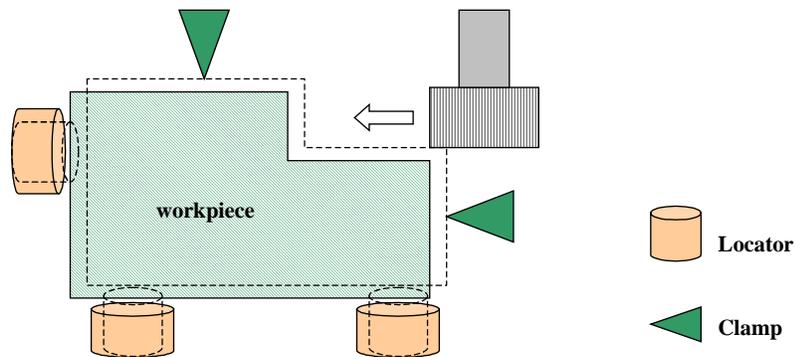
Figure 7.1 Workpiece Stability

Fixture stability analysis has two major functions – stability verification and clamping force optimization. Stability verification verifies existing fixture designs – it checks workpiece stability under gravity force, clamping forces, and machining forces. Clamping force optimization, on the other hand, assists with fixture design process – it finds the minimal required clamping force to stabilize the workpiece.

7.1.   Stability Verification

With the kinetic fixture model, we are able to calculate the reaction forces at locating points when an external force is applied on the workpiece. Using this result, the workpiece stability can be verified.

Workpiece stability is defined so that there is no slippage between any locating point and the workpiece surface. This criterion is further discussed as follows.

7.1.1.   Stability Criteria

This section will first illustrate the condition for a point to remain in contact with a surface, and then list the criteria of fixturing stability.

<u>Friction Cone</u>

As we know, the condition for a point in contact with the surface is that the contact force falls within the friction cone (Figure 7.2).
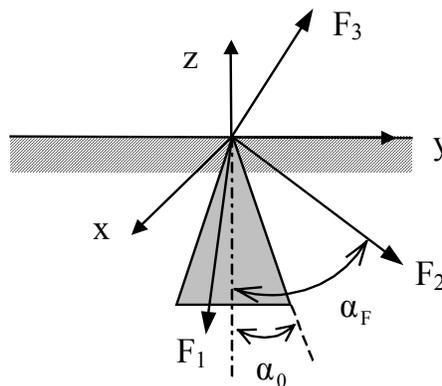
Figure 7.2 Friction Cone and Contact Stability Index

In the figure, three forces are exerted onto the surface at the contact point. F1 falls within the friction cone (shaded area), it will remain in contact with the surface; F2 falls outside the cone but still points towards the inside of the surface, it will cause slippery; F3 points towards the outside of the surface, it will cause the separation from the surface.

The friction cone is defined by the maximum friction force limitation:

$$-\infty \leq \frac{f}{\mu \cdot N} \leq -1$$

(7.1)

where f is the friction force, μ is the static friction coefficient, and N is the normal force.

Contact Stability Index (CSI)

To evaluate the stability at a contact point, it is desirable to have a quantitative measurement. Also it is desirable the measurement be normalized, so that the stability index can be read directly from the value. To fulfill the requirements, the contact stability index (CSI) is defined to measure the stability of a contact point. It will have the following properties:

· $-1 \leq CSI < 0$ – outside the friction cone, unstable.

· $CSI = 0$ – on the friction cone, marginally stable.

· $0 < CSI \leq 1$ – inside the friction cone, stable.

To satisfy the requirements above, CSI is formulated as following:

$$CSI = \begin{cases} 1.0 - \dfrac{\alpha_F}{\alpha_0} & \alpha_F \leq \alpha_0 \\ -\dfrac{\alpha_F - \alpha_0}{\pi - \alpha_0} & \alpha_F > \alpha_0 \end{cases}$$

(7.2)

where (Figure 7.2),

    · α_0 is the angle (radius) of the friction cone,

    · α_F is the angle (radius) between force vector and "-z" axis.

This can be visually illustrated in Figure 7.2.

Fixturing Stability Criteria

After obtaining the CSI, it is easy to check the fixturing stability. It requires that every locating point remain in contact with the workpiece surface. That is, at each locating point $CSI \geq 0$.

7.1.2.   Clamping Sequence and Stability

To solve a stability problem, we can treat all the locating points as contact points in the kinetic model, and combine the gravity force, clamping forces, and machining forces as a single external wrench.

However this scheme is only true if all the clamps are applied all at one time. When friction forces are taken into consideration, the stability problem becomes clamping sequence dependent. This is because when the clamps are applied one by one, the previously applied clamp also serves as a new contact point as the next clamp is applied.

From the kinetic model (Chapter 4), we know the stability problem is a linear system. Thus a multi-load stability problem can be decomposed into several independent stability problems. Each next step contains one more contact point from the previous step. And the final solution is the combination of all solutions from sub-steps.

For example, the stability problem shown in (Figure 7.3) can be decomposed into four sub-problems (Figure 7.4), each with its own contact points and external forces.
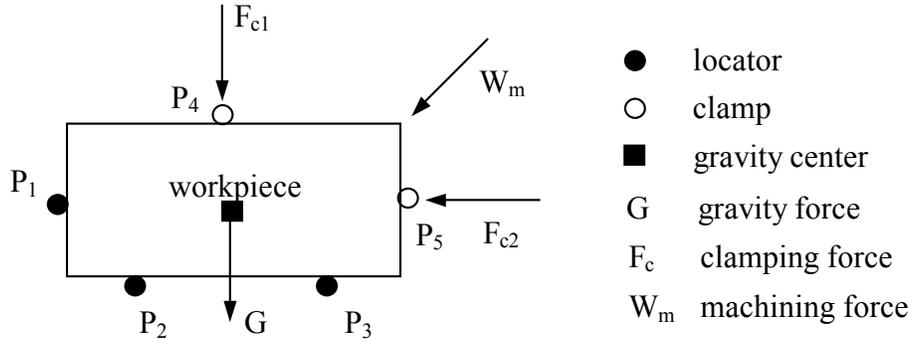
Figure 7.3 Multi-Load Stability Problem
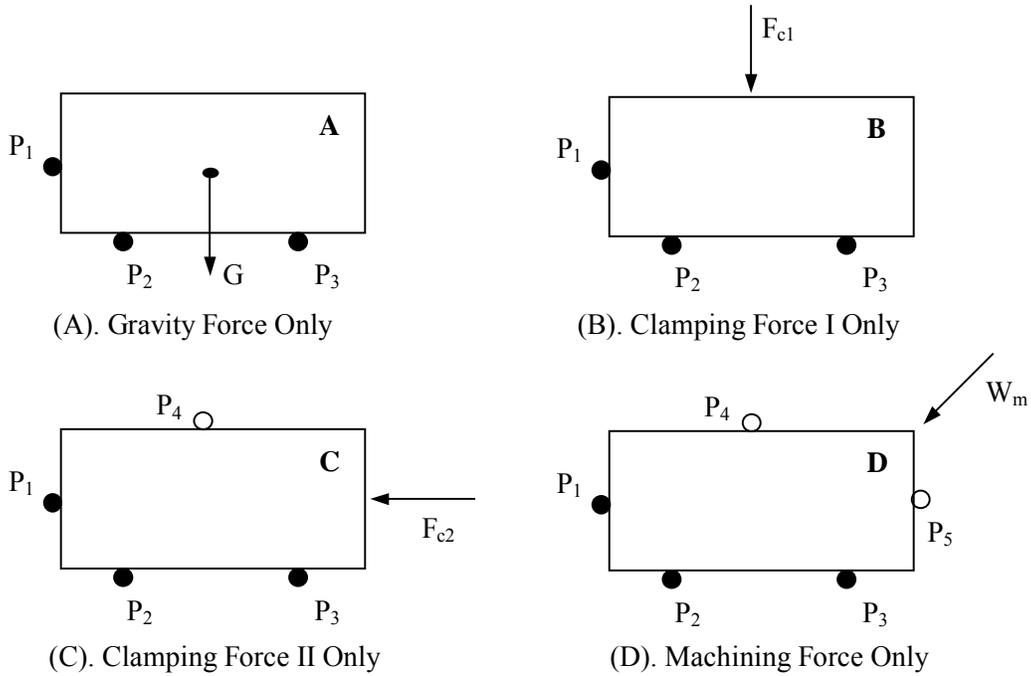
Figure 7.4 Stability Decomposition

In Step A (Figure 7.4-A), the workpiece is placed on the three locating points. In this step, these three locating points serve as the contact points, and the gravity force serves as the external force.

In Step B (Figure 7.4-B) clamping force F_{c1} is applied. The contact points are still the three locating points, and the external force is the clamping force F_{c1}.

In Step C (Figure 7.4-C), the clamping point from previous step becomes a new contact point. So there are total four contact points, and the external force is clamping force F_{c2}.

In Step D (Figure 7.4-D), there are total five contact points: three locating points and two clamping points. And the external force in this step is the machining force.

When checking the stability in each stage, the contact points displacements and reaction forces in LCS is the sum of those in current and all previous steps. In Figure 7.4, if the contact point displacement and reaction forces in each stage are $\{d_i^L\}$ and $\{f_i^L\}$ ($i = A, B, C, D$), then we have:

	Displacements in LCS	Reaction Forces in LCS
Step A	$\{d^L\} = \{d_A^L\}$	$\{f^L\} = \{f_A^L\}$
Step B	$\{d^L\} = \{d_A^L\} + \{d_B^L\}$	$\{f^L\} = \{f_A^L\} + \{f_B^L\}$
Step C	$\{d^L\} = \{d_A^L\} + \{d_B^L\} + \{d_C^L\}$	$\{f^L\} = \{f_A^L\} + \{f_B^L\} + \{f_C^L\}$
Step D	$\{d^L\} = \{d_A^L\} + \{d_B^L\} + \{d_C^L\} + \{d_D^L\}$	$\{f^L\} = \{f_A^L\} + \{f_B^L\} + \{f_C^L\} + \{f_D^L\}$

Table 7.1 Stability Decomposition

For a workpiece to be stable throughout the loading/fixturing/machining processes, it must be stable under each of the steps listed above.

7.2. Minimal Clamping Force

Some fixture designs rely on friction forces to stabilize the workpiece. In such cases, the clamping forces can be optimized (minimized) so that there is no excessive forces and unnecessary workpiece deformation.

The clamping forces are optimized by the following rule: if certain contact points are found to need larger normal force to maintain stable, all clamping forces will be searched and the "most helpful" clamping forces will be adjusted. And this is done through the CSI matrix.

7.2.1. CSI Matrix

Assume a fixture with m locating points (L1, …, Li, …, Lm) and n clamping points (C1, …, Cj, …, Cn). To evaluate the effect at locating point Li by clamping force at point Cj, we set a unit clamping force at Cj, and find out the CSI at Li α_{ij} by Equation 7.2. After finding CSI at all locating points by all clamping points, we get the CSI matrix as follows:

$$[C] = \begin{bmatrix} \alpha_{11} & \cdots & \alpha_{1j} & \cdots & \alpha_{1n} \\ \vdots & \ddots & & & \\ \alpha_{i1} & & \alpha_{ij} & & \\ \vdots & & & \ddots & \\ \alpha_{m1} & & & & \alpha_{mn} \end{bmatrix} \qquad (7.3)$$

α_{ij} shows how the jth clamp affects the ith locator stability. $\alpha > 0$ means the clamp is stabilizing the contact at the locating point, while $\alpha < 0$ means the clamp is causing slippage at the locating point (see CSI). Below is an illustrated table for the effects:

	Clamp 1	…	Clamp j	…	Clamp n
Locator 1	α_{11}	…	α_{1j}	…	α_{1n}
:	:		:		:
Locator i	α_{i1}	…	α_{ij}	…	α_{in}
:	:		:		:
Locator m	α_{m1}	…	α_{mj}	…	α_{mn}

Table 7.2 CSI Matrix

For example, the CSI matrix for the following 3-locator-2-clamp example would be:
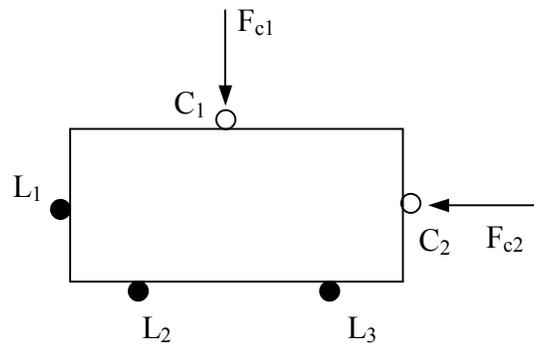
Figure 7.5 An Example of CSI Matrix

$$[C] = \begin{bmatrix} -0.25 & 1.0 \\ 1.0 & -0.5 \\ 1.0 & -0.5 \end{bmatrix}$$

From this CSI matrix, we can see clamping force at point C1 decreases contact stability at locating point L1 (-0.25), but increases it at L2 (1.0) and L3 (1.0); clamping force at point C2 increase contact stability at L1 (1.0) but decrease it at L2 (-0.5) and L3 (-0.5).

7.2.2. Minimal Clamping Forces

From the CSI matrix example in the last section, we can find how a clamping force affects the contact stability at each locating point.

After solving the stability equation, if we find the contact stability index (CSI) at locating point Li is less than zero, we will adjust the clamping forces according their CSI at point Li, and then re-solve the stability equation with adjusted clamping forces. This procedure is repeated until the workpiece is stable, or the maximal number of iteration reach, which means there is no solution for such case.

If the ith locating point is not stable, for each clamping point, its clamping force is adjusted by the following equation:

$$f = f_0 \cdot [1 + pos(C_{ij})] \quad (j = 1 \cdots n) \tag{7.4}$$

where,

· f_0 is the force before adjustment.

· f is the force after adjustment.

· $pos(x) = \begin{cases} x & x \geq 0 \\ 0 & x < 0 \end{cases}$

· C_{ij} is the element in CSI matrix at i^{th} row and j^{th} column.

An example, if there are 3 locating points and 3 clamping points, the CSI matrix would look like:

$$[C] = \begin{bmatrix} 0.25 & 1.0 & -0.5 \\ 1.0 & 0.0 & -0.5 \\ 1.0 & -0.5 & -0.25 \end{bmatrix}$$

If we found the CSI at locating point L1 is negative, we want to adjust the clamping forces by their CSI at this point (1st row in matrix), and we would:

· Increase clamping force at C1 by 25%;

· Increase clamping force at C2 by 100%;

· Keep clamping force at C3 unchanged.

The interval size can be adjusted to achieve best result.

7.3.   Summary

In this chapter, fixturing stability is defined as being stable (no slippage) at all contact points. Stability at each contact point is determined using the friction cone and CSI, and the force at the contact point can be calculated with the fixture kinetic model. For multi-clamp stability problems, clamping sequence is considered and the problem is decomposed into single clamp problems.

The CSI Matrix can be constructed with CSI at all contact points. Based on the CSI Matrix, the minimal clamping forces can be optimized.

Chapter 8.   Accessibility Analysis

When selecting a locating/clamping position on a workpiece surface, one important consideration is the ergonomics of the fixturing. If two locating positions (A and B) are both valid from tolerance and stability points of view (Figure 8.1), which one should be chosen as the best one? Obviously position B is better because it is more accessible by the locator. This chapter defines this accessibility for both positions on surface and a surface as a whole.
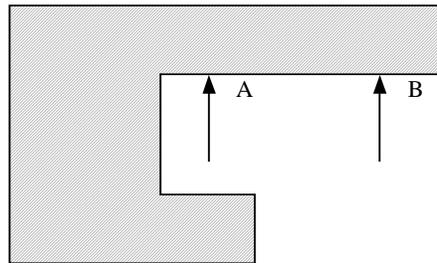
Figure 8.1 Accessibility Analysis

Fixturing accessibility is defined as the ease with which a locator or clamp approaches the fixturing point / surface. An obscured fixturing surface (which has lower accessibility) will result in difficulties of locating and clamping. The concept of accessibility can also be applied in search of locating surfaces and positions.

There are two types of accessibility. Point accessibility, which is used to evaluate how accessible a particular position on a surface, and surface accessibility, which is used to evaluate the overall accessibility of a surface.

Point accessibility is evaluated based on the Accessible Cylinder, a concept developed to describe the accessible area and directions near the point accessed. Surface accessibility is calculated using surface discretization method (Li et al., 1999). It is an overall evaluation of all discretized point accessibilities on that surface.

8.1.   Locator Bounding Cylinder

To implement the algorithm, the complicated locator geometry must be simplified for rapid evaluation. Here, the cylinder type bounding box (or bounding cylinder) is used to represent locators. Each locator is described using two parameters (Figure 8.2):

- R_L - Locator's bounding radius
- H_L - Locator's bounding height
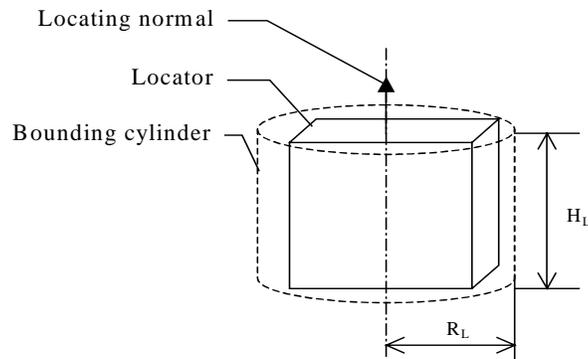
Figure 8.2 Locator Bounding Cylinder

8.2.   Accessible Height H_A

The accessible height H_A is defined as the distance from the locating position, along the surface normal direction at that position, to the point first blocked by the workpiece

geometry. This is illustrated in the following figure, H_{A1} and H_{A2} is the accessible heights for position A and B, respectively.
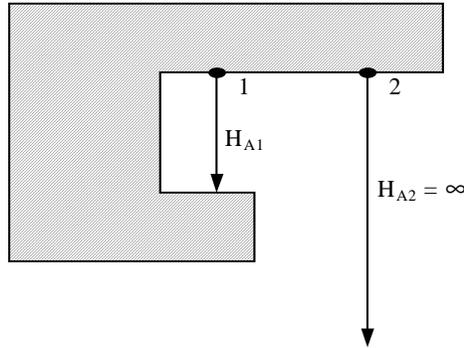
Figure 8.3 Accessible Height

Because position B has no obstruction along the normal direction, it would have the infinite accessible height. The infinite number will cause trouble in both accessible radius calculation (next section) and in computer implementation. So in order to eliminate the infinite, the accessible height's "satisfactory factor" K_H is introduced. The K_H is defined as following:

If $H_A > K_H \cdot H_L$, then let $H_A = K_H \cdot H_L$.

For example, if the designer thinks an accessible height of three times of the locator height is "very accessible", then $K_H = 3$. In computer implementation, K_H can be an option that allows user modification.

8.3.   Accessible Radius R_A

As with accessible height, the accessible radius R_A is defined in this section. The accessible radius R_A is defined as following:

If we construct a cylinder using the locating position's normal direction as the cylinder axis, and the satisfactory accessible height $(K_H \cdot H_L)$ as the cylinder height, the accessible radius R_A is the maximal radius the cylinder can be constructed without interfere with the workpiece geometry (Figure 8.4).
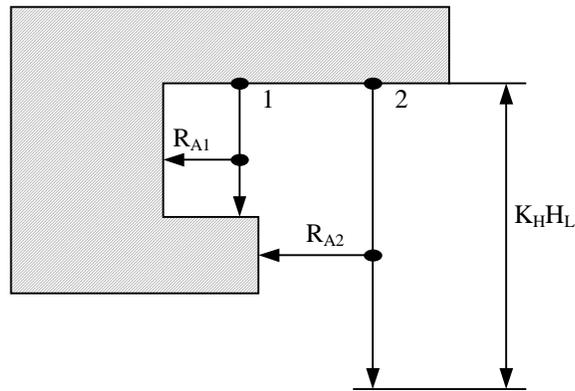
Figure 8.4 Accessible Radius

Similar to the accessible height, a "satisfactory factor" K_R is introduced:

If $R_A > K_R \cdot R_L$, then let $R_A = K_R \cdot R_L$.

8.4.   Accessible Cylinder

From the above sections, we can see that at a given locating position, a cylinder can be constructed using the accessible height H_A and the accessible radius R_A. This cylinder

illustrates the volume in 3D space that can be accessed by a locator, and it is called the "accessible cylinder". The volume of the accessible cylinder is essential for evaluating the accessibility of certain position, and its relation with the locator's bounding cylinder determines the accessibility.

In the next section, the accessibility of a point is calculated based on the concept of accessible cylinder.

8.5.   Point Accessibility A_P

Point accessibility A_P is the accessibility when a locator approaches a position on a workpiece surface. It is desirable that the point accessibility is normalized into range [0,1], so a designer can easily know the accessibility of certain position by looking at the value of accessibility. To achieve this, let's first look at some cases:

- If $\dfrac{H_A}{H_L} < 1$, which means the accessible height is less than the locator's bounding height, the position is not accessible, and the point accessibility A_P should have value 0.

- If $\dfrac{R_A}{R_L} < 1$, which means the accessible radius is less than the locator's bounding radius, the position is not accessible, and the point accessibility A_P should have value 0.

- If $\dfrac{H_A}{H_L} \geq K_H$ and $\dfrac{R_A}{R_L} \geq K_R$, which means the accessible height and accessible radius are both "satisfactory", the point accessibility A_P should have value 1.

Base on these observations, we can conclude the formula for calculating the point accessibility:

$$A_P = \frac{H_A - H_L}{(K_H - 1) \cdot H_L} \cdot \frac{R_A - R_L}{(K_R - 1) \cdot R_L}$$

(8.1)

This formula satisfies all the case above and normalized the point accessibility in the range of [0,1].

8.6. Surface Accessibility A_S

The calculation of Surface Accessibility A_S is similar as that of Li's et al., 1999. The surface is first discretized into grids (Figure 8.5).
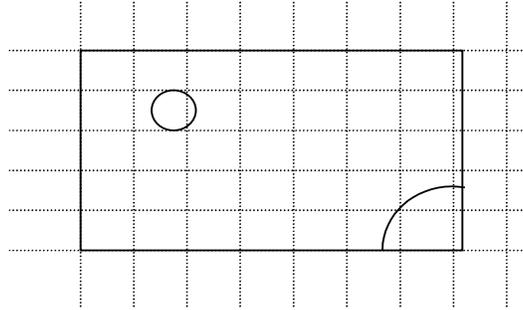
Figure 8.5 Surface Discretization

The point accessibility for the center point of each grid is calculated and the surface accessibility is the average of all point accessibility:

$$A_S = \frac{\sum_{i=1}^{n} A_{Pi}}{n}$$

(8.2)

Where n is the number of grids on a surface.

8.7.   Summary

Fixturing accessibility refers to the ease with which a locator or clamp approaches the fixturing surface/point. There are two types of accessibility – point accessibility and surface accessibility – for both a point and a surface.

The point accessibility is evaluated based on the volume of the "accessible cylinder" at this point. It depends on the accessible radius and height at the point, and on the bounding size of the locator/clamp. The surface accessibility is calculated based on all point accessibilities on that surface, using the surface discretization technique.

Chapter 9.　Algorithms

In previous chapters, the theoretical models for fixture verification have been created. However, without proper algorithms, theoretical models cannot be implemented by computer to generate solutions. Many theoretical solutions, if implemented improperly, would be too expensive for computing – they take too much time to get the results. In these cases, more efficient algorithms must be devised to shorten the computing time. This chapter lists several algorithms developed by this study for CAFDV, which are critical to the overall performance.

9.1.　Locator Layout Optimization

Locator layout optimization has been discussed in Section 5.2, and here the flowchart for locator layout optimization is presented (Figure 9.1).

```
                         ┌─────────────────┐
                         │      Start      │
                         └────────┬────────┘
                                  │
                                  ▼
    ┌──────────────────────────────────────────────────────────┐
    │  • Get locating surfaces and related locator type          │
    │  • Generate locating point initial positions               │
    │  • Determine searchable area for each locating point        │
    │  • Determine the constraints between locating points        │
    └──────────────────────────┬───────────────────────────────┘
                               │◄──────────────────────────────┐
                               ▼                                │
    ┌──────────────────────────────────────────────────────────┐│
    │Loop through each locating points:                          ││
    │  • Compare the LPI with LPIs when the point is at          ││
    │    one of four neighborhood positions                      ││
    │  • Place the locating point to the position with the       ││
    │    greatest LPI                                             ││
    └──────────────────────────┬───────────────────────────────┘│
                               ▼                                 │
         ╱─────────────────────────────────────╲       Y        │
        ⟨  Has any locating point been optimized  ⟩──────────────┘
         ╲         (repositioned)?              ╱
                               │ N
                               ▼
    ┌──────────────────────────────────────────────────────────┐
    │         Maximum LPI reached, stop optimization             │
    └──────────────────────────┬───────────────────────────────┘
                               ▼
    ┌──────────────────────────────────────────────────────────┐
    │                     Post Process                           │
    └──────────────────────────┬───────────────────────────────┘
                               ▼
                         ┌─────────────────┐
                         │      End        │
                         └─────────────────┘
```
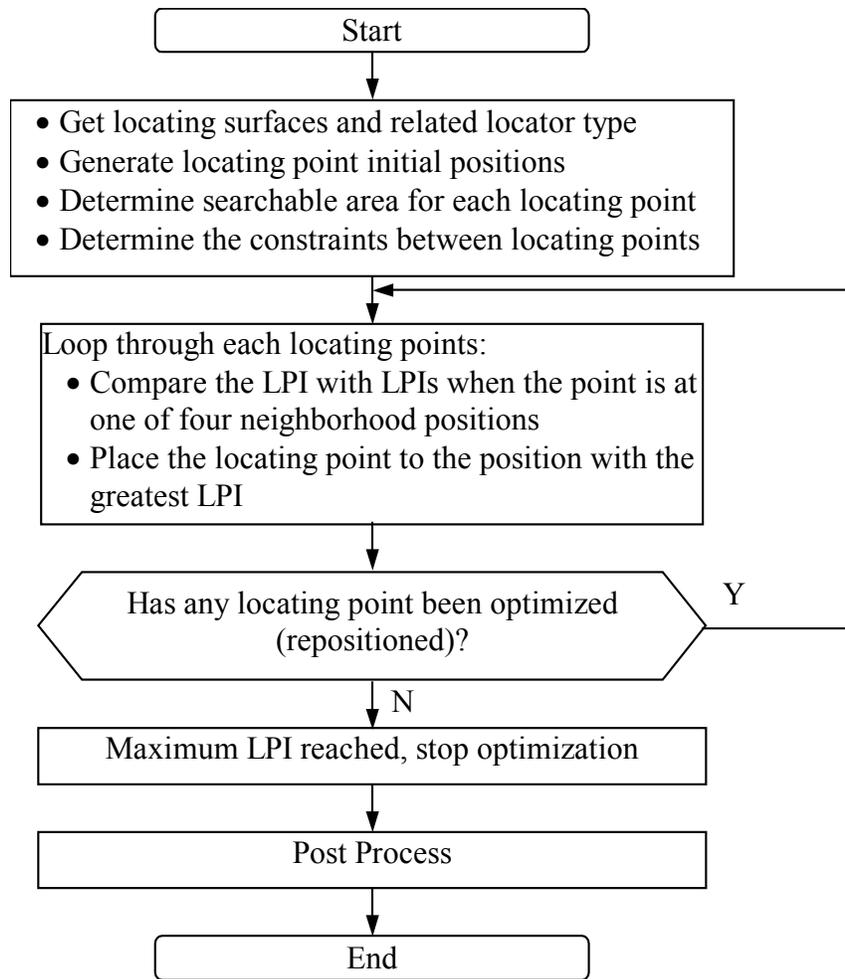
Figure 9.1 Layout Optimization Flowchart

9.2.   Machining Surface Accuracy Check

Machining surface accuracy check has been discussed in Section 6.3, and its flowchart is
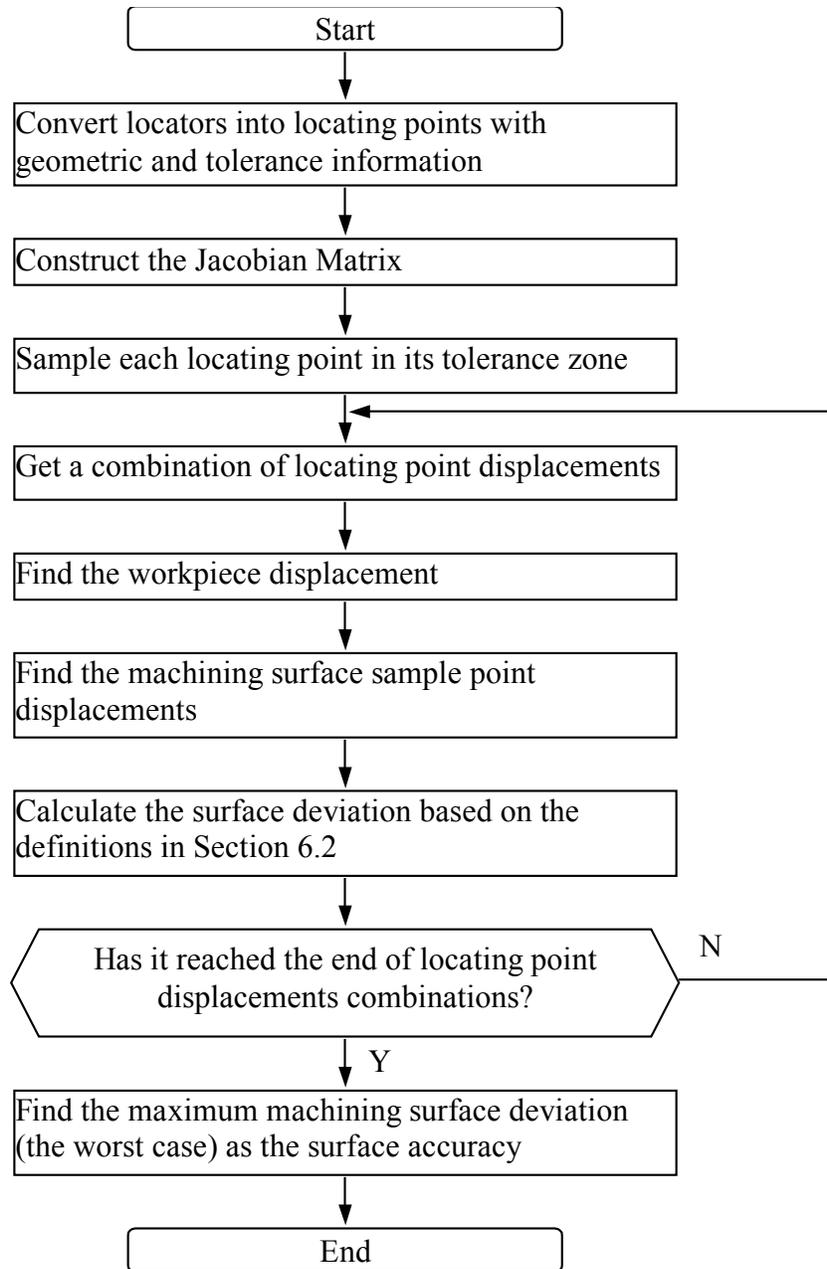
presented here (Figure 9.2).

```
                        ┌──────────────────┐
                        │      Start       │
                        └──────────────────┘
                                 │
                                 ▼
        ┌──────────────────────────────────────────────────┐
        │ Convert locators into locating points with       │
        │ geometric and tolerance information              │
        └──────────────────────────────────────────────────┘
                                 │
                                 ▼
        ┌──────────────────────────────────────────────────┐
        │ Construct the Jacobian Matrix                    │
        └──────────────────────────────────────────────────┘
                                 │
                                 ▼
        ┌──────────────────────────────────────────────────┐
        │ Sample each locating point in its tolerance zone │
        └──────────────────────────────────────────────────┘
                                 │
                                 ▼
        ┌──────────────────────────────────────────────────┐
        │ Get a combination of locating point displacements│
        └──────────────────────────────────────────────────┘
                                 │
                                 ▼
        ┌──────────────────────────────────────────────────┐
        │ Find the workpiece displacement                  │
        └──────────────────────────────────────────────────┘
                                 │
                                 ▼
        ┌──────────────────────────────────────────────────┐
        │ Find the machining surface sample point          │
        │ displacements                                    │
        └──────────────────────────────────────────────────┘
                                 │
                                 ▼
        ┌──────────────────────────────────────────────────┐
        │ Calculate the surface deviation based on the     │
        │ definitions in Section 6.2                       │
        └──────────────────────────────────────────────────┘
                                 │
                                 ▼
        ╱──────────────────────────────────────────╲   N
       ⟨    Has it reached the end of locating point  ⟩────┐
        ╲      displacements combinations?          ╱      │
                                 │ Y                        │
                                 ▼                          │
        ┌──────────────────────────────────────────────────┐│
        │ Find the maximum machining surface deviation     ││
        │ (the worst case) as the surface accuracy         ││
        └──────────────────────────────────────────────────┘│
                                 │
                                 ▼
                        ┌──────────────────┐
                        │       End        │
                        └──────────────────┘
```

Figure 9.2 Machining Surface Accuracy Check Flowchart

9.3. Jacobian Matrix Implementation

The Jacobian Matrix contains matrix inverse and derivative operations, thus efficient algorithm must be present to ensure the performance. The procedure of finding the Jacobian Matrix is detailed below.

9.3.1. Workpiece Location and Transformation Matrix

The workpiece location $\{q\} = \{\alpha, \beta, \gamma, x_w, y_w, z_w\}$ is a vector of six independent variables, each representing a degree of freedom of the workpiece. In operation, a 4×4 transformation matrix $[T]$ is used instead of using the q directly. The transformation matrix $[T]$ is calculated following the ZYX convention, which means:

- $[T]$ starts as a 4x4 identity matrix:

$$[T_1] = \begin{bmatrix} 1 & 0 & 0 & 0 \\ 0 & 1 & 0 & 0 \\ 0 & 0 & 1 & 0 \\ 0 & 0 & 0 & 1 \end{bmatrix}$$

- Rotate $[T]$ around X-axis by an angle of α

$$[T_2] = \begin{bmatrix} 1 & 0 & 0 & 0 \\ 0 & \cos\alpha & -\sin\alpha & 0 \\ 0 & \sin\alpha & \cos\alpha & 0 \\ 0 & 0 & 0 & 1 \end{bmatrix}$$

- Rotate $[T]$ around Y-axis by an angle of β

$$[T_3] = \begin{bmatrix} \cos\alpha & 0 & \sin\alpha & 0 \\ 0 & 1 & 0 & 0 \\ -\sin\alpha & 0 & \cos\alpha & 0 \\ 0 & 0 & 0 & 1 \end{bmatrix} \cdot [T_2]$$

- Rotate $[T]$ around Z-axis by an angle of γ

$$[T_4] = \begin{bmatrix} \cos\alpha & -\sin\alpha & 0 & 0 \\ \sin\alpha & \cos\alpha & 0 & 0 \\ 0 & 0 & 1 & 0 \\ 0 & 0 & 0 & 1 \end{bmatrix} \cdot [T_3]$$

- Translate [T] by vector (x_w, y_w, z_w)

$$[T_W] = \begin{bmatrix} 1 & 0 & 0 & x_w \\ 0 & 1 & 0 & y_w \\ 0 & 0 & 1 & z_w \\ 0 & 0 & 0 & 1 \end{bmatrix} \cdot [T_4]$$

By following the above procedures, the workpiece location can be represented as:

$$T_W = \begin{bmatrix} R_W & | & P_W \\ \hline 0 & | & 1 \end{bmatrix}$$

(9.1)

where,

$$R_w = \begin{bmatrix} cb \cdot cc & -ca \cdot sc + sa \cdot sb \cdot cc & sa \cdot sc + ca \cdot sb \cdot cc \\ cb \cdot sc & ca \cdot cc + sa \cdot sb \cdot sc & -sa \cdot cc + ca \cdot sb \cdot sc \\ -sb & sa \cdot cb & ca \cdot cb \end{bmatrix}$$

$$\{P_w\} = \{x_w, y_w, z_w\}^T$$

$$sa = \sin(\alpha) \quad sb = \sin(\beta) \quad sc = \sin(\gamma)$$
$$ca = \cos(\alpha) \quad cb = \cos(\beta) \quad cc = \cos(\gamma)$$

9.3.2. Transformation Matrix to Workpiece Location Conversion

In most CAD system, the workpiece location $\{q\} = \{\alpha, \beta, \gamma, x_w, y_w, z_w\}$ cannot be retrieved directly. Instead, the transformation matrix [T] representing the workpiece location is readily to be retrieved from CAD. Therefore the workpiece location $\{q\}$ needs

to be converted from transformation matrix [T]. Observing the transformation matrix in previous section allows us to get the workpiece location {q} as following:

$$x_w = T[0][3]$$

$$y_w = T[1][3]$$

$$z_w = T[2][3]$$

$$\alpha = arctan2(T[2][1], T[2][2])$$

$$\beta = arctan2\left(T[2][0], \frac{T[2][1]}{\sin(\alpha)}\right)$$

$$\alpha = arctan2(T[1][0], T[0][0])$$

Notes:

- The matrix index is 0-based, which mean the index in a 4x4 matrix would be 0-3.
- The function arctan2 (y, x) is used to return an angle in the range of [-PI, PI], it corresponds with the standard C/C++ function atan2 (y, x).

9.3.3. Inverse of Transformation Matrix

From the previous section we can see that the transformation matrix [T] is a function of the workpiece location {q}, $T_w = T_w(q) = T_w(\alpha, \beta, \gamma, x_w, y_w, z_w)$. So, once the workpiece location {q} is known, the inverse of the transformation matrix can be computed mathematically instead of numerically. This will greatly improve the computing performance. Here T_w^{-1} is constructed by reversing the procedures above:

- Translate [T] by vector $(-x_w, -y_w, -z_w)$
- Rotate [T] around Z-axis by an angle of $-\gamma$

- Rotate [T] around Y-axis by an angle of $-\beta$

- Rotate [T] around X-axis by an angle of $-\alpha$

The reversed matrix will be:

$$T_w^{-1} = \left[\begin{array}{c|c} R_w^r & P_w^r \\ \hline 0 & 1 \end{array} \right]$$

(9.2)

where,

$$R_w^r = R_w^{-1} = \begin{bmatrix} cb \cdot cc & cb \cdot sc & -sb \\ sa \cdot sb \cdot cc - ca \cdot sc & sa \cdot sb \cdot sc + ca \cdot cc & sa \cdot cb \\ ca \cdot sb \cdot cc + sa \cdot sc & ca \cdot sb \cdot sc - sa \cdot cc & ca \cdot cb \end{bmatrix}$$

(9.3)

$$P_w^r = -R_w^r \cdot P_w$$

(9.4)

We can see the inverse of the transformation matrix T_w^{-1} is also a function of the workpiece location q, $T_w^{-1} = T_w^{-1}(q) = T_w^{-1}(\alpha, \beta, \gamma, x_w, y_w, z_w)$. This is very nice since we can now get its derivatives over location q by direct computation instead of numerical approach.

9.3.4. Distance Between Locator and Locating Surface

The surface representation in workpiece local coordinate system (LCS):

$$f = Ax + By + Cz + D = n \cdot p = 0$$

(9.5)

where, (A, B, C) is the normalized surface normal direction, $n(A, B, C, D)$ is the surface parameter vector, $p(x, y, z, 1)$ is a point in 3-dimensional space, it is extended by adding a '1' at the end for matrix manipulation (Figure 9.3).
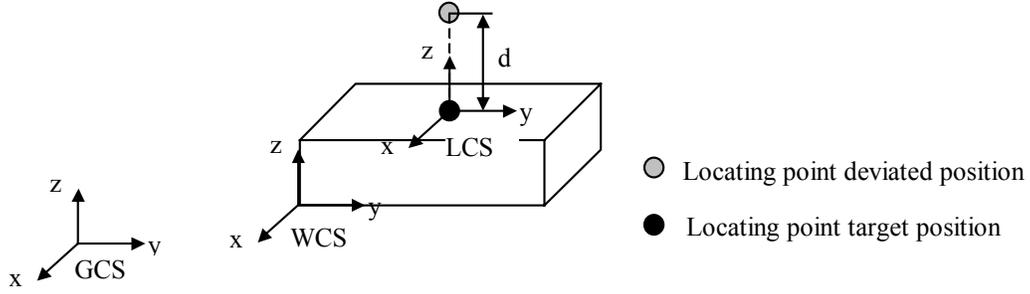
Figure 9.3 Distance Between Locating Point and Surface

If there is a point in workpiece LCS $p^L(x^L, y^L, z^L, 1)$, the distance from the point to the plane is:

$$d = Ax^L + By^L + Cz^L + D = n \cdot p^L \qquad (9.6)$$

Once the point in GCS $p^G(x^G, y^G, z^G, 1)$ and the workpiece location are know, the point in LCS $p^L(x^L, y^L, z^L, 1)$ can be calculated as:

$$p^L = T_w^{-1} \cdot p^G \qquad (9.7)$$

where T_w is the 4×4 transformation matrix representing the workpiece location. Thus, the distance from the point in GCS $p^G(x^G, y^G, z^G, 1)$ to the surface will be:

$$d = n \cdot p^L = n \cdot T_w^{-1} \cdot p^G \qquad (9.8)$$

From the earlier section we know T_w^{-1} is a function of workpiece location q,

$T_w^{-1} = T_w^{-1}(q) = T_w^{-1}(\alpha, \beta, \gamma, x_w, y_w, z_w)$, now we can see the distance d is also a function of

q, $d = d(q) = d(\alpha, \beta, \gamma, x_w, y_w, z_w)$.

9.3.5. Partial Derivatives of Workpiece Location

In constructing the Jacobian Matrix, the partial derivatives of the distance {d} over workpiece location {q} are to be calculated. From the previous section we can derive the derivatives symbolically:

$$d = n \cdot p^L = n \cdot T_w^{-1} \cdot p^G = n \cdot T_w^{-1}(\alpha, \beta, \gamma, x_w, y_w, z_w) \cdot p^G \tag{9.9}$$

$$\frac{\partial d}{\partial q} = \frac{\partial(n \cdot T_w^{-1} \cdot p^G)}{\partial q} = n \cdot \frac{\partial T_w^{-1}(\alpha, \beta, \gamma, x_w, y_w, z_w)}{\partial q} \cdot p^G \tag{9.10}$$

From the section (inverse of transformation matrix), we can derive the partial derivatives of the matrix symbolically:

$$T_w^{-1} = \left[\begin{array}{c|c} R_w^r & P_w^r \\ \hline 0 & 1 \end{array}\right] \Rightarrow \frac{\partial T_w^{-1}}{\partial q} = \left[\begin{array}{c|c} \partial R_w^r / \partial q & \partial P_w^r / \partial q \\ \hline 0 & 1 \end{array}\right] \tag{9.11}$$

By taking the derivatives of the inverse transformation matrix, we can get the derivatives for each variable in the workpiece location $q(\alpha, \beta, \gamma, x_w, y_w, z_w)$:

$$\begin{cases} \dfrac{\partial R_w^r}{\partial \alpha} = \begin{bmatrix} 0 & 0 & 0 \\ ca \cdot sb \cdot cc + sa \cdot sc & ca \cdot sb \cdot sc - sa \cdot cc & ca \cdot cb \\ -sa \cdot sb \cdot cc + ca \cdot sc & -sa \cdot sb \cdot sc - ca \cdot cc & -sa \cdot cb \end{bmatrix} \\ \dfrac{\partial P_w^r}{\partial \alpha} = -\dfrac{\partial R_w^r}{\partial \alpha} \cdot P_w \end{cases} \tag{9.12}$$

$$\begin{cases} \dfrac{\partial R_w^r}{\partial \beta} = \begin{bmatrix} -sb \cdot cc & -sb \cdot sc & -cb \\ sa \cdot cb \cdot cc & sa \cdot cb \cdot sc & -sa \cdot sb \\ ca \cdot cb \cdot cc & ca \cdot cb \cdot sc & -ca \cdot sb \end{bmatrix} \\ \dfrac{\partial P_w^r}{\partial \beta} = -\dfrac{\partial R_w^r}{\partial \beta} \cdot P_w \end{cases} \tag{9.13}$$

$$\begin{cases} \dfrac{\partial R_w^r}{\partial \gamma} = \begin{bmatrix} -cb*sc & cb*cc & 0 \\ -sa*sb*sc - ca*cc & sa*sb*cc - ca*sc & 0 \\ -ca*sb*sc + sa*cc & ca*sb*cc + sa*sc & 0 \end{bmatrix} \\ \dfrac{\partial P_w^r}{\partial \gamma} = -\dfrac{\partial R_w^r}{\partial \gamma} \cdot P_w \end{cases}$$

$$(9.14)$$

$$\begin{cases} \dfrac{\partial R_w^r}{\partial x_w} = \begin{bmatrix} 0 & 0 & 0 \\ 0 & 0 & 0 \\ 0 & 0 & 0 \end{bmatrix} \\ \dfrac{\partial P_w^r}{\partial x_w} = \begin{bmatrix} -(cb \cdot cc) & -(sa \cdot sb \cdot cc - ca \cdot sc) & -(ca \cdot sb \cdot cc + sa \cdot sc) \end{bmatrix}^{\mathrm{T}} \end{cases}$$

$$(9.15)$$

$$\begin{cases} \dfrac{\partial R_w^r}{\partial y_w} = \begin{bmatrix} 0 & 0 & 0 \\ 0 & 0 & 0 \\ 0 & 0 & 0 \end{bmatrix} \\ \dfrac{\partial P_w^r}{\partial y_w} = \begin{bmatrix} -(cb \cdot sc) & -(sa \cdot sb \cdot sc + ca \cdot cc) & -(ca \cdot sb \cdot sc - sa \cdot cc) \end{bmatrix}^{\mathrm{T}} \end{cases}$$

$$(9.16)$$

$$\begin{cases} \dfrac{\partial R_w^r}{\partial z_w} = \begin{bmatrix} 0 & 0 & 0 \\ 0 & 0 & 0 \\ 0 & 0 & 0 \end{bmatrix} \\ \dfrac{\partial P_w^r}{\partial z_w} = \begin{bmatrix} sb & -(sa \cdot cb) & -(ca \cdot cb) \end{bmatrix}^{\mathrm{T}} \end{cases}$$

$$(9.17)$$

After finding the partial derivatives of the transformation matrix, we can now substitute them back and get the partial derivatives of the distance.

9.3.6.   Jacobian Matrix

Now the Jacobian Matrix is finally ready to be constructed. By following the procedures in the previous sections, we can get all the derivatives of each locating point to its surface. Fill them in the Jacobian Matrix and we have:

$$[J] = \begin{bmatrix} \dfrac{\partial d_1}{\partial x_w} & \dfrac{\partial d_1}{\partial y_w} & \dfrac{\partial d_1}{\partial z_w} & \dfrac{\partial d_1}{\partial \alpha} & \dfrac{\partial d_1}{\partial \beta} & \dfrac{\partial d_1}{\partial \gamma} \\ \dfrac{\partial d_2}{\partial x_w} & \ddots & & & & \dfrac{\partial d_2}{\partial \gamma} \\ \vdots & & & & & \vdots \\ \dfrac{\partial d_m}{\partial x_w} & \cdots & & & & \dfrac{\partial d_n}{\partial \gamma} \end{bmatrix}$$

(9.18)

9.4.   Fixture Stiffness Matrix

The Fixture Stiffness Matrix is theoretically a large matrix. It is a 27x27 matrix for a fixture with six locating points and 3 clamping points. Matrices of such size could be very computing-expensive. Therefore a more efficient algorithm is required.

The major adaptation from pure methodology to computer implementation is the matrix operation. From the matrices listed in those equations, we can see that most matrices ($\left[R_G^L\right]$, $\left[k^L\right]$, $\left[R_G^L\right]^{-1}$) are diagonal and contain many zeros. So if we are able to compute at the contact point level, with only small matrices ($\left[R_{Gi}^L\right]$, $\left[k_i^L\right]$, $\left[R_{Gi}^L\right]^{-1}$), then we can significantly improve the computing efficiency by both eliminating void

operations (multiply by zeros) and avoiding large matrices that take large blocks of memory space.

By examining the procedures of establishing the equilibrium equation, we know that we can compute the extended stiffness matrix for each contact point [Ki] and then assemble them together to get the final extended stiffness matrix [K]. This procedure is presented by the following equation:

$$[K] = \sum [K_i]$$

(9.19)

$$[K_i] = -[\Sigma_i] \cdot \left[R_{Gi}^L\right] \cdot \left[k_i^L\right] \cdot \left[R_{Gi}^L\right]^{-1} \cdot [J_i]$$

(9.20)

where [K$_i$] is the individual extended stiffness matrix for contact point i.

9.5.   Tolerance Specification Optimization

Tolerance specification optimization finds the minimal requirements for locator tolerances. Because there are many possible locator tolerance combinations that satisfy the machining surface tolerance specification, it is impossible to distribute locator tolerances directly from machining surface tolerance. The algorithm used here is to try a set of locator tolerances first, and adjust the tolerances based on the output machining surface accuracy. A flowchart is shown in Figure 9.4.
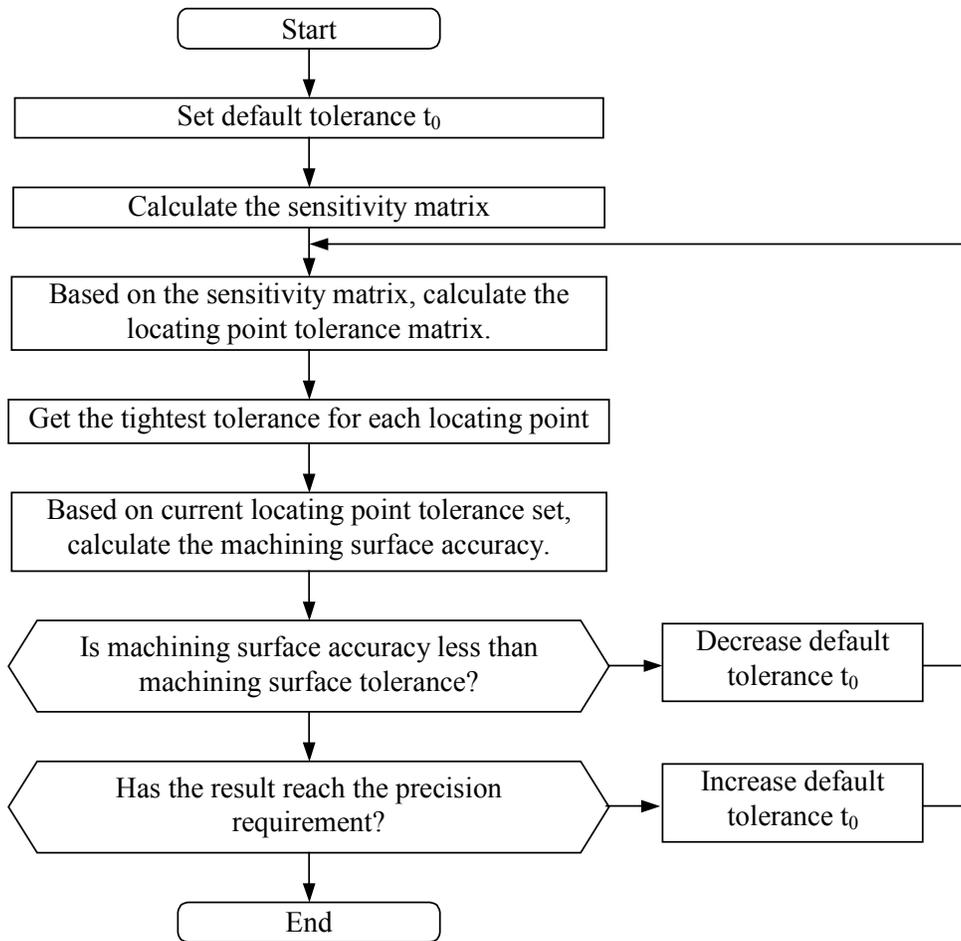
Figure 9.4 Tolerance Assignment Flowchart

Chapter 10. Case Studies and Software Design

In this chapter we will go through a case study with the CAFDV software developed, to demonstrate the methodologies discussed in earlier chapters.

10.1.   CAD Integration

CAFDV is integrated with CAD (in this case with I-DEAS 8), and Figure 10.1 shows the startup screen of the software.

I-DEAS Window   CAFDV Window
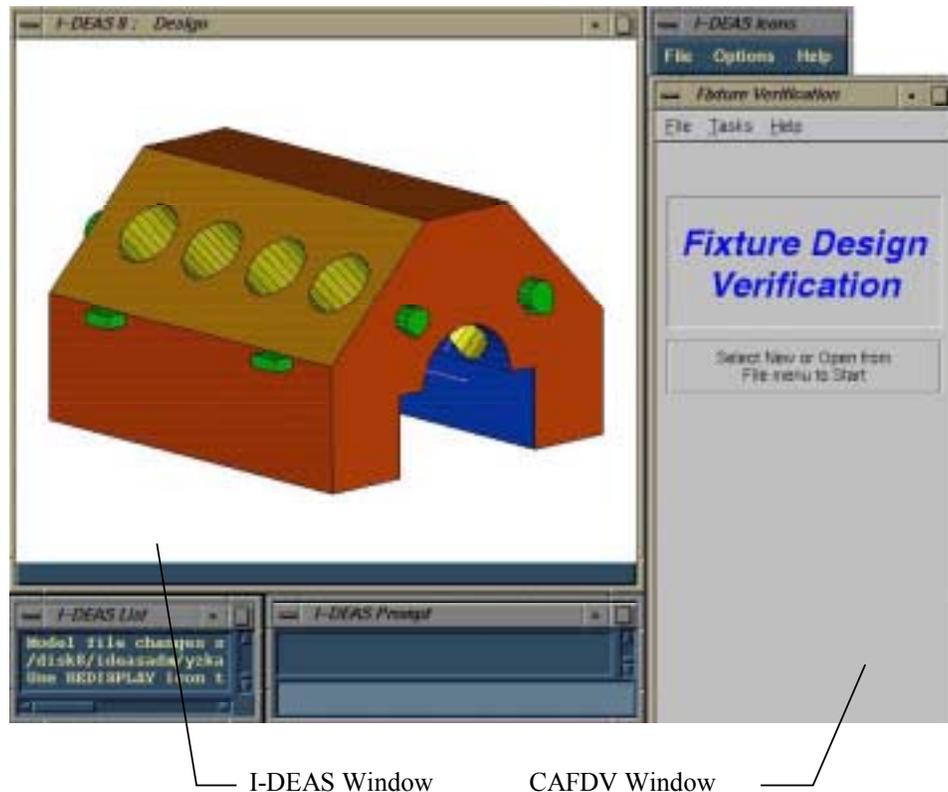
Figure 10.1 CAFDV CAD Integration – Startup Screen

10.2. Setup Information

The setup information for this case study is listed as follows.

Workpiece – The workpiece is a simplified V-8 engine block from a real case (Figure 10.2). It is position so that its WCS is coincident with GCS, in other words, the transformation matrix from WCS to GCS is a 4x4 identity matrix.
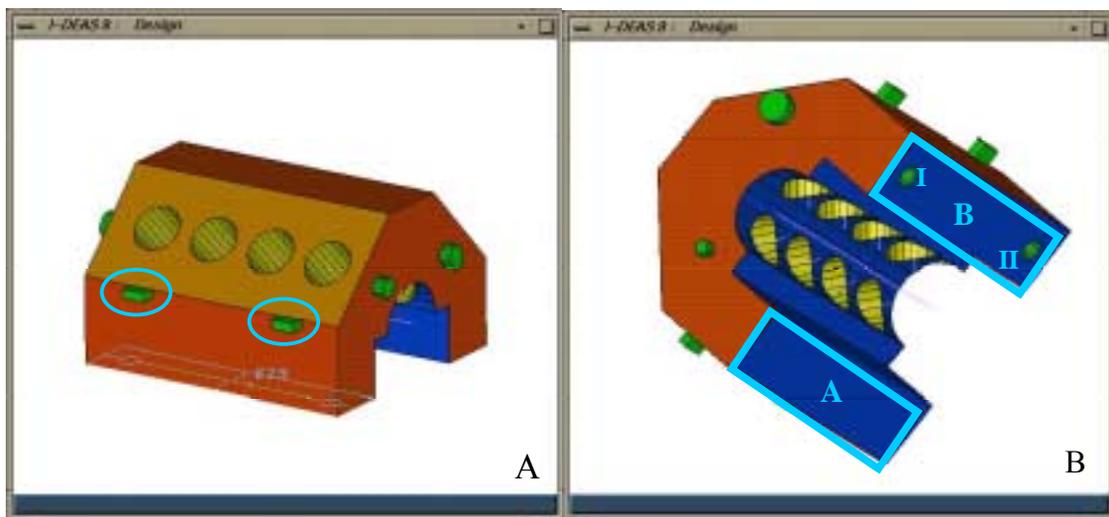
Figure 10.2 Case Setup Information

Machining Surfaces – The machining surfaces under this setup are the bottom surfaces of the four lugs on both sides of the engine block (as circled in Figure 10.2-A). Each machining surface has two tolerances – a surface profile of 0.08 and a parallelism of 0.04, with the bottom-locating surface as datum.

Locating Surfaces and Locators – There are two "point" type locators on surface A, and one "point" type locator on surface B. A "short round pin" locator and a "short diamond pin" locator are placed in the holes on surface B (Figure 10.2-B).

10.3. Locating Points

Users can choose locator type, set locator parameters, and pick locator position interactively with CAD system (Figure 10.3). There are five locators:

- · Locator 1 – "point" type locator, on surface A.
- · Locator 2 – "point" type locator, on surface A.
- · Locator 3 – "point" type locator, on surface B.
- · Locator 4 – "short-round pin" type locator, inside hole I on surface B.
- · Locator 5 – "short-diamond pin" type locator, inside hole II on surface B.
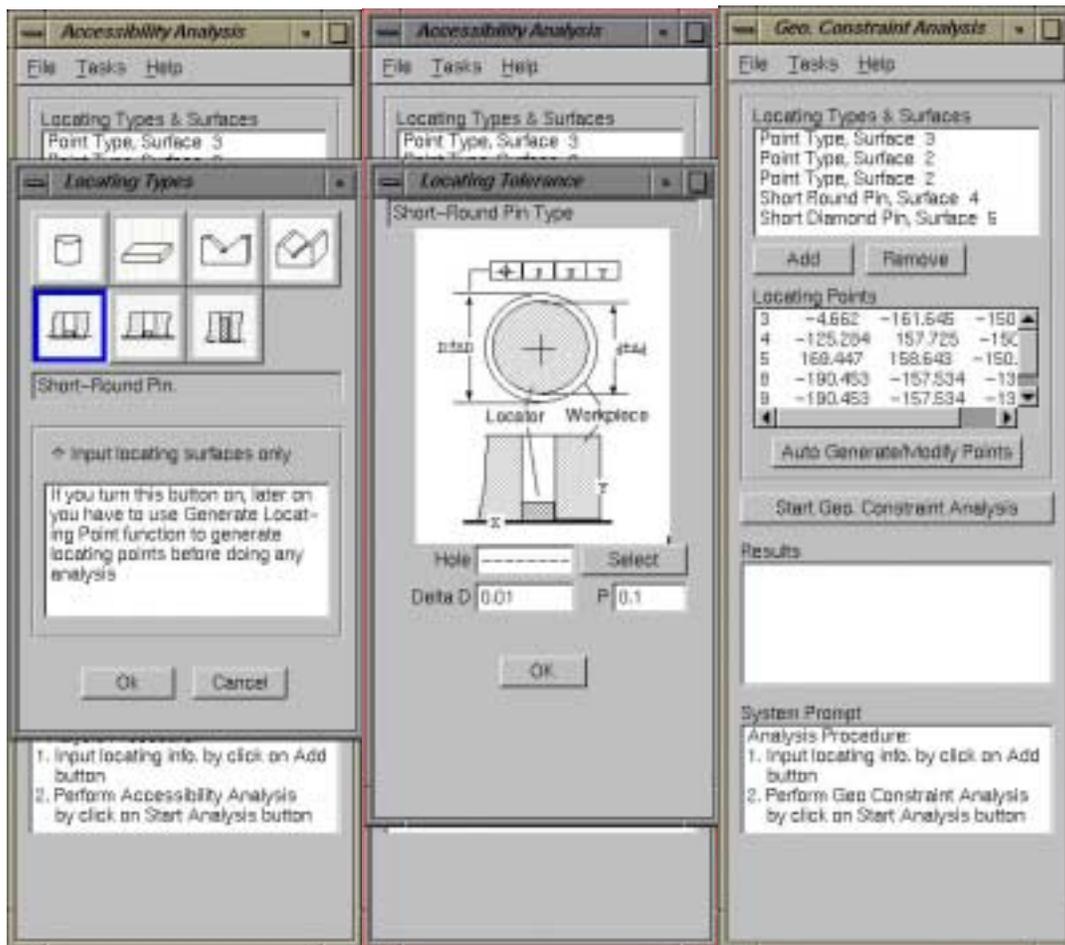
Figure 10.3 Locator Selection and Positioning

After locators are selected and positioned, they are converted into equivalent locating points. Below is the list of the six locating points converted from locators, including their position and surface normal direction.

Locating Points:

· Point 1 – from Locator 1

```
Position:  -1.2528e+02   1.5772e+02  -1.5000e+02
Normal:     0.0000e+00   0.0000e+00  -1.0000e+00
```

· Point 2 – from Locator 2

```
Position:   1.6945e+02   1.5864e+02  -1.5000e+02
Normal:     0.0000e+00   0.0000e+00  -1.0000e+00
```

· Point 3 – from Locator 3

```
Position:  -4.6620e+00  -1.6164e+02  -1.5000e+02
Normal:     0.0000e+00   0.0000e+00  -1.0000e+00
```

· Point 4 – from Locator 4

```
Position:  -1.9045e+02  -1.5753e+02  -1.3000e+02
Normal:    -1.0000e+00   0.0000e+00   0.0000e+00
```

· Point 5 – from Locator 4

```
Position:  -1.9045e+02  -1.5753e+02  -1.3000e+02
Normal:     0.0000e+00  -1.0000e+00   0.0000e+00
```

· Point 6 – from Locator 5

```
Position:   1.8977e+02  -1.5753e+02  -1.3000e+02
Normal:     0.0000e+00  -1.0000e+00   0.0000e+00
```

10.4. Jacobian Matrix and Locating Performance Index

Based on the workpiece location (in this case a 4x4 identity matrix), locating point positions and normal directions, the Jacobian Matrix can be computed as in Section 9.3. In this case, the Jacobian Matrix is:

```
0.0000e+00  0.0000e+00  1.0000e+00  1.5772e+02  1.2528e+02  0.0000e+00
0.0000e+00  0.0000e+00  1.0000e+00  1.5864e+02 -1.6945e+02  0.0000e+00
0.0000e+00  0.0000e+00  1.0000e+00 -1.6164e+02  4.6620e+00  0.0000e+00
1.0000e+00  0.0000e+00  0.0000e+00  0.0000e+00 -1.3000e+02  1.5753e+02
0.0000e+00  1.0000e+00  0.0000e+00  1.3000e+02  0.0000e+00 -1.9045e+02
0.0000e+00  1.0000e+00  0.0000e+00  1.3000e+02  0.0000e+00  1.8977e+02
```

The rank of this Jacobian Matrix is 6, indicating the workpiece is well constrained. The Locating Performance Index (LPI) can be calculated once the Jacobian Matrix is available, following procedures in Section 5.1:

LPI(1) = 3.58304e+007

If the locator layout changes so that locator 2 is closer to locator 1 at new position:

```
Position:   0.0000e+00   1.5864e+02  -1.5000e+02
Normal:     0.0000e+00   0.0000e+00  -1.0000e+00
```

The new LPI is then computed to be:

LPI(2) = 1.52546e+007

Comparing LPI(1) with LPI(2), we can see the previous layout has a greater LPI, thus better overall locating accuracy.

10.5. Locator Tolerance Assignment

To satisfy the two tolerances specifications of the machining surface, locator tolerances are assigned following the procedures discussed in Section 6.4. Below is the list of locator tolerances assigned. The notations are illustrated in Figure 10.4, as more details can be found in Appendix A.
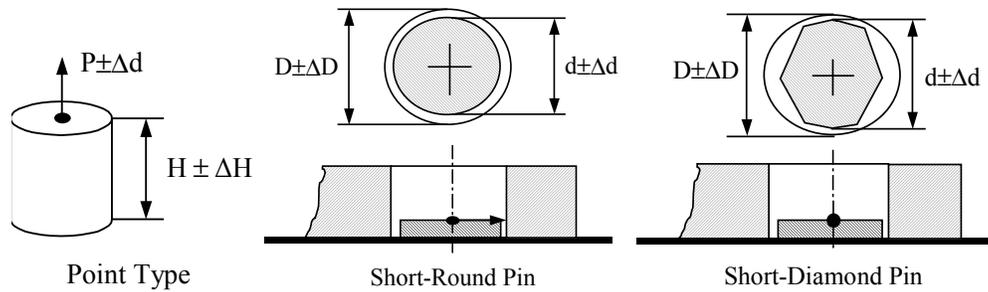
Figure 10.4 Locator Tolerances

- Locator 1 – "point" type locator.

    · Δh = 0.0193046

- Locator 2 – "point" type locator.

    · Δh = 0.0225628

- Locator 3 – "point" type locator.

    · Δh = 0.0128038

- Locator 4 – "short-round pin" type locator.

    · D = 34.0137 (from workpiece)

    · d = 33.9827

    · Δd = 0.0210339

    · ΔD = 0.01

- Locator 5 – "short-diamond pin" type locator.

    · D = 33.9791 (from workpiece)

    · d = 33.948

    · Δd = 0.0210339

    · ΔD = 0.01

10.6.   Machining Surface Accuracy Check

If the locator tolerances are known, we can also check the machining surface accuracy. If we use the tolerances assigned in the previous step to check the surface profile, we will get the profile as 0.0770921, which is slightly less than the specified 0.08. This result also validates the correctness of tolerance assignment.

If we change the tolerance of locator 1 from 0.0193046 to 0.15, and do the accuracy check again. This time the surface profile accuracy is calculated to be 0.0710263 (Figure 10.5). The result is in agreement with the fact that when the locator tolerance tightens, it provides higher machining accuracy.
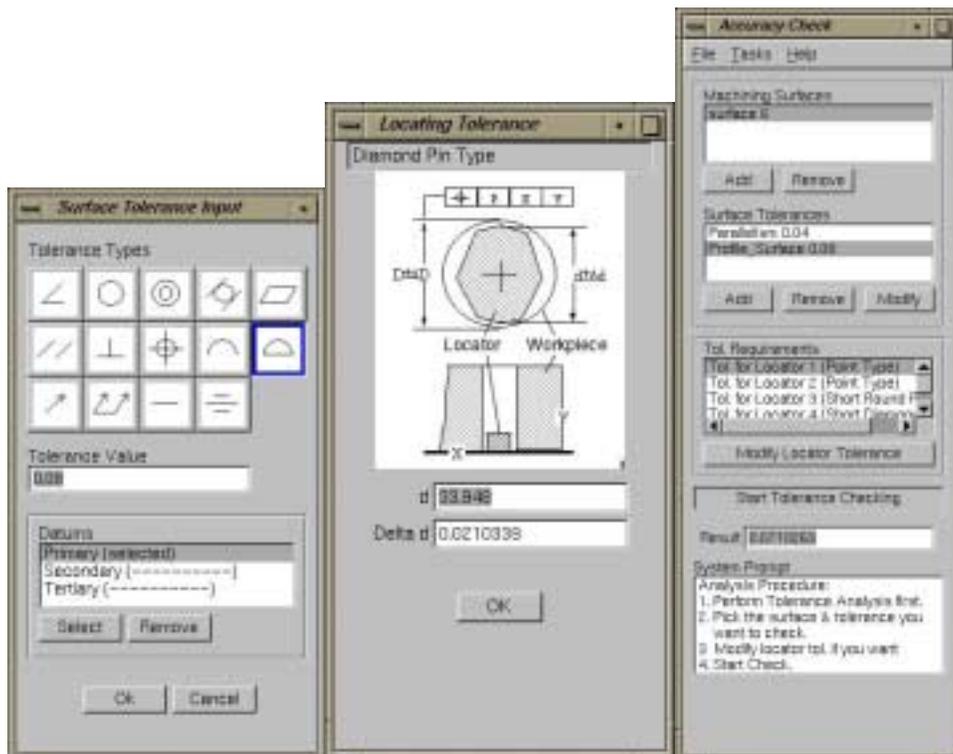
Figure 10.5 Tolerance Assignment and Accuracy Check

10.7.   Stability and Fixture Stiffness Matrix

Locators are converted into locating points, and their stiffness are converted as described in Appendix A. With locating point stiffness, the Fixture Stiffness Matrix can be constructed. In this case, it is:

```
-1.0000e+06  0.0000e+00  0.0000e+00  0.0000e+00  1.3000e+08 -1.5753e+08
 0.0000e+00 -2.0000e+06  0.0000e+00 -2.6000e+08  0.0000e+00  6.8000e+05
 0.0000e+00  0.0000e+00 -3.0000e+06 -1.5472e+08  3.9508e+07  0.0000e+00
 0.0000e+00 -2.6000e+08 -1.5472e+08 -1.0997e+11  7.8760e+09  8.8400e+07
 1.3000e+08  0.0000e+00  3.9508e+07  7.8760e+09 -6.1330e+10  2.0479e+10
-1.5753e+08  6.8000e+05  0.0000e+00  8.8400e+07  2.0479e+10 -9.7100e+10
```

The input cutting force is a series of forces in time, and the workpiece stability is solved at each time step. At each time step, the external forces include gravity force, clamping forces and cutting forces. The following is the cutting force data used in this case – there are total five steps, each step has position, direction and magnitude of the cutting force.

```
5

0.0 0.0 250
0.0 -1.0 0.0
1.0E+01

0.0 0.0 250
-1.0 0.0 0.0
2.0E+01

0.0 0.0 250
-1.0 0.0 0.0
3.0E+01

0.0 0.0 250
-1.0 0.0 0.0
4.0E+01

0.0 0.0 250
-1.0 0.0 0.0
3.0E+01
```

The reaction forces can be calculated following the discussion in Section 4.5. The reaction forces at each locating point are illustrated in the output chart (Figure 10.6).
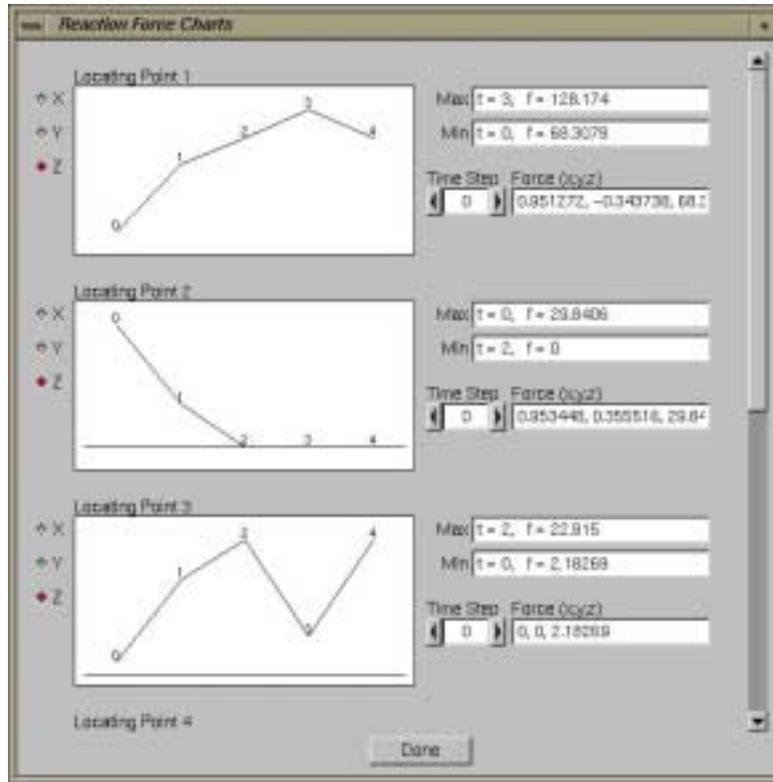
Figure 10.6 Reaction Force Chart

10.8. Software Architecture

A realistic and non-trivial problem facing CAFDV software design is the variety of today's CAD systems and operating systems. To maximize the portability of CAFDV among different CAD systems and operating systems and to minimize the maintaining cost, the CAFDV software is divided and capsulated into modules, so that the common modules can be reused as much as possible.

Figure 10.1 shows the diagram of the software architecture. The CAFDV software contains four modules (shaded in the figure), and each module is functionally self-contained. An arrow from module A to B indicates the dependency of module B on A.
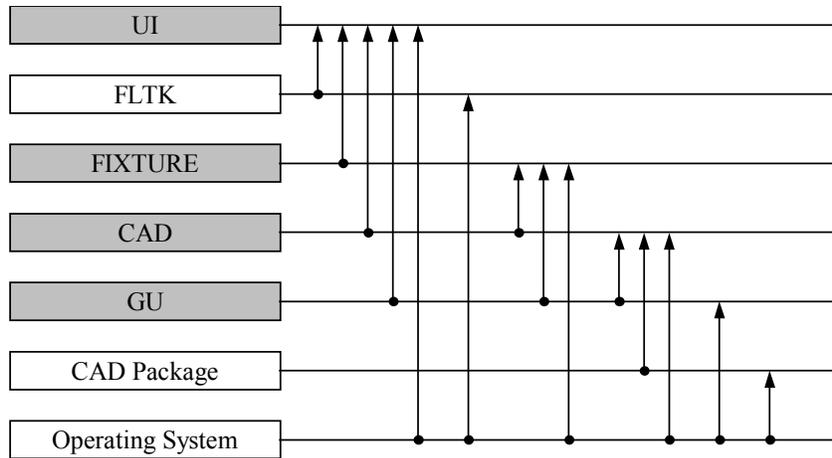
Figure 10.7 CAFDV Software Architecture

The table below lists the descriptions of all modules.

Module Name	Description
UI	Functions related to user interface, such as the windows, menu bars, dialog boxes etc.
FLTK	FLTK is a third party multi-platform user interface library.
FIXTURE	Functions related to fixture design algorithms, such as finding the Jacobian Matrix, tolerance assignment etc.
CAD	Functions related to CAD functions, such as selecting a surface interactively, getting the part name, mass center, etc.
GU	General Utilities. This is a set of functions as a utility library. It includes data structure, matrix, geometry and other utilities.
CAD Package	The API (application program interface) provided by CAD package (we used I-DEAS) to allow access to its geometry data.
Operating System	We used IRIX.

Table 10.1 CAFDV Software Modules

Chapter 11. Summary

This chapter gives a summary of this study. It includes two parts – contributions and future works.

11.1. Contributions

With two fixture models, four areas of applications, and the development of the software, this work presents the framework for the Computer-Aided Fixture Design Verification (CAFDV).

In this work, two fixture models – geometric and kinetic – are established. In the geometric model, the Jacobian Matrix links the workpiece displacement with locator displacements. In the kinetic model, the Fixture Stiffness Matrix links the external force with workpiece displacement and fixture deformation.

Four areas of applications are explored with the fixture models. 1). Locating performance analysis defines the Locating Performance Index (LPI), which can also be used to optimize the locator layout. 2). Tolerance analysis is able to predict the machining surface accuracy based on locator tolerances, and is able to assign the locator tolerances based on machining surface tolerance. Surface sensitivities on locators are defined for tolerance distribution. 3). Stability analysis defines the workpiece stability criteria with CSI, and a CSI matrix is used to find the minimal clamping forces. 4). Accessibility analysis defines the point and surface accessibility, which helps to improve ergonomics aspect of a fixture design.

For computer implementation, algorithms for the Jacobian Matrix and the Fixture Stiffness Matrix are listed, along with other algorithms and software design issues.

11.2. Future Works

Due to the scope of this study, it does not contain every possible area of CAFDV. Several possible areas for future study are listed below.

At system level, loading/unloading accessibility would be a complement application in addition to the three applications studied here. Loading/unloading accessibility measures the ease with which a workpiece can be loaded to or unloaded from the fixture. It had been studied by Asada (1985), and it is also an application of the geometric model.

At application level, current stability analysis is modeled as a static problem with rigid workpieces. Future studies include extending the current model into a dynamics problem, and taking into account the workpiece deformation. The workpiece deformation could be solved with FEA.

In current tolerance analysis application, machining surface error only includes that caused by locator manufacturing and positioning errors. It would be ideal to also include errors caused by workpiece and fixture deformation, which could be obtained from stability analysis. The tolerance analysis considering all above factors will generate more complete and accurate results.

References

[ANSI, 1995] American National Standard Institute, 1995, ANSI Y14.5M – 1994, Dimensioning and Tolerancing, The American Society of Mechanical Engineers, New York.

[Asada and By, 1985] Asada, H; By, A; "Kinematic Analysis of Workpart Fixturing for Flexible Assembly with Automatically Reconfigurable Fixtures", IEEE J. of Robotics and Automation, Vol. 1, 1985, pp. 86-94.

[Aspragathos and Dimitros, 1998] Aspragathos, N. A.; Dimitros, J. K.; "A Comparative Study of Three Methods for Robot Kinematics", IEEE Transactions on Systems, Man, and Cybernetics – Part B: Cybernetics, Vol. l. 28, No. 2, pp 135-145, April 1998.

[Bai Y. and Rong Y., 1995], Bai, Y; Rong, Y; "Establishment of modular fixture component assembly relationship for automated fixture design," Symposium on Computer-aided Tooling, ASME IMECE, San Francisco, CA, Nov. 12-17, MED-Vol. 2-1, pp. 805-816.

[Bicchi, 1995] Bicchi, A; "On the Closure Properties of Robotic Grasping", The International Journal of Robotics Research, Vol.14, No. 4, August 1995.

[Chang and Wysk, 1985] Chang, T. C.; Wysk, R. A.; "An Introduction to Automated Process Planning Systems", Englewood Cliffs, NJ: Prentice-Hall, 1985.

[Chen, 1995] Chen, Y. C.; "Proper Clamping Sequences in the Fixturing of Prismatic Workpieces," Proceedings of the IEEE International Symposium on Assembly and Task Planning, August 10-11, 1995, pp. 368-373.

[Chou et al., 1989] Chou, Y. C.; Chandru, V.; Barash, M. M.; "A Mathematical Approach to Automatic Configuration of Machining Fixtures: Analysis and Synthesis", Journal of Engineering for Industry, November 1989, Vol. 111, pp. 299-306.

[Chou, 1993] Chou, Y. C.; "Automated Fixture Design for Concurrent Manufacturing Planning," Concurrent Engineering: Research and Applications, Vol. 1, pp. 219-229.

[Choudhuri and DeMeter, 1999] Choudhuri, S.A.; De Meter, E.C.; "Tolerance analysis of machining fixture locators," Journal of Manufacturing Science and Engineering, Transactions of the ASME, Vol. 121, No. 2, 1999, pp. 273-281.

[Cogun, 1992], Cogun, C.; "Importance of the Application Sequence of Clamping Forces on Workpiece Accuracy," Journal of Engineering for Industry, Transactions of the ASME, Vol. 114, No. 4, Nov 1992, pp. 539-543.

[DeMeter, 1998] DeMeter, E. C.; "Fast Support Layout Optimization," International Journal of Machine Tools & Manufacture, Vol. 38, No. 10-11, October-November 1998, pp. 1221-1239.

[Elber, 1994] Elber, G.; "Accessibility in 5-Axis Milling Environment," Computer-Aided Design, Vol. 26, No. 11, pp. 196-202.

[Hu and Rong, 2000] Hu, W.; Rong, Y.; "Fast Interference Checking Algorithm for Automated Fixture Design Verification," International Journal of Advanced Manufacturing Technology, Vol. 16, No. 8, 2000, pp. 571-581.

[Huang et al, 1997] Huang, S. H.; Zhang, H.C.; Oldham W. J. B.; "Tolerance Analysis for Setup Planning: A Graph Theoretical Approach", International Journal of Production Research, Vol. 35, No. 4, 1997, pp. 1107-1124.

[Huang, 1998] Huang, S. H.; "Automated Setup Planning for Lathe Machining", Journal of Manufacturing System, Vol. 17, No. 3, 1998, pp. 196-208.

[Jayaram et al, 2000] Jayaram, S.; El-Khasawneh, B.S.; Beutel, D. E.; "Fast Analytical Method to Compute Optimum Stiffness of Fixturing Locators," CIRP Annals - Manufacturing Technology, Vol. 49, No. 1, 2000, pp. 317-320.

[Joneja and Chang, 1999] Joneja, A.; Chang, T. C.; "Setup and Fixture Planning in Automated Process Planning Systems", IIE Transactions, Vol. 31, 1999, pp. 653-665.

[Kashyap and DeVries, 1999] Kashyap, S.; DeVries, W. R.; "Finite Element Analysis and Optimization in Fixture Design," Structural Optimization, Vol. 18 No. 2-3 October 1999, pp. 193-201.

[King and Ling, 1995] King, L. S.; Ling, F.; "Force analysis based analytical framework for automatic fixture configuration," American Society of Mechanical Engineers,

Manufacturing Engineering Division, MED v 2-1, November 12-17, 1995, pp. 789-800.

[Laperriere and ElMaraghy, 2000] Laperriere, L; ElMaraghy, H. A.; "Tolerance Analysis and Synthesis Using Jacobian Transforms", Annals of the CIRP, Vol. 49, January 2000, pp 317-320.

[Lee and Cutkosky, 1991] Lee, S. H. and Cutkosky, M. R.; "Fixture Planning with Friction," Journal of Engineering for Industry, Vol. 113, 1991, pp. 320-327.

[Li et al., 1999] Li, J.; Ma W; Rong, Y; "Fixturing Surface Accessibility Analysis for Automated Fixture Design", Int. J. of Production Research, 1999, Vol. 37, No. 13, pp. 2997-3016.

[Ma et al., 1999] Ma, W.; Li, J.; Rong, Y.; "Development of automated fixture planning systems," International Journal of Advanced Manufacturing Technology, Vol 15, No. 3, 1999, pp. 171-181.

[Lim and Menq, 1994] Lim, C. P.; Menq, C. H. "CMM Feature Accessibility and Path Generation", International Journal of Production Research, 1994, Vol. 32, No. 3, pp. 597-618.

[Ohwovoriole, 1981] Ohwovoriole, M. S.; (1981), "An Extension of Screw Theory", Journal of Mechanical Design, October 1981, Vol. 103, pp 725-735.

[Ong and Nee, 1998] Ong, S. K.; Nee, A. Y. C.; "Systematic Approach for Analyzing the Fixturability of Parts for Machining," Journal of Manufacturing Science and Engineering, Transactions of the ASME, Vol. 120, No. 2, May 1998, pp. 401-408.

[Rong et al., 1994] Rong, Y.; Wu, S.; Chu, T. P.; "Automated Verification of Clamping Stability in Computer-Aided Fixture Design", Computers in Engineering, Proceedings of the International Conference and Exhibit v /1, September 1994, pp. 421-426.

[Rong et al., 1995a] Rong, Y.; Liu, X.; Wen, A.; "Computer-Aided Setup Planning and Fixture Design", Int. J. of Intelligent Automation and Soft Computing, Vol. 3, No. 3, 1997, pp. 191-206; partially presented at 27th CIRP Int. Seminar on Manufacturing Systems, Ann Arbor, MI, May 1995.

[Rong et al., 1995b] Rong, Y.; Li, W.; Bai, Y.; "Locator Error Analysis for Fixturing Accuracy Verification", ASME Computer in Engineering, Boston, MA, September 1995, pp. 825-832.

[Rong and Bai, 1996] Rong, Y.; Bai, Y.; "Machining Accuracy Analysis for Computer-Aided Fixture Design", J. of Manufacturing Science and Engineering, Vol. 118, August 1996, pp. 289-300.

[Rong and Zhu, 1999] Rong, Y; Zhu, Y; "Computer-Aided Fixture Design", Marcel Dekker Inc., NY, 1999.

[Sakurai, 1992] Sakurai, H.; "Automatic Setup Planning and Fixture Design for Machining," Journal of Manufacturing Systems, Vol. 11, No. 1, 1992, pp. 30-37.

[Shimoga, 1996] Shimoga, K. B. "Robot Grasp Synthesis Algorithms: A Survey". The International Journal of Robotics Research. Vol. 15, No. 3, June 1996, pp. 230-266.

[Sugar and Kumar, 2000] Sugar, T. G.; Kumar, V.; "Metrics for Analysis and Optimization of Grasps and Fixtures," Proceedings - IEEE International Conference on Robotics and Automation, Vol. 4, April 2000, pp. 3561-3566.

[Trappey and Liu, 1992] Trappey, A. J. C.; Liu, C. R.; "Automatic Workholding Verification System", Robotics and Computer-Integrated Manufacturing, Vol. 9, No. 4-5, August-October 1992, pp. 321-326.

[Trappey et al., 1995] Trappey, A. J. C.; Su, C. S.; Hou, J. L.; "Computer-Aided Fixture Analysis Using Finite Element Analysis and Mathematical Optimization Modeling," American Society of Mechanical Engineers, Manufacturing Engineering Division, MED v 2-1, November 12-17, 1995, pp 777-787.

[Wang, 1999] Wang, M. Y.; "Automated Fixture Layout Design for 3D Workpieces," Proceedings - IEEE International Conference on Robotics and Automation, v 2, May 10-5 1999, pp. 1577-1582.

[Wu et al., 1995] Wu, N. H.; Chan, K. C.; Leong, S. S.; "Fixturing Verification Based On the Analysis of Multi-Discipline Frictional Contacts", American Society of

Mechanical Engineers, Manufacturing Engineering Division, MED v 2-1, November 12-17, 1995, pp. 735-744.

[Xiong, 1993] Xiong, Y. L.; "Theory and Methodology for Concurrent Design and Planning of Reconfiguration Fixture," Proceedings - IEEE International Conference on Robotics and Automation, Vol. 3, May 2-6, 1993, pp. 305-311.

[Xiong and Xiong, 1998] Xiong, C.; Xiong, Y.; "Stability Index and Contact Configuration Planning for Multifingered Grasp", Journal of Robotic Systems, Vol. 15, No. 4, 1998, pp. 183-190.

[Xiong et al., 1999] Xiong, C.; Li, Y.; Xiong, Y; Ding, H.; Huang, Q; "Grasp Capability Analysis of Multifingered Robot Hands", Robotics and Autonomous Systems, Vol. 27, 1999, pp. 211-224.

[Xiuwen et al., 1996] Xiuwen, G.; Fuh, J. Y. H.; Nee, A. Y. C.; "Modeling of Frictional Elastic Fixture-Workpiece System for Improving Location Accuracy," IIE Transactions (Institute of Industrial Engineers), Vol. 28, No. 10, October 1996, pp. 821-827.

[Zhang et al., 1995] Zhang, Y. F.; Nee, A. Y. C.; Ong; S. K.; "A Hybrid Approach for Set-up Planning", International Journal of Advanced Manufacturing Technology, Vol. 10, 1995, pp. 183-190.

Appendix A.   Locators and Locating Points

There exist many types of locators in fixture design, and each with its unique geometry and other properties. It is desirable for the fixture models to handle different types of locators regardless of their detailed geometry, and be extended to include other types.

For this purpose, locators are abstracted in the analysis process as points only. Since the contact between locator and workpiece is the most important function for locators, they are converted into equivalent locating points. A locator and its equivalent locating points constrain the same number of DOFs of the workpiece, provide the same accuracy, and have the same stiffness.

A.1.   Geometry Conversion

The conversion of geometry information (position and normal direction) between locators and locating points is shown in Figure A.1. The number of locating points associated with a locator equals the number of DOFs of the workpiece constrained by the locator. Currently seven commonly used locators are included in the work. More locator types can be added in similar procedures.

Point Type	Plane Type	Short V	Long V
Short Round Pin	Short Diamond Pin	Long Round Pin	
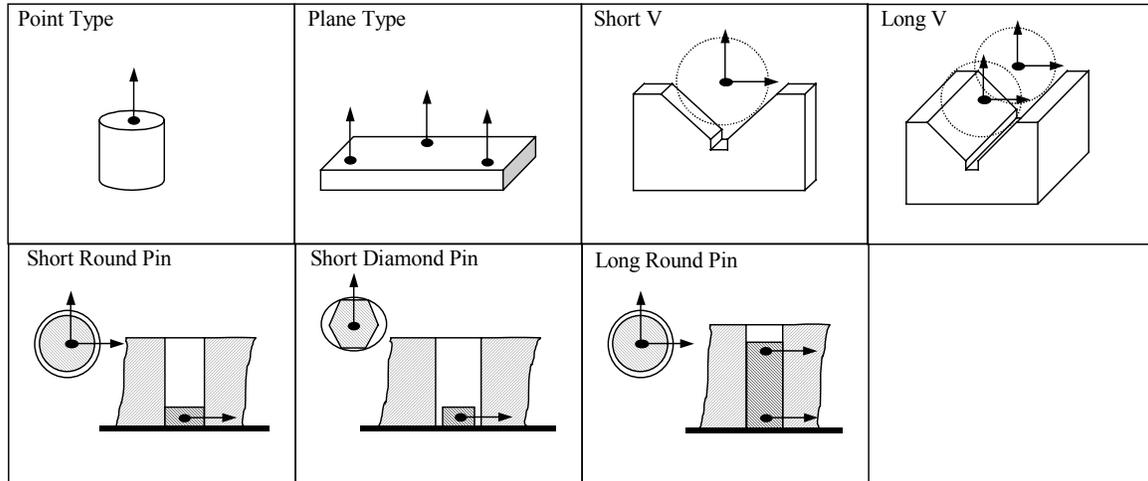
Figure A.1. Locator Types and Locating Points

In Figure A.1, each locating point is represented by a position and a normal direction. There are cases that two locating points share the same position but have different normal directions.

The conversion of tolerance and stiffness between locators and locating points is more complicated, as discussed in the following sections.

A.2.   Tolerance Conversion

Tolerance verification checks the machining surface accuracy, with the given locator tolerances. Those locator tolerances need to be converted into locating point tolerances first, before they can be used for calculating machining surface deviation. On the other hand, when doing the locator tolerance assignments, the tolerance for each locating point is first assigned, and it needs to be converted into locator tolerance to be understood by design engineers.

Each locator has different types of tolerances, and each locating point has a tolerance along its normal direction ($\pm\Delta d$). Conversions between locator and locating point tolerance are listed below.

A.2.1.　Point Type

- $\Delta d = \Delta H$
- $\Delta H = \Delta d$

A.2.2.　Plane Type

- $\Delta d_1 = \Delta d_2 = \Delta d_3 = F$
- $F = \min\{\Delta d_1 \quad \Delta d_2 \quad \Delta d_3\}$
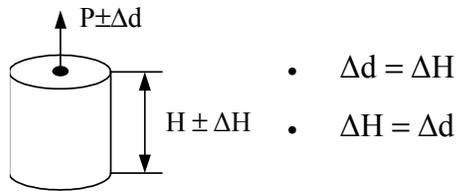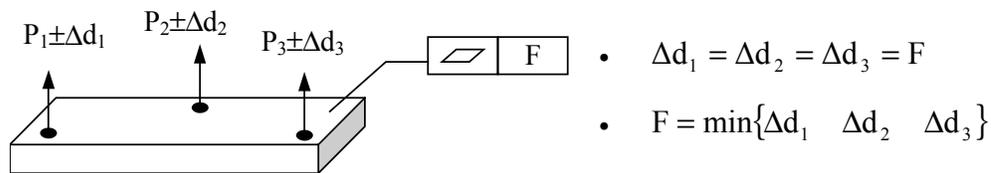
A.2.3.　Short-V Type (V-Pad) and Long-V Type (V-Block)

$$\begin{cases} \Delta d_{1(3)} = \Delta H + \dfrac{\Delta D \cdot \sin(\alpha/2)}{2} + \dfrac{\Delta D \cdot \cos(\alpha/2) \cdot \Delta\alpha}{4 \cdot [1 - \cos^2(\alpha/2)]} \\ \Delta d_{2(4)} = \Delta W \end{cases}$$

$$\begin{cases} \Delta H = t \cdot \sin(\alpha/2) \\ \Delta W = t \cdot \cos(\alpha/2) \\ \Delta\alpha = t/D \\ \text{where,} \quad t = \min\{\Delta d_1 \quad \Delta d_2\}/3 \end{cases}$$
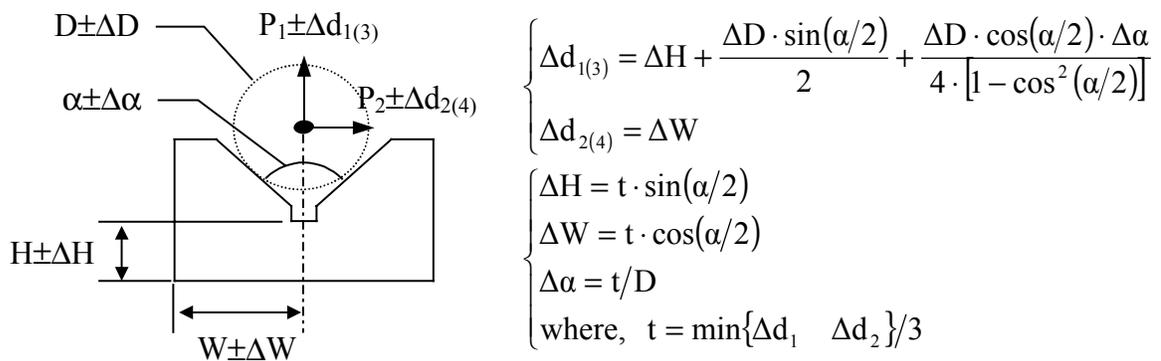
A.2.4. Short Round Pin Type

$$\Delta d_1 = \Delta d_2 = \frac{\Delta D + \Delta d}{2}$$

$$\begin{cases} d = D - \Delta D - t/2 \\ \Delta d = t/2 \\ \text{where,} \quad t = \min\{\Delta d_1 \quad \Delta d_2\} \times 2 - \Delta D \end{cases}$$
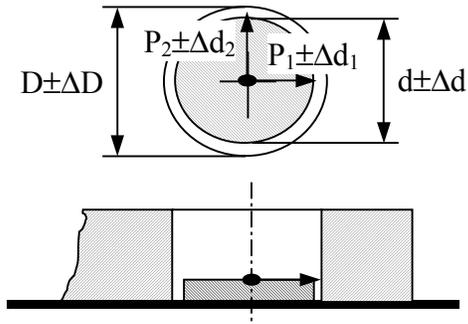
A.2.5. Short Diamond Pin Type

$$\Delta d_1 = \Delta d_2 = \frac{\Delta D + \Delta d}{2}$$

$$\begin{cases} d = D - \Delta D - t/2 \\ \Delta d = t/2 \\ \text{where,} \quad t = \min\{\Delta d_1 \quad \Delta d_2\} \end{cases}$$
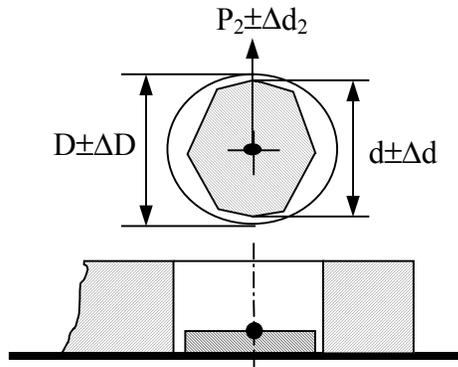
A.2.6. Long Pin Type
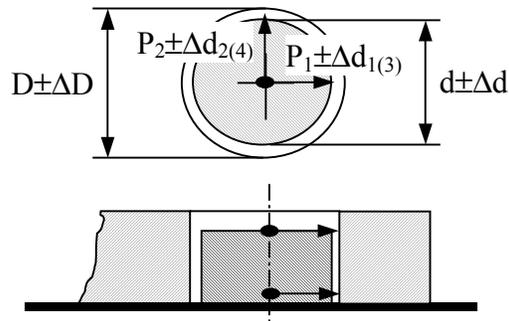
$$\Delta d_1 = \Delta d_2 = \Delta d_3 = \Delta d_4 = \frac{\Delta D + \Delta d}{2}$$

$$\begin{cases} d = D - \Delta D - t/2 \\ \Delta d = t/2 \\ \text{where,} \quad t = \min\{\Delta d_1 \quad \Delta d_2 \quad \Delta d_3 \quad \Delta d_4\} \times 2 - \Delta D \end{cases}$$

A.3.   Stiffness Conversion

For a locator or a clamp, its stiffness is determined by its geometry and material. The stiffness for each locator type is determined using FEA method. The FEA data is listed in the next section, and below is the list of stiffness for each type of locator

In the FEA analysis, the material selected is carbon tool steel, with an elastic modulus of 29E6 psi, a shear modulus of 12E6 psi, and a Poisson's ratio of 0.32. A 10-node tetrahedral element, SOLID92 is used for the locators and clamps.

A.3.1.   Point Type
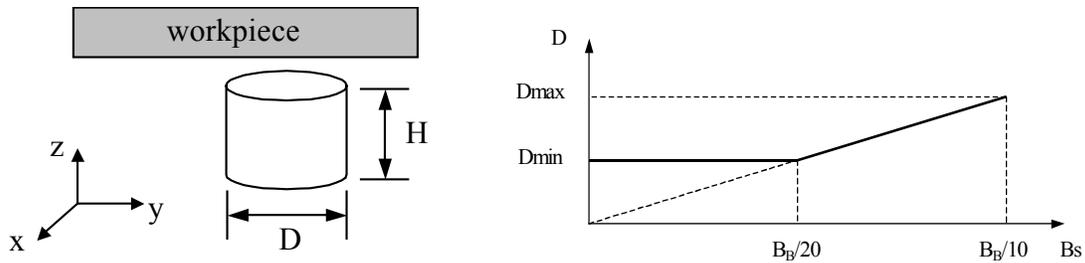
$$D = \begin{cases} D_{min} & B_S \leq B_B/2 \\ B_S/10 & B_B/2 \leq B_S \leq B_B \\ D_{max} & B_S = B_B \end{cases}$$

$$H = D$$

where,

- Bs – Smaller edge length of locating surface bounding box.
- B_B – Largest edge length of workpiece bounding box.
- $D_{min} = B_B/20$
- $D_{max} = B_B/10$

$$\text{Stiffness - } \begin{cases} S_z = 1.60E + 07 \cdot D \\ S_x = S_y = 2.58E + 06 \cdot D \end{cases}$$

A.3.2. Plane Type
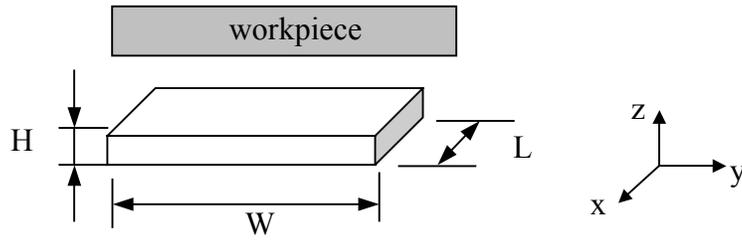
$W = B_{Smax}$

$L = B_{Smin}$

$H = W/6$

where,

- Bsmin – Smaller edge length of locating surface bounding box.

- Bsmax – Larger edge length of locating surface bounding box.

Stiffness -
$$\begin{cases} Sz = 3.37E + 07 \cdot WLH^{-0.7} \\ Sx = Sy = 3.11E + 06 \cdot WLH^{-1} \end{cases}$$

A.3.3. Short-V
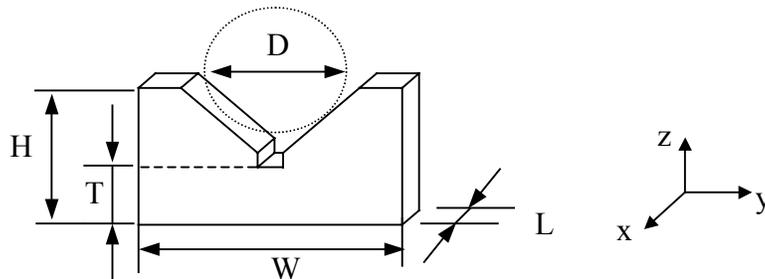
$W = 2D$

$L = W/5 = 2D/5$

$H = D$

$T = 3D/5$

Stiffness -
$$\begin{cases} Sz = 4.83E + 06 \cdot W \\ Sx = 1.48E + 06 \cdot W \\ Sy = 6.54E + 05 \cdot W \end{cases}$$

A.3.4. Long-V
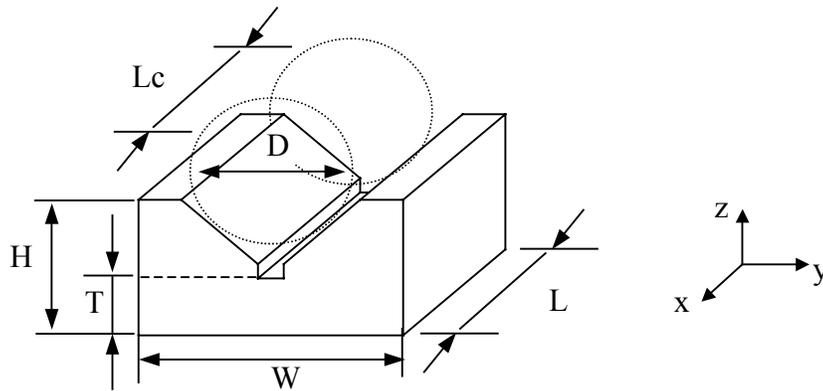
$W = 2D$

$L = Lc$

$H = D$

$T = D/2$

$$\alpha = \frac{Lc}{2D/5}$$

Stiffness – its stiffness can be derived based on short-v stiffness:

$$\text{Stiffness -} \begin{cases} Sz = \alpha \cdot 4.83E + 06 \cdot W \\ Sx = \alpha \cdot 1.48E + 06 \cdot W \\ Sy = \alpha \cdot 6.54E + 05 \cdot W \end{cases}$$

A.3.5. Short-Round Pin
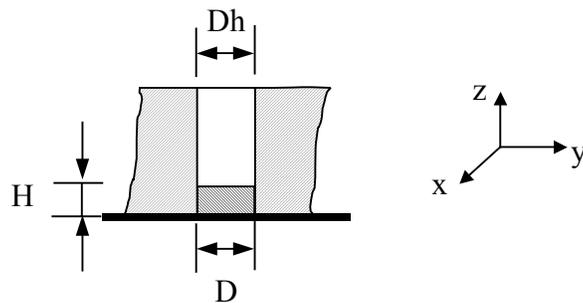
$D = Dh$

$H = D/2$

$$\text{Stiffness -} \begin{cases} Sz = 3.25E + 07 \cdot D \\ Sx = Sy = 9.62E + 06 \cdot D \end{cases}$$

A.3.6.   Short-Diamond Pin
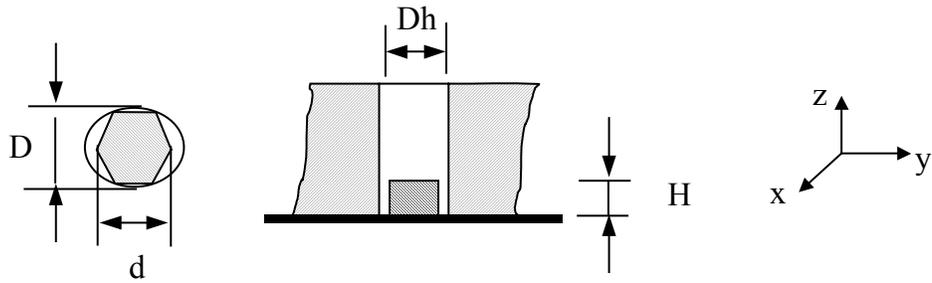
$D = Dh$

$d = 2D/3$

$H = D/2$

$$\text{Stiffness -} \begin{cases} Sz = 2.06E + 07 \cdot D \\ Sx = 4.55E + 06 \cdot D \\ Sy = 6.33E + 06 \cdot D \end{cases}$$

A.3.7.   Long-Round Pin
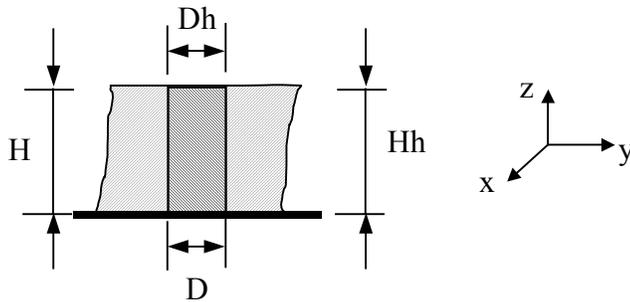
$D = Dh$

$H = Hh$

$$\alpha = \frac{H}{D/2}$$

Stiffness – its stiffness can be derived based on short-round pin stiffness.

$$\text{Stiffness -} \begin{cases} Sz = \alpha^{-0.7} \cdot 3.25E + 07 \cdot D \\ Sx = Sy = \alpha^{-1} \cdot 9.62E + 06 \cdot D \end{cases}$$

A.4.   Locator Stiffness Estimation

The stiffness conversions listed in the previous section are estimated with FEA (finite element analysis) package ANSYS. The original testing data and the curve fitting results are listed here.

A.4.1.   Point Type
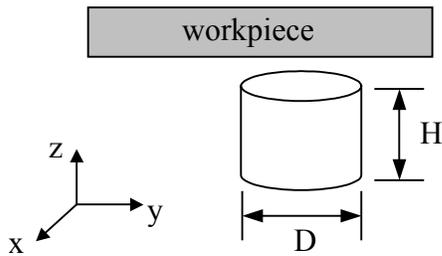
D	H	f(z)	dz_max
0.05	0.05	1	1.29E-06
0.1	0.1	1	7.18E-07
0.2	0.2	1	3.11E-07

D	H	f(x)	dx_max
0.05	0.05	1	7.18E-06
0.1	0.1	1	3.69E-06
0.2	0.2	1	1.86E-06

Point Type Locator Stiffness (z direction)

dz_max

$dz = 6.24\text{E-}08D^{-1}$

(D)

Point Type Locator Stiffness (x direction)

dx_max

$dx = 3.88\text{E-}07D^{-1}$

(D)
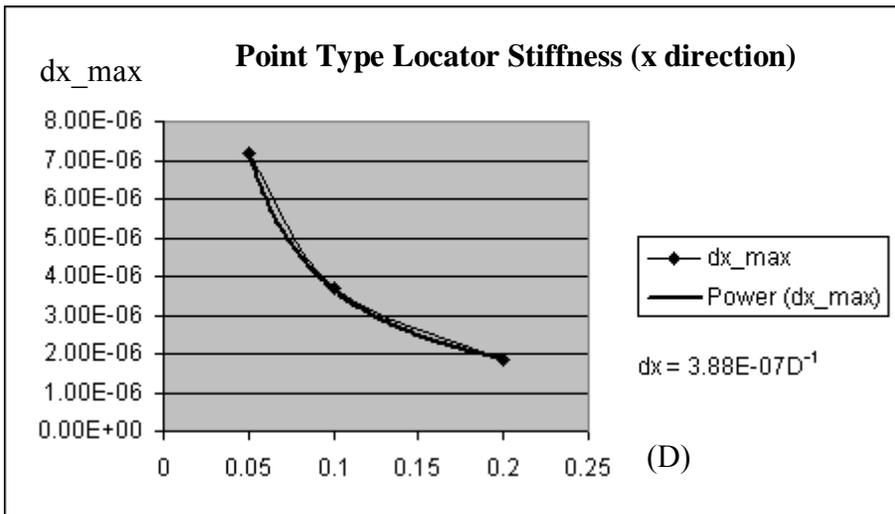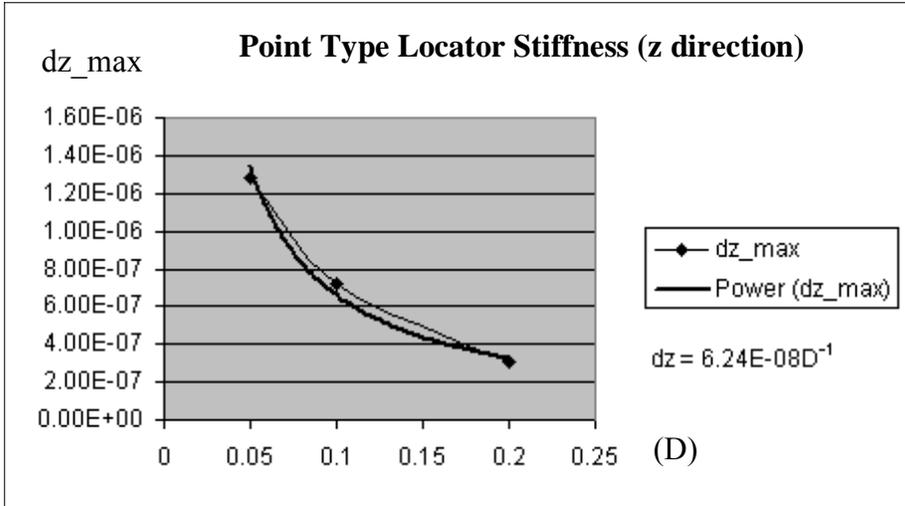
A.4.2. Plane Type
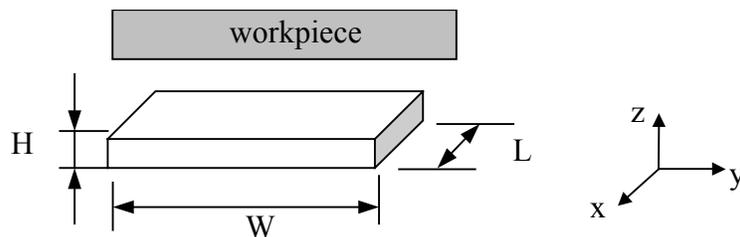
W	L	H	f(z)	dz_max
0.3	0.3	0.05	1	3.74E-08
0.3	0.3	0.1	1	5.91E-08
0.3	0.3	0.2	1	9.79E-08

0.6   0.3   0.05   1   1.81E-08

Plane Type Locator Stiffness (z direction)

dz_max

$$dz = 2.97E\text{-}08 W^{-1}L^{-1}H^{0.7}$$

(H)
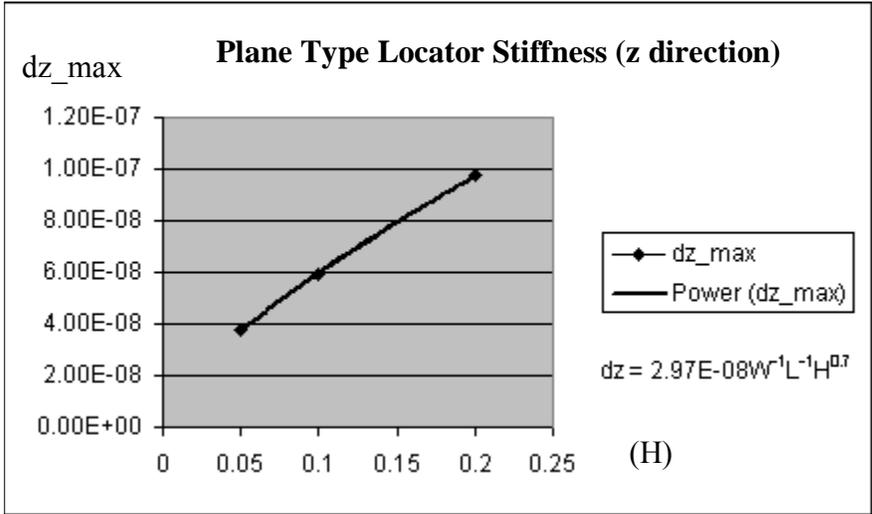
W	L	H	f(y)	dy_max
0.3	0.3	0.05	1	7.90E-08
0.3	0.3	0.1	1	1.59E-07
0.3	0.3	0.2	1	3.82E-07
0.6	0.3	0.05	1	3.82E-08

W	L	H	f(x)	dy_max
0.6	0.3	0.05	1	4.42E-08

Point Type Locator Stiffness (y direction)

dy_max

$$dy = 3.22E\text{-}07 W^{-1}L^{-1}H$$

(H)
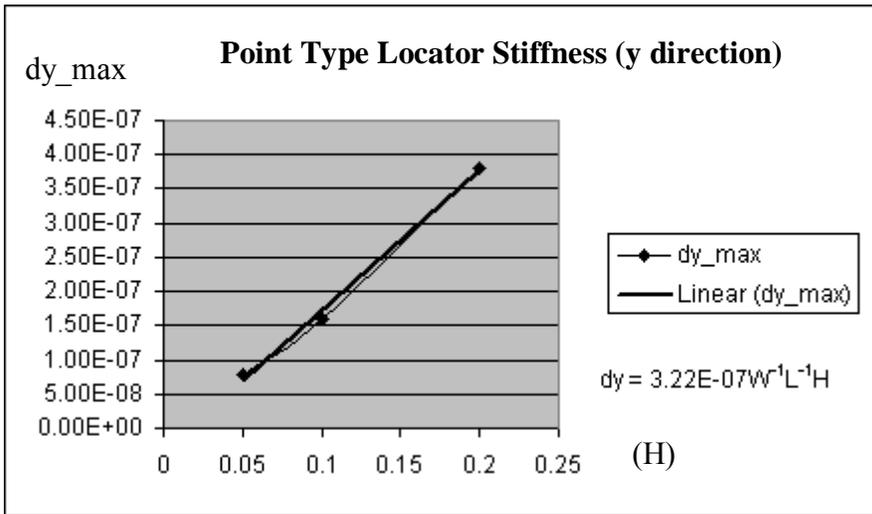
A.4.3.   Short-V and Long-V
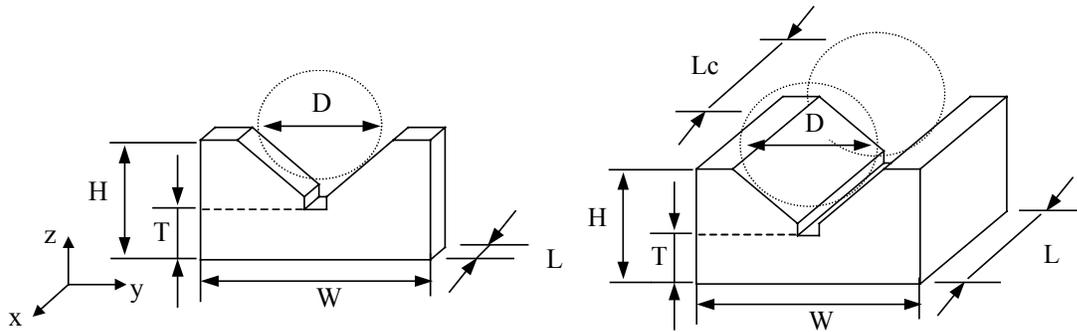
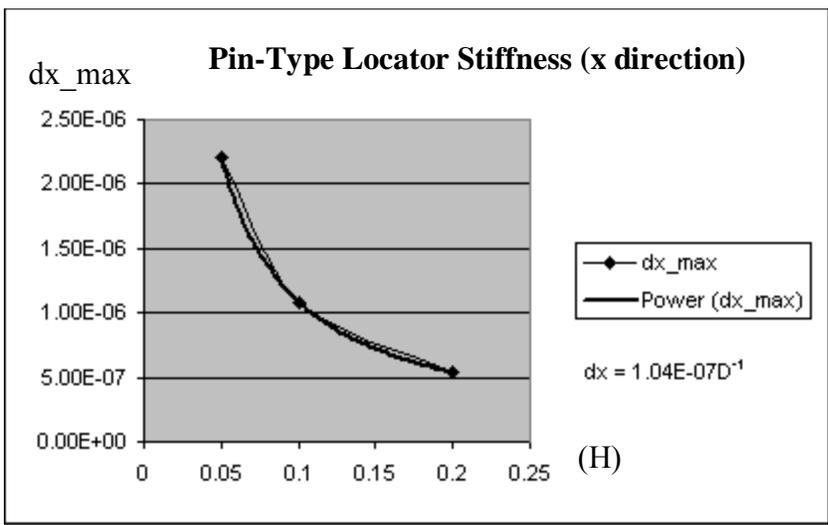| W	L	H	T	f(z)	dz_max
0.025	0.005	0.0125	0.0075	1	8.23E-06
0.05	0.01	0.025	0.015	1	4.12E-06
0.1	0.02	0.05	0.03	1	2.06E-06
0.2	0.04	0.1	0.06	1	1.03E-06
0.4	0.08	0.2	0.12	1	5.14E-07
0.8	0.16	0.4	0.24	1	2.60E-07
0.1	0.04	0.05	0.03	1	1.21E-06

V-Type Locator Stiffness (z direction)

$dz = 2.07E{-}07 W^{1}$

(H)
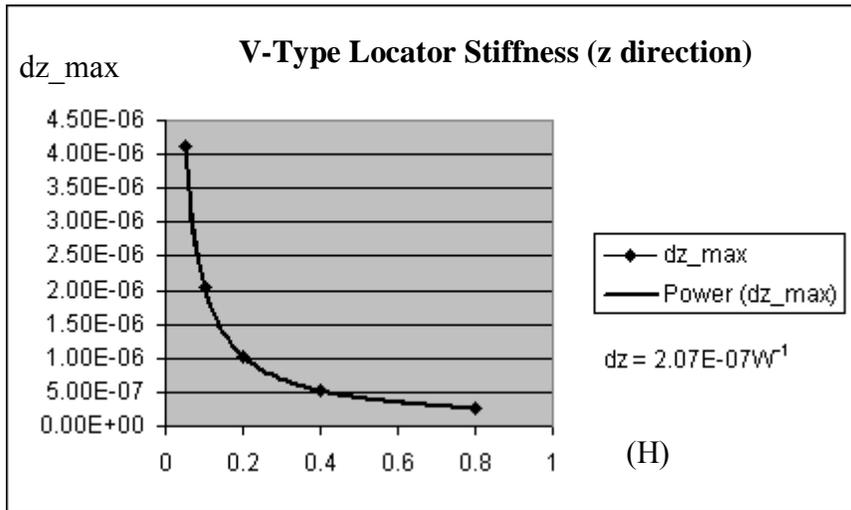
W	L	H	T	f(x)	dx_max
0.1	0.02	0.05	0.03	1	6.77E-06
0.2	0.04	0.1	0.06	1	3.38E-06
0.4	0.08	0.2	0.12	1	1.69E-06

V-Type Locator Stiffness (x direction)

dx_max

$dx = 6.77E\text{-}07 W^1$

(H)
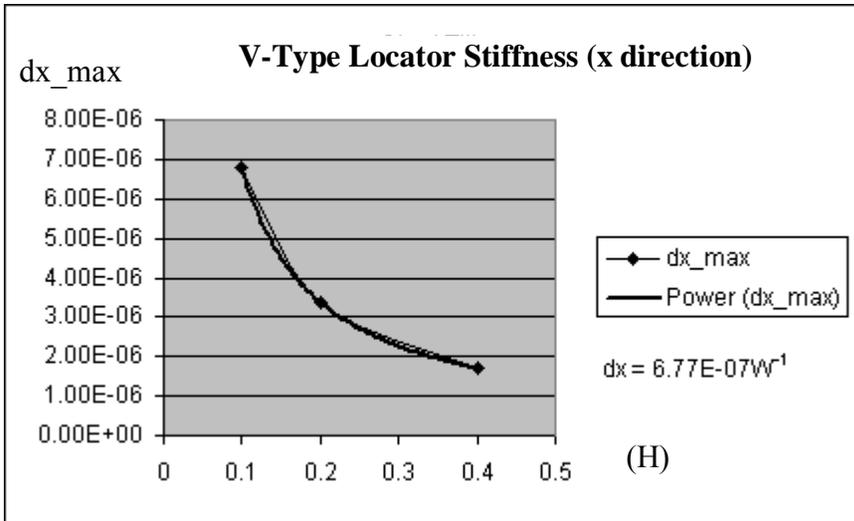
A.4.4. Short-Round Pin and Long-Round Pin
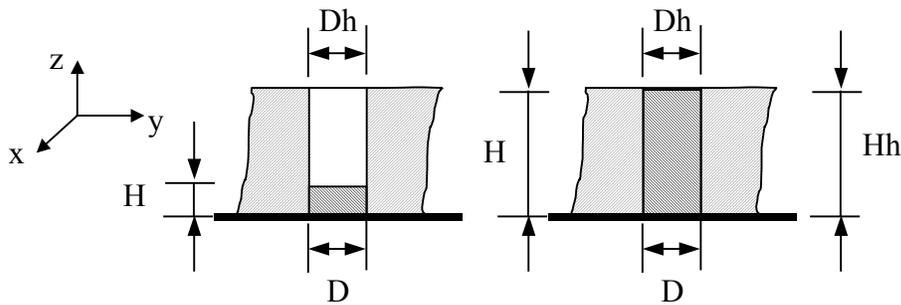
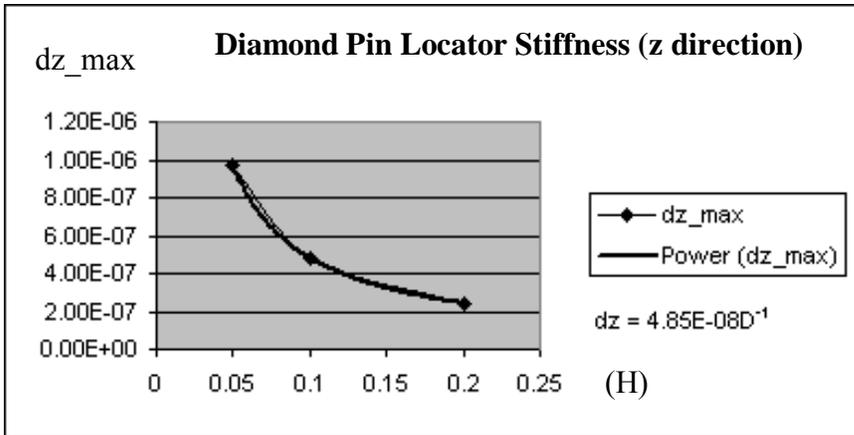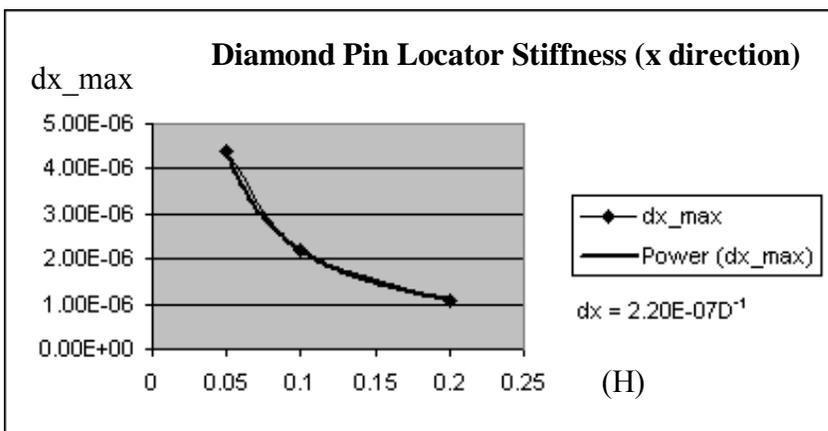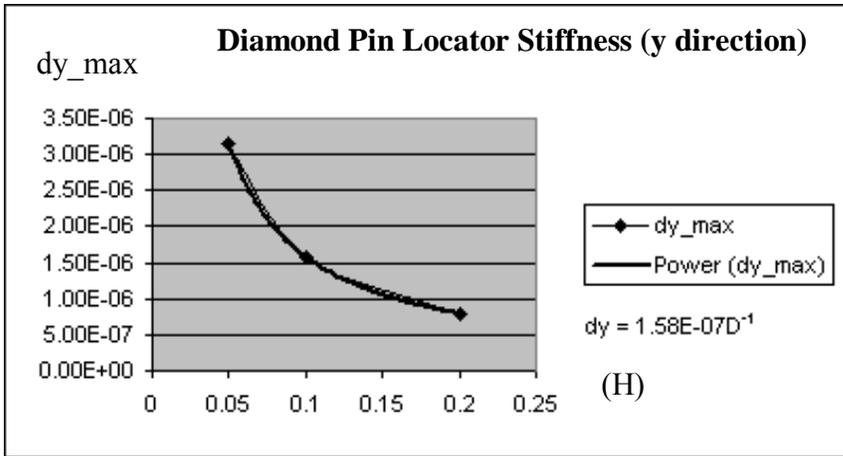| D	H	f(z)	dz_max
0.05	0.025	1	6.97E-07
0.1	0.5	1	3.34E-07
0.2	1	1	1.65E-07
0.05	0.5	1	1.16E-06
0.05	1	1	1.63E-06

Pin-Type Locator Stiffness (z direction)

dz_max

dz = 3.08E-08D^{-1}

(H)
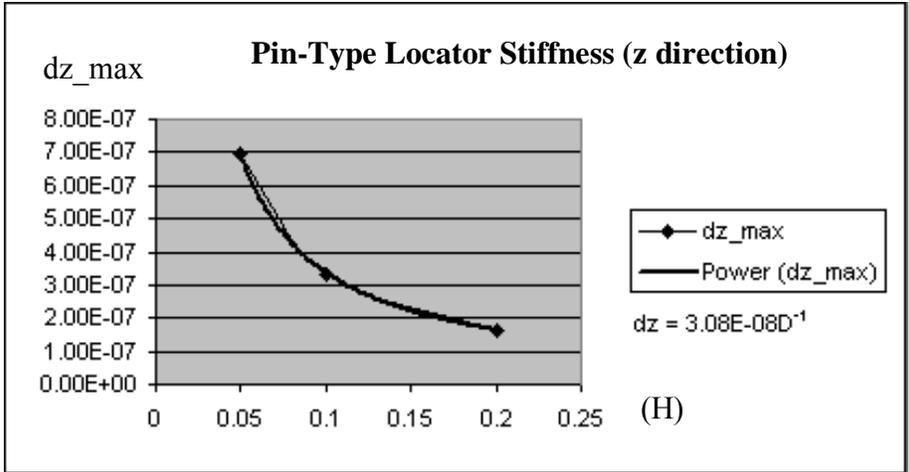
D	H	f(x)	dx_max
0.05	0.025	1	2.21E-06
0.1	0.5	1	1.09E-06
0.2	1	1	5.37E-07
0.05	0.5	1	7.16E-06
0.05	1	1	1.88E-05

Pin-Type Locator Stiffness (x direction)

dx_max

dx = 1.04E-07D^{-1}

(H)

A.4.5.   Short-Diamond Pin
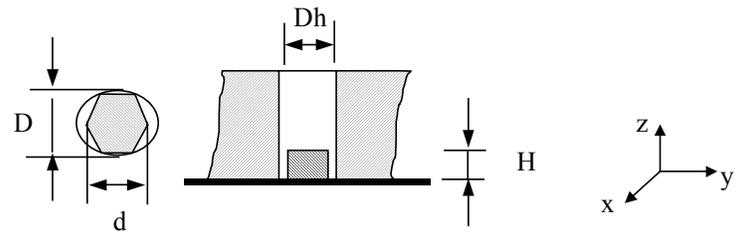
D	H	f(z)	dz_max
0.05	0.025	1	9.66E-07
0.1	0.5	1	4.83E-07
0.2	1	1	2.42E-07

Diamond Pin Locator Stiffness (z direction)

dz_max

$dz = 4.85E\text{-}08 D^{-1}$

(H)

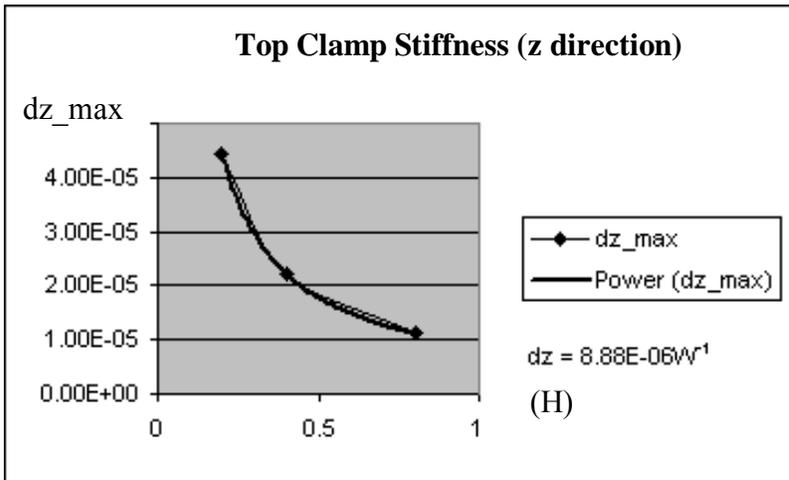| D	H	f(x)	dx_max
0.05	0.025	1	4.39E-06
0.1	0.5	1	2.19E-06
0.2	1	1	1.10E-06

Diamond Pin Locator Stiffness (x direction)

dx_max

$dx = 2.20E\text{-}07 D^{-1}$

(H)

D	H	f(y)	dy_max
0.05	0.025	1	3.16E-06
0.1	0.5	1	1.58E-06
0.2	1	1	7.91E-07

Diamond Pin Locator Stiffness (y direction)

dy_max

$dy = 1.58E\text{-}07D^{-1}$

(H)

A.4.6. Top Clamp

W	L	H	T	f(z)	dz_max
0.2	0.05	0.03	0.04	1	4.45E-05
0.4	0.1	0.06	0.08	1	2.22E-05
0.8	0.2	0.12	0.16	1	1.11E-05

Top Clamp Stiffness (z direction)

dz_max

$dz = 8.88E\text{-}06W^{-1}$

(H)

W	L	H	T	f(x)	dx_max
0.2	0.05	0.03	0.04	1	6.00E-06
0.4	0.1	0.06	0.08	1	3.00E-06
0.8	0.2	0.12	0.16	1	1.50E-06

113

Top Clamp Stiffness (x direction)

dx_max

dx = 1.20E-06W^1

(H)
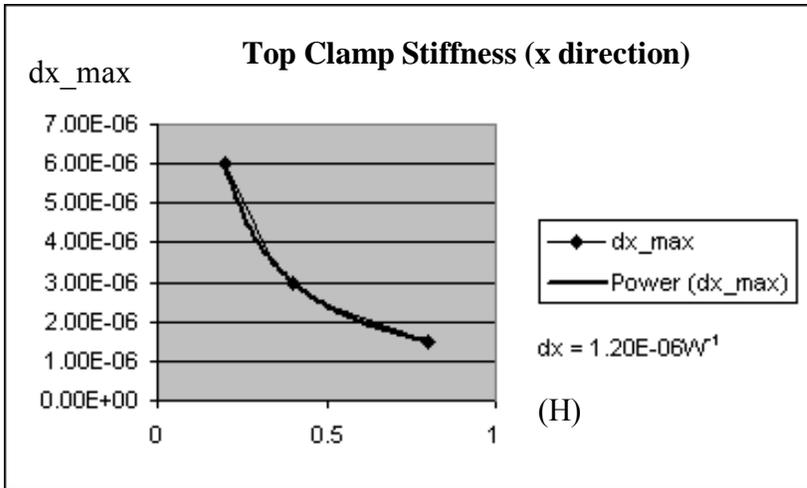
W	L	H	T	f(y)	dy_max
0.2	0.05	0.03	0.04	1	2.71E-05
0.4	0.1	0.06	0.08	1	1.35E-05
0.8	0.2	0.12	0.16	1	6.75E-06

Top Clamp Stiffness (y direction)

dy_max

dy = 5.40E-06W^1

(H)
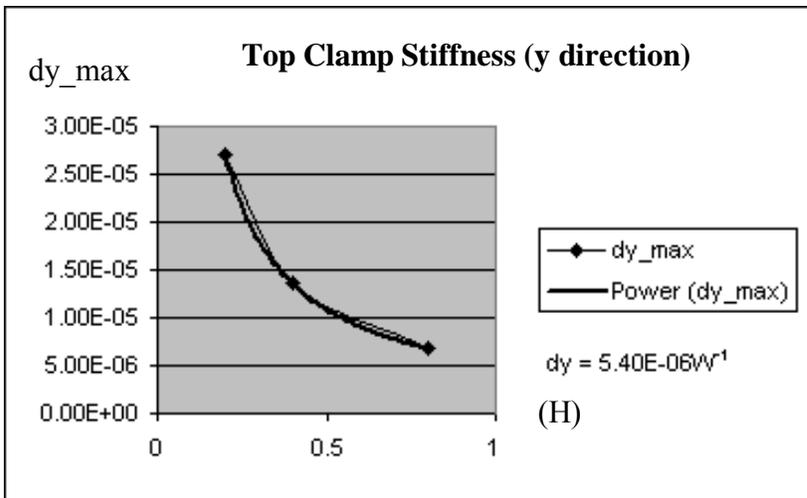
Appendix B.   Clamping Position Determination

After we have the locating plan and clamping surfaces, we can determine the clamping positions automatically. The algorithm here is used to quickly generate, in general cases, feasible clamping plans without getting too sophisticated.

B.1.   Initial Positions

First, each locating point is projected along the opposite of its normal direction. If an intersection exists on one of the clamping surfaces, then that intersection is selected as one clamping point. In Figure B.1, locating point L1 is projected and has an intersection C1, so point C1 is found as the clamping point for L1.
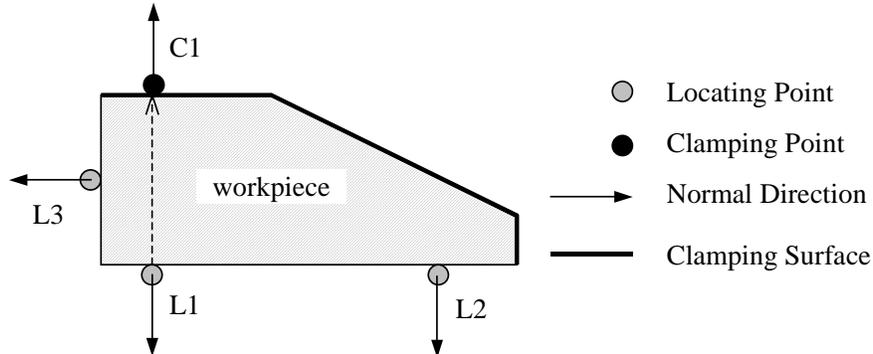
Figure B.1. Initial Clamping Position Generation (1)

If no surface with an opposite normal direction can be found, then the surface with closest opposite normal direction is used instead. In Figure B.2, locating point L2 has no "opposite" surface, so it is projected back to have the intersection C2, which is the

115

clamping point for L2. In such case, the angle between locating and clamping point normal directions is required to be large enough, i.e., $\alpha > 145$ (degree).
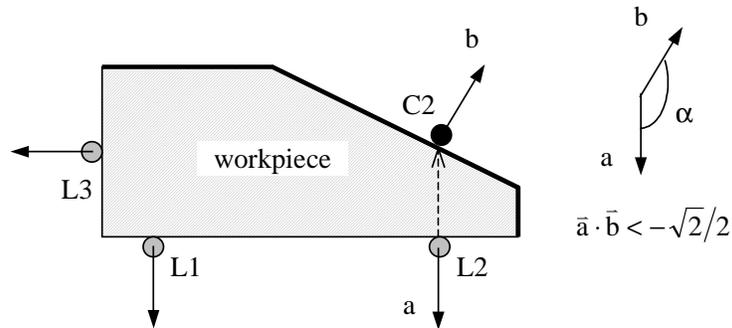

Figure B.2. Initial Clamping Position Generation (2)

If there is a surface that satisfies the normal direction requirement, but there is no intersection, then a "virtual point" is first generated. Then the virtual point is adjusted onto the surface as the clamping point. In Figure B.3, locating point L3 is projected back to have the virtual intersection V3, it is then adjust onto the clamping surface at position C3. The distance d between surface edge and final position C3 is set in the algorithm and can be modified by the user.
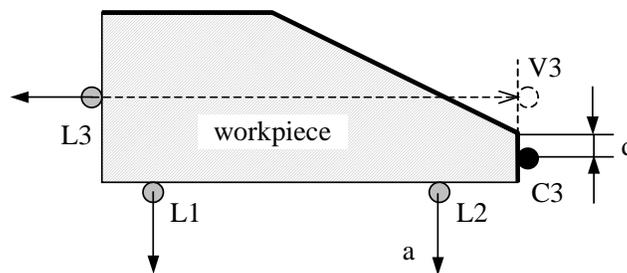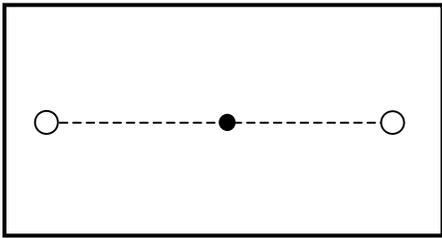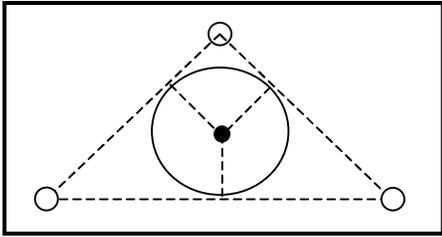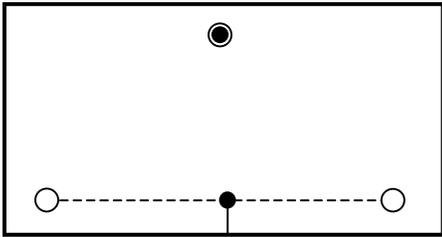

Figure B.3. Initial Clamping Position Generation (3)

B.2.   Clamping Points Adjustment

Users are allowed to set the number of clamping points on each surface. In cases where the user defined number does not equal to the program generated number, clamping points will be adjusted to match the user defined number. The adjustment is list in the table below.

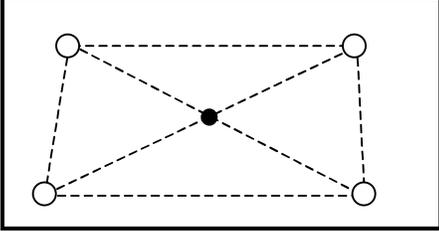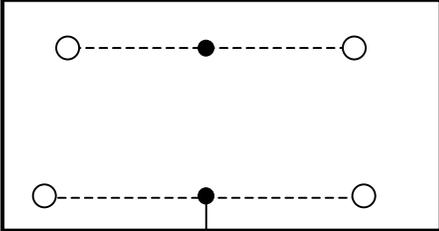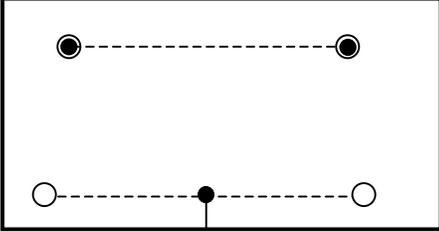| Program Number	User Defined Number	Clamping Points Adjustment
2	1	The center of the two auto generated points. ○ auto generated positions ● positions after modification
3	1	The point that its distances to the three edges are equal. ○ auto generated positions ● positions after modification
3	2	Comparing the center points of three edges, one clamping point is the center point so that its distance to the edge of clamping surface is the shortest. The other clamping point is the auto generated one against the first clamping point. ○ auto generated positions ● positions after modification
4	1	The center point.

		○ auto generated positions ● positions after modification
4	2	Comparing the center points of four edges, one clamping points is the center point that its distance to the edge of clamping surface is the shortest. The other clamping point is the center point against the first clamping point. ○ auto generated positions ● positions after modification
4	3	Comparing the center points of four edges, one clamping points is the center point that its distance to the edge of clamping surface is the shortest. The other two clamping points is the two auto generated ones against the first clamping point. ○ auto generated positions ● positions after modification

Table B.1 Clamping Points Adjustment

Note: if the clamping points are not in the accessible area, the nearest point in the accessible area is used.

Appendix C.   Transformation of Point Displacement

This section shows how to transform a point displacement from one coordinate system to another. Here we use the local coordinate system (LCS) as the original CS, and the global coordinate system (GCS) as the new CS to be transformed to.

Assume the 4x4 transformation matrix from LCS to GCS is $\left[T_G^L\right] = \begin{bmatrix} \left[R_G^L\right] & \vdots & \left[P_G^L\right] \\ \hdashline 0 & \vdots & 1 \end{bmatrix}$, where $\left[R_G^L\right]$ is the 3x3 rotation matrix, and $\left[P_G^L\right]$ is the 3x1 translation part.

If the point positions in LCS before and after displacement are $\left\{p_1^L\right\}$ and $\left\{p_2^L\right\}$, then their positions in GCS before and after displacement are:

$$\left\{p_1^G\right\} = \left[R_G^L\right] \cdot \left\{p_1^L\right\} + \left[P_G^L\right]$$

$$\left\{p_2^G\right\} = \left[R_G^L\right] \cdot \left\{p_2^L\right\} + \left[P_G^L\right]$$

Then we have the displacement after transformation:

$$\left\{\Delta p^G\right\} = \left\{p_2^G\right\} - \left\{p_1^G\right\} = \left[R_G^L\right] \cdot \left(\left\{p_2^L\right\} - \left\{p_1^L\right\}\right) = \left[R_G^L\right] \cdot \left\{\Delta p^L\right\} \qquad (C.1)$$

From this equation, we can see that the point displacement in GCS is only related with the orientation of LCS, but not its position. This conclusion allows us to simply the algorithm in finding the Fixture Stiffness Matrix.